Electronic components & applications

Vol. 1, No. 2
February 1979

incorporating Philips Electronic Applications Bulletin and Mullard Technical Communications

ISSN 0141–6219

Electronic components & applications

Volume 1, No. 2 February 1979

Contents

Printed in The Netherlands
by Eindhovensche Drukkerij

Solar energy serving everyday needs: In northerly latitudes the winter sun is never high in the sky and often overcast, but even during the severe winter of 1979 the solar panel atop the further of the two masts in the photograph demonstrated that it was able to supply the round-the-clock energy requirements of the motorists' emergency telephone in the foreground. The article beginning on page 109 describes the construction and operation of such panels and how they can be integrated into complete energy systems.

2/3 inch Plumbicon* tube with enhanced performance

A. A. J. FRANKEN

In a new version of the 2/3 inch Plumbicon tube, lag is minimised and resolution enhanced by the use of a thinner photoconductive layer in combination with a new diode gun. This results in a highly versatile camera tube suited to ENG, EFP and general studio applications.

The last few years have seen an upsurge in the development of portable TV cameras for electronic news gathering (ENG). Such cameras must be of lightweight construction and must consume little power. Use of the 2/3 inch Plumbicon tube type XQ1427 results in these requirements being met with ease. Moreover, because of its fast response (i.e. low lag) and high sensitivity, this tube is well suited to operation under the low light conditions often encountered in ENG applications. Its small size, however, does result in some sacrifice of resolution.

Besides ENG applications, recent trends indicate that the 2/3 inch camera tube is also suitable for studio use (e.g. continuity, interviews and news reading) and for electronic field production (EFP). However, since the requirements for ENG and studio applications are not the same, they necessarily call for some differences in tube characteristics. A TV camera designed for use outdoors (e.g. for ENG) must be able to cope with scenes containing rapidly moving objects (dynamic scenes) such as those encountered in sporting events. It must also remain usable over a wide range of lighting conditions and ambient temperatures. The most important parameters for camera tubes used in ENG applications are therefore, high *sensitivity*, good *dynamic resolution* especially in low light conditions, and good *highlight handling*. In contrast, camera tubes used in EFP and studio applications will normally be exposed to well lit scenes, and therefore low lag and good dynamic resolution are already assured (Ref. 2). However, the recording of programme material is a major application of EFP and studio cameras, and requires a high signal/noise ratio (for editing etc.) which in turn demands good *'static' resolution*.

A need has arisen therefore to adapt the 2/3 inch Plumbicon tube type XQ1427 for EFP and studio use, without sacrifice of the characteristics that make it suitable for ENG applications. Development of a 'diode gun' has made a significant contribution towards fulfilling this need. To explain its action however, we must first consider the influence of certain design parameters on two important aspects of camera tube performance.

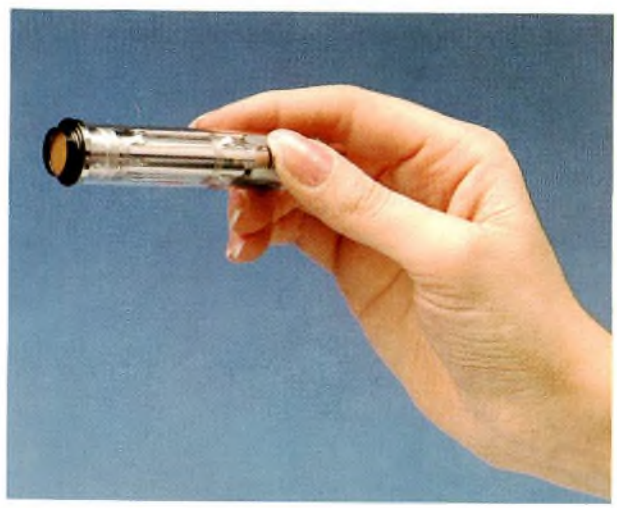

74XQ Plumbicon tube incorporating the new 'diode gun'

* Trademark of N.V. Philips' Gloeilampenfabrieken for television camera tubes.

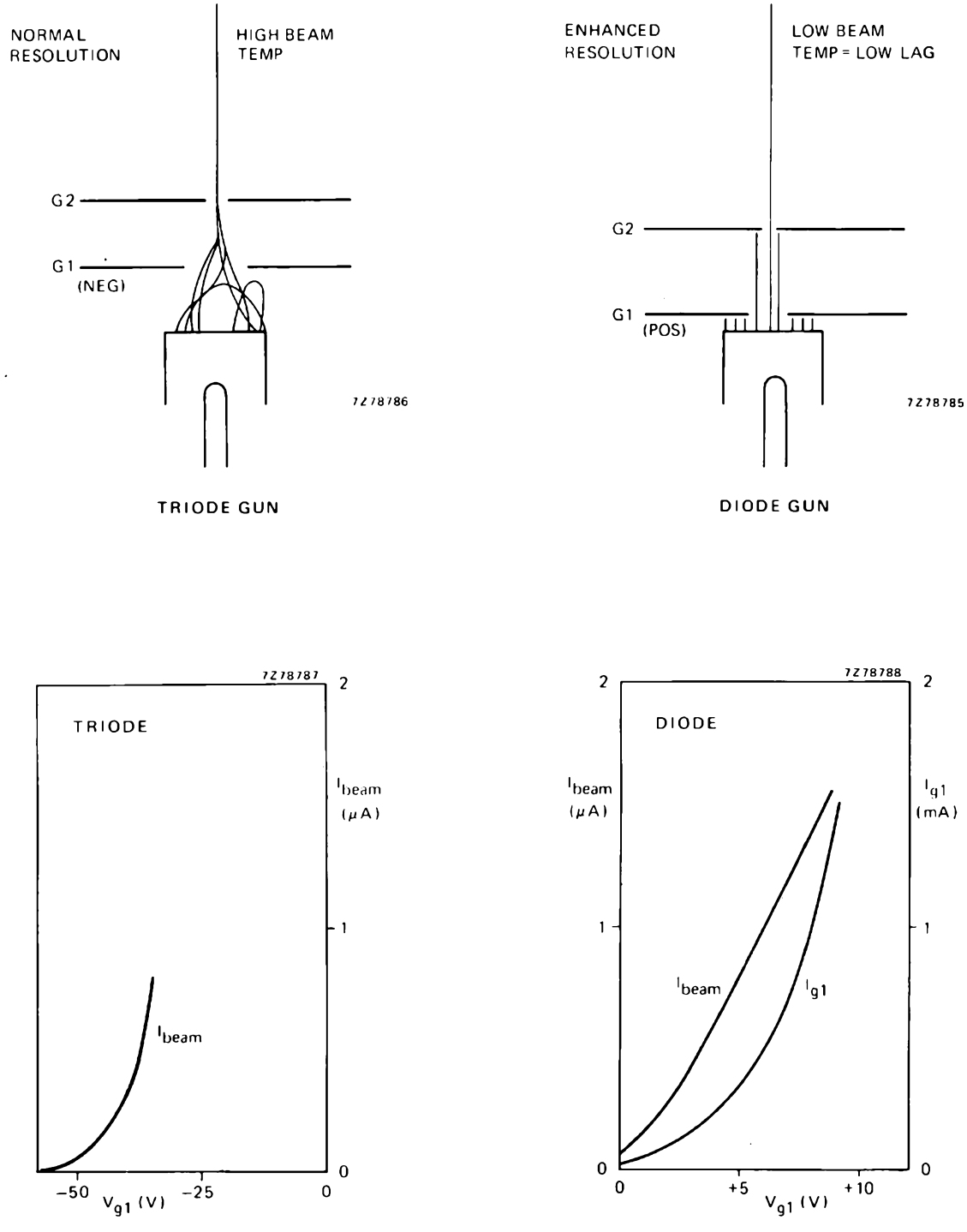

Fig.1 Comparison between the conventional triode gun with beam crossover, and the new 'diode gun' without beam crossover

LAG AND RESOLUTION

Table 1 shows the dependence of *lag* and *resolution* on the characteristics of the photoconductive layer and electron beam.

TABLE 1
Resolution and lag in a camera tube, determined by photoconductive layer and electron beam.

	photoconductive layer (thickness)	electron beam (current density)
resolution	dispersion of light and charge	spot diameter
lag	layer capacitance C_{layer}	beam resistance R_{beam}

The lag of a conventional vidicon tube is determined principally by that of the photoconductive layer (photoconductive lag). In a Plumbicon tube however, the photoconductive lag is negligible. The lag in this type of tube can be attributed to the process by which the electron beam recharges the photoconductive layer (beam discharge lag, Refs. 1 and 2). Beam discharge lag varies directly with the photoconductive layer capacitance C_{layer} and the differential beam resistance R_{beam} (Ref. 2).

The 'static' resolution of a camera tube is determined by the *modulation depth*, which is defined as the ratio (expressed as a percentage) of the amplitudes of a 4 MHz and 0.5 MHz (320 and 40 TV lines) squarewave signal as measured on a waveform monitor. The modulation depth varies inversely with the thickness of the target material, a thinner target resulting in increased modulation depth due to reduced light and charge dispersion. However, since C_{layer} is inversely proportional to target thickness, simply reducing the latter will increase C_{layer} and thereby, increase lag. Thus if static resolution is to be improved by reducing layer thickness, some means must be found to compensate the increase in C_{layer}. This can be done by reducing differential beam resistance so that good dynamic resolution is maintained.

CONCEPT OF A NEW TUBE WITH 'DIODE GUN'

In a conventional triode gun, the grid and anode converge the electrons emitted by the cathode to produce a 'crossover' in the electron beam. An analysis of the axial velocities of electrons in this configuration reveals an excess of fast electrons compared with the Maxwellian distribution emitted by the cathode. This can be attributed to the high degree of electron interaction occurring in the beam, particularly in the vicinity of the crossover.

It can be shown (Refs. 2 and 3), that the differential beam resistance is given by:

$$R_{beam} = \frac{kT_O}{ei}$$

where T_O is the effective cathode temperature, i is the photoconductive layer charging current, e is the charge on an electron (1.6×10^{-19} coulombs) and k is Boltzmann's constant (1.38×10^{-23} joules/K). T_O can be regarded as a measure of the beam temperature which is itself a function of the electron velocity distribution. An increase in mean electron velocity therefore, results in a corresponding increase in T_O which leads in turn, to a proportional increase in R_{beam}.

The differential beam resistance can be reduced by eliminating the crossover. This can be accomplished by means of the 'diode gun', which is a positive grid triode operating in the diode mode (Fig. 1), the grid drawing a current of a few milliamperes. The effect of the positive grid is to reduce beam convergence, and thereby to eliminate the crossover. In this way R_{beam} is reduced, and the consequent reduction in lag permits the use of thinner targets to increase modulation depth, and improve 'static' resolution.

PERFORMANCE

Lag and modulation depth

Figure 2 compares the lag and modulation depth of the standard XQ1427, an experimental XQ1427 with a thinner photoconductive layer and finally, the new tube development type 74XQ with the thinner layer and the 'diode gun'. Also shown is the performance of a tube with a selenium-based photoconductive layer, and it is evident from the figure, that the performance of this tube is similar to that of the experimental XQ1427 with the thinner layer. The figure illustrates also that the 74XQ tube combines the low lag of the standard XQ1427 with the increased modulation depth of the experimental XQ1427 tube.

Use of bias light to minimise lag

The equation for R_{beam} shows that it varies inversely with the charging current i. The beam resistance and hence the lag, can therefore be reduced by offsetting the zero point of the charging current. This is effected by projecting a bias light onto the photoconductive layer. The results of using a bias light are shown in Fig. 3.

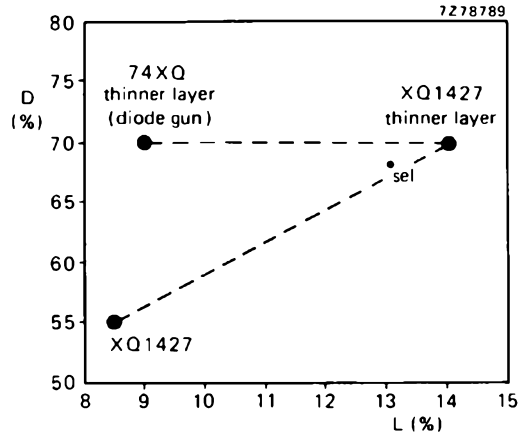

Fig.2 Decay lag L, in third field, and modulation depth D of 2/3 inch tubes. Decay lag was measured in white light with a 20 nA signal and a 300 nA beam current (measured after 60 ms). Modulation depth was measured in white light with a 150 nA signal current and a 300 nA beam current (V_{mesh} = 750 V)

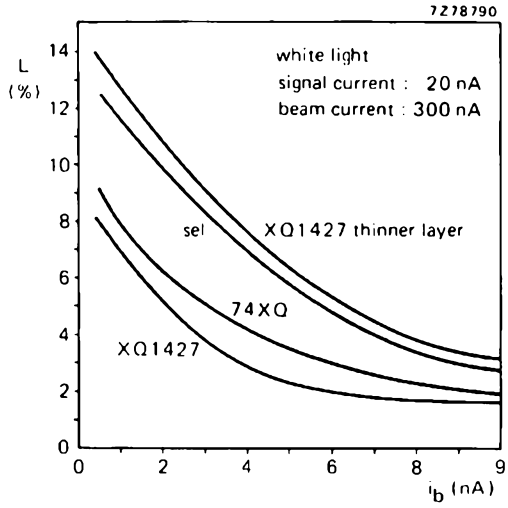

Fig.3 Decay lag in third field (60 ms) as a function of bias light current i_b (including dark current)

Sensitivity

Table 2 shows that the XQ1427 and the 74XQ are equally sensitive to blue light, and that the difference in sensitivity to other colours is only slight.

TABLE 2

Sensitivity in μA/lumen of some 2/3 inch camera tubes.

	white	red	green	blue
XQ1427	400	125	140	32
{ XQ1427 thinner layer / 74XQ }	350	115	120	32
selenium	280	90	90	27

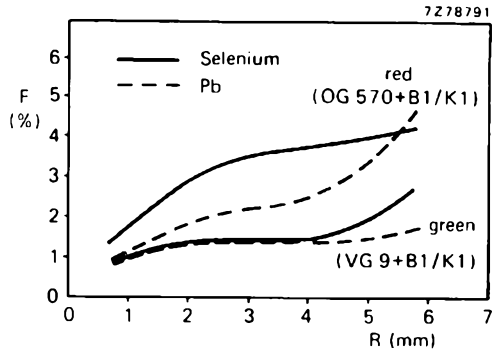

Fig.4 Flare F in the centre of the image as a function of the radius R of the irradiated area for Plumbicon (Pb) and selenium-based tubes.
Scanned area 6.6 x 8.8 mm², R_{max} = 5.5 mm

Flare

Flare occurs in any optical system and is caused by internal reflections. The method of measuring flare in a camera tube was described in a previous article (Ref. 3).

The low flare of the Plumbicon tube is due primarily to the use of the 'anti-halation' disc. This is located in front of the target and serves in addition to keep dust particles away from the focal plane to prevent them from becoming visible when small lens apertures are used. In the 74XQ further attention has been given to the problem of minimising internal reflections, resulting in a significant reduction in flare.

Figure 4 compares the flare, measured separately for red and green light, for the Plumbicon and selenium-based tubes. The flare is greater for red light than it is for green simply because the photoconductive layer has a higher reflectivity for red light. The flare for blue light is barely measurable.

Registration

Registration of the tubes in a colour camera improves with reduced mesh-to-layer spacing. This reduction however, increases the signal electrode output capacitance and consequently degrades the signal/noise ratio. The electron gun in the Plumbicon tube is produced to such close dimensional tolerances that the stringent registration requirements for broadcasting are met, whilst keeping output capacitance down to approximately 2.5 pF.

Burning-in

The 74XQ, like the XQ1427, performs excellently with respect to highlight burning-in, after-images of highlights seldom persisting for more than a few seconds.

Performance at elevated temperatures

As stated earlier, ENG requirements demand that the camera tube be able to operate over a wide range of ambient temperatures. Because high temperatures accelerate ageing of the photoconductive layer, the camera should be designed in such a way that the target temperature remains below 50 °C.

Faceplate temperatures of up to 70 °C have been recorded in cameras used in direct sunlight. The effect of such temperatures on camera tube life expectancy is therefore of interest. In Fig. 5, plots are shown of the white and the red sensitivity, as functions of operating time. The tubes were operated for a time at 60 °C before measurements were made. Only the red sensitivity increased slightly, the white sensitivity remaining constant.

Other parameters, such as white spot occurrence, blue and green sensitivity, burning-in, modulation depth and lag, remained unchanged as functions of operating time at 60 °C.

Experiments carried out on tubes with selenium-based layers show a significant decrease in white and red sensitivity and an increase in burning-in and white spot occurrence, after a few days. The Plumbicon tube however, continuously operated at 60 °C, retains its good performance for periods of several weeks.

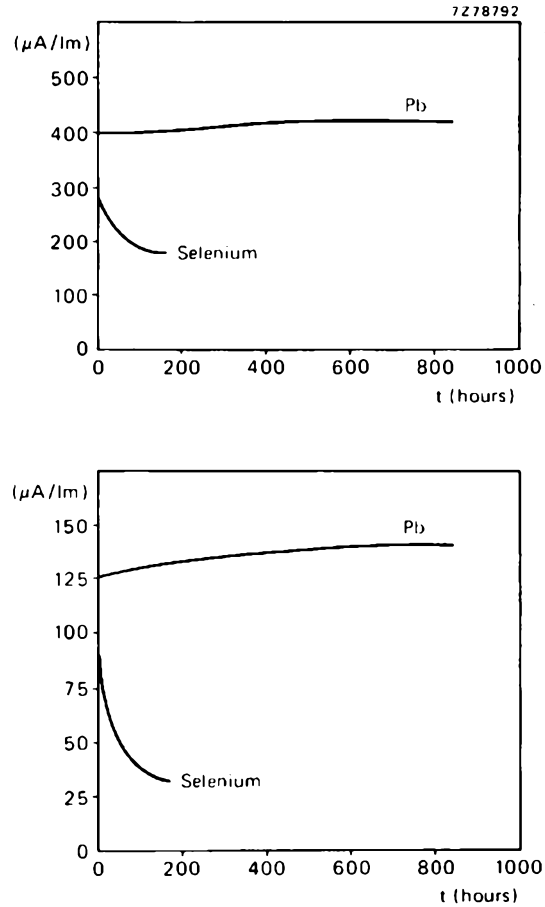

Fig.5 White sensitivity (top) and red sensitivity (bottom) as functions of operating time at 60 °C

Highlight handling

To achieve good highlight handling, a camera tube should operate with a high beam current. For the 74XQ tube, this causes only slight loss of modulation depth and increase in lag. Nevertheless, continuous operation with a high beam current must be avoided since it reduces the life of the tube. A more satisfactory method is to increase the beam current automatically, only when the beam scans a highlight on the target. This technique, which is known as 'dynamic beam control' (DBC), 'automatic beam optimalisation' (ABO) or 'comet tail suppression' (CTS), is suitable for many portable TV cameras.

The new 'diode gun' of the 74XQ camera tube, when operated with DBC, has enough beam reserve for correct highlight handling of at least 4 lens stops over a signal current of 200 nA. A major problem in the design of DBC circuits is instability. However, owing to the high slope of the diode characteristic in the diode gun (Fig. 1), only a few volts on the grid are necessary to produce a high beam current, thereby minimising the possibility of instability.

TABLE 3
Comparative performance of Plumbicon and selenium-based tubes.

	modulation depth white	decay lag after 60 ms 20/300 nA 5 nA bias light	sensitivity (μA/lumen) red	green	blue	flare R = 2.3 mm red	burn-in time	operating life at 60 °C	application
XQ1427	55%	2.5%	125	140	32*	2%	seconds	weeks	ENG, EFP
XQ1427 with thinner layer	70%	6%	115	120	32*	2%	seconds	weeks	
74XQ (diode gun)	70%	3.5%	115	120	32*	2%	seconds	weeks	ENG, EFP studio
selenium	70%	6%	90	90	27	3.2%	tens of seconds	days	ENG, EFP.

* 38 μA/lm measured without B1/K1 filter.

Table 3 summarises performance characteristics of the three Plumbicon tubes discussed here and for comparison, those of a tube having a selenium target.

CONCLUSION

The 2/3 inch Plumbicon tube type XQ1427 is extremely well suited to ENG applications. The new Plumbicon tube, development type 74XQ, with its 'diode gun' will provide excellent 'static' resolution, low lag and hence good dynamic resolution, high sensitivity and good highlight handling. These characteristics place it in an unrivalled position as a multi-purpose camera tube, suited to ENG, EFP and general purpose studio applications.

NOTES

Measuring conditions:

Modulation depth: all measurements were made with an infrared reflecting filter (Balzers B1/K1) in the light path (tungsten lamp, colour temperature 2856 K).

Additional filters were inserted in the light path for the measurements with coloured light.

Red: Schott OG570, thickness 3 mm
Green: Schott VG9, thickness 1 mm
Blue: Schott BG12, thickness 3 mm.

All measurements on the Plumbicon tubes, except the blue sensitivity, refer to tubes with extended red sensitivity. The blue sensitivity increases to 38 μA/lm when measured without B1/K1 filter.

Since the control grid in the 74XQ draws current, it is not interchangeable with the XQ1427 without modification of the camera.

REFERENCES

1. HEYNE, L. 1956–1958. Acta Electronica 1-2, 124.
2. POLDER, L. J. v. d. 1967. Philips Research Reports 22, 178-207.
3. FRANKEN, A. 1978. Electronic Components and Applications 1, 57-59.

Erratum, E.C.A. 1 No. 1

In the article on the 25 mm Plumbicon tube, the lower figure on page 58 should be labelled Fig.2 and its caption should read, 'Frequency dependence of modulation depth, measured with square-wave test patterns.'

Philips' LDK14, which is fitted with 2/3 inch Plumbicon tubes, weighs only 5.5 kg, setting a new standard for ENG and EFP colour cameras

Digital control of radio and audio equipment

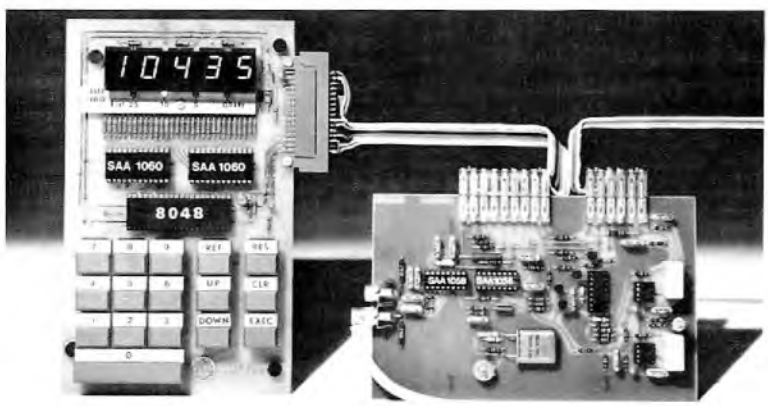

This is the first microcomputer-controlled tuning system to be specifically designed for a.m. and f.m. radios. The system uses a LOCMOS frequency synthesiser in a phase locked loop to provide digitally-controlled tuning and programme pre-selection. A 4½ digit LED display of the tuned frequency is provided. The system can be extended to give additional displays of programme and channel numbers, and can easily be adapted for remote control.

Recent advances in integrated circuit technology have so reduced the cost of integrating complex electronic functions that the use of MSI and LSI circuits can now be extended to domestic radios and audio equipment. This means that the long felt need to improve the performance and control facilities for this class of equipment can now be realised to the benefit of both the manufacturer and the user.

Some of the more significant improvements offered by the use of complex integrated circuits are as follows.

- Digital frequency and channel indicators which are much more accurate than conventional dials or tuning meters. Elimination of tuning dials also eases styling restrictions.
- Improved tuning stability in a.m. and f.m. radios. By using a phase-locked-loop frequency synthesiser and a microcomputer, it is possible to design a tuning system that can automatically select stereo broadcasts, traffic information services, transmissions with signal strength above a predetermined threshold, etc.
- Electromechanical preset tuning units can be replaced by digital programme selection via a voltage synthesiser.
- The remaining potentiometers and switches can be eliminated from radio/audio equipment by using digital control via microcomputer and D to A converters. The equipment can then be easily converted for remote control.

New integrated circuits and associated systems for implementing these improvements will be introduced during the course of 1979. An article on the first of them is published in this issue of Electronic Components and Applications. The others will be discussed in future issues.

Part 1 - Frequency measurement and display system for a.m. and f.m. radios

J. VAN STRAATEN

The described system based on two ICs can be used with v.h.f. (f.m.), short-wave, medium-wave and long-wave and can be programmed to compensate for a wide range of intermediate frequencies. Being self-contained, it can be easily added to existing mains-powered receivers and can also be adapted for battery-powered radios. A 4½ digit LED display indicates frequency or channel number.

This system has been specifically designed to measure the frequency to which an a.m./f.m. radio is tuned and to provide a digital LED display of either the tuned-frequency or the associated v.h.f. channel number.

The system counts the number of receiver local oscillator cycles that occur during a predetermined period, subtracts a programmable intermediate frequency from the count and feeds the resultant frequency to a display decoder/driver. The output from the decoder is displayed in the form of 4½ seven-segment digits or, in the case of v.h.f., there is an option of displaying the associated two-digit channel number.

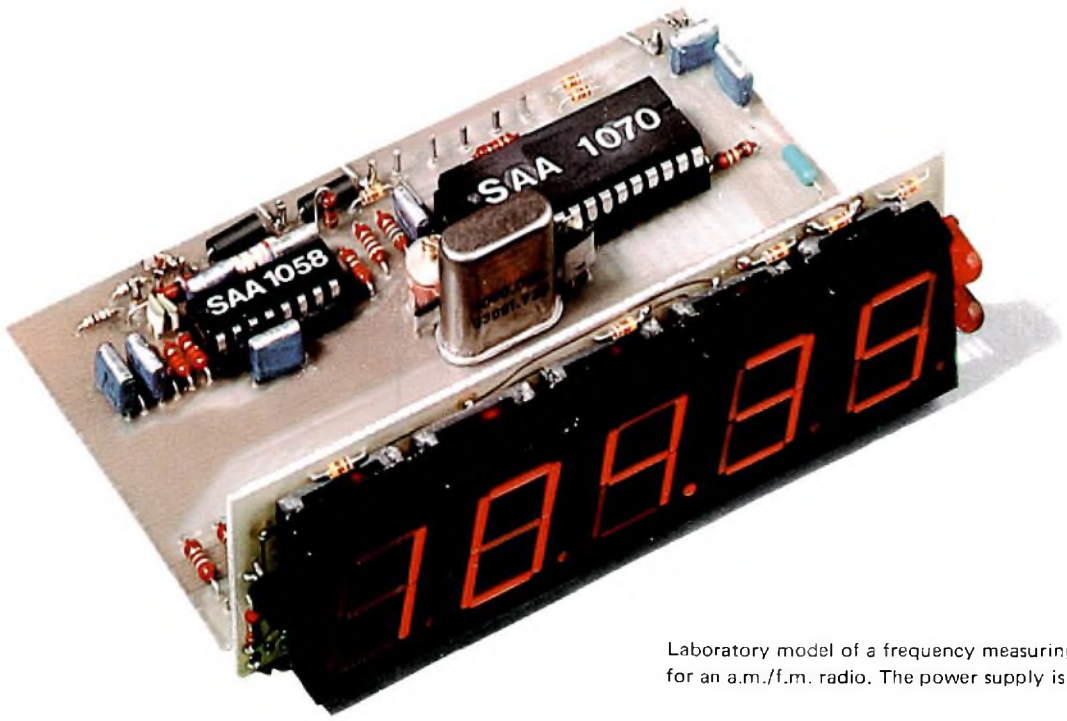

Laboratory model of a frequency measuring and display system for an a.m./f.m. radio. The power supply is not shown.

Since the system requires only two integrated circuits and a few passive peripheral components in addition to the display, it occupies very little printed-wiring board area. Furthermore, it can be programmed to operate on long-wave, medium-wave, short-wave and v.h.f. in association with a wide range of intermediate frequencies. The system can therefore be very easily added to the majority of existing radio receiver designs.

The following are features of the system:

- mains zero-crossing switching to reduce interference,
- multiple sampling to stabilise display during short-term local oscillator drift,
- requires only a single 8 V a.c. supply,
- suitability for use with a wide range of intermediate frequencies: for a.m., 449 kHz to 472 kHz; for f.m. 10.6 MHz to 10.775 MHz,
- compact circuitry with few peripheral components,
- facilities for 'freezing', testing and blanking the display:
  - v.h.f. channel number: +02 to +74 to within 0.1 MHz,
  - v.h.f. frequency, up to 109.3 MHz to within 0.05 MHz,
  - s.w. frequency, up to 19 995 kHz to within 5 kHz,
  - m.w./l.w. frequency, up to 1999 kHz to within 1 kHz,
- flicker suppression,
- high input sensitivity allows direct drive from radio local oscillators.

BRIEF SYSTEM DESCRIPTION

The principle of the frequency measuring and display system is illustrated by the block diagram in Fig. 1. The main components of the system are an integrated programmable pre-scaler (SAA1058), an integrated display interface and frequency counter (SAA1070), a 4 MHz quartz crystal and a 4½-digit seven-segment LED display.

The pre-scaler contains a preamplifier with inputs for a.m. and f.m. local oscillator signals, a frequency divider and two output amplifiers for driving ECL or MOS

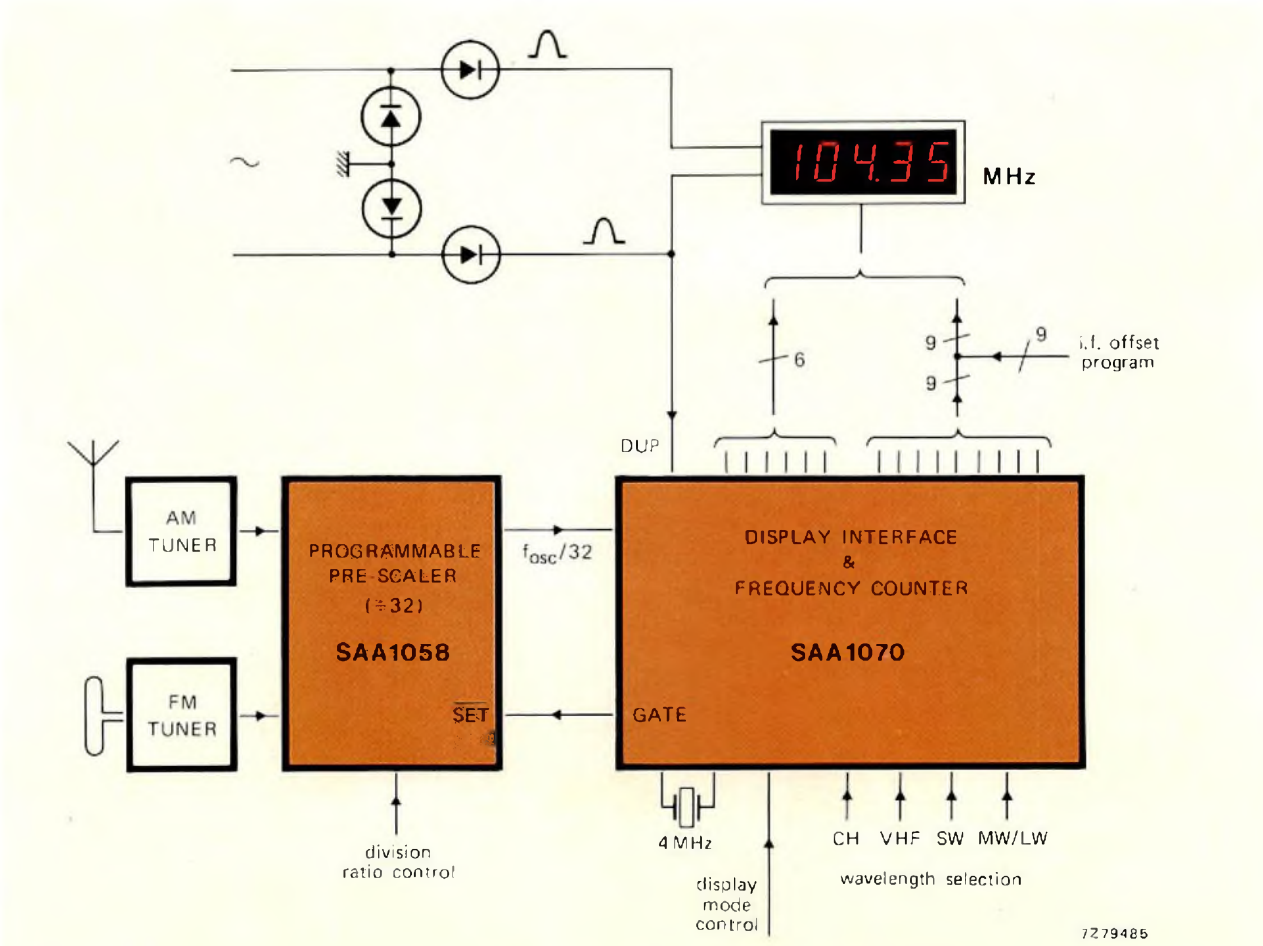

Fig.1 Block diagram of a digital frequency indicator

circuits. The high input sensitivity of 5 mV for a.m. and 10 mV for f.m. oscillator signals allows the system to be directly connected to the radio local oscillators without an amplifier interface.

The pre-scaler divides the local oscillator frequency by 32 and provides a square-wave output to the integrated frequency counter/display driver. The frequency is then measured by counting the number of negative-going transitions that occur during a period defined by a crystal-controlled pulse generator. The same pulse generator presets the pre-scaler at the start of each counting period to minimise indecisive counting and thereby reduce display flicker. Nine of the fifteen output pins of the SAA1070 are also used to program the system for use with the appropriate intermediate frequencies for s.w./m.w./l.w. and v.h.f.

Selection of wavelength and display mode (frequency/channel number/display test/display blanking) is effected by connecting one of four pins of the SAA1070 to the supply return line. Applying a mains-frequency half-sinewave to the DUP input of the circuit results in minimum interference radiation by synchronising the switching of the display segments with the zero crossing of the display drive voltage. The circuit is capable of directly driving the segments of the LED display so that discrete driver transistors are not required.

THE INTEGRATED CIRCUITS

Programmable Pre-scaler

The SAA1058 is a multi-stage divider with an externally selectable division ratio of 32:1 or 33:1. This facility allows the circuit to also be used in frequency synthesiser systems such as our microcomputer-controlled phase-locked-loop tuning system which requires the use of both ratios. In the system being described, only the 32:1 division ratio is used.

Figure 2 is a simplified functional block diagram of

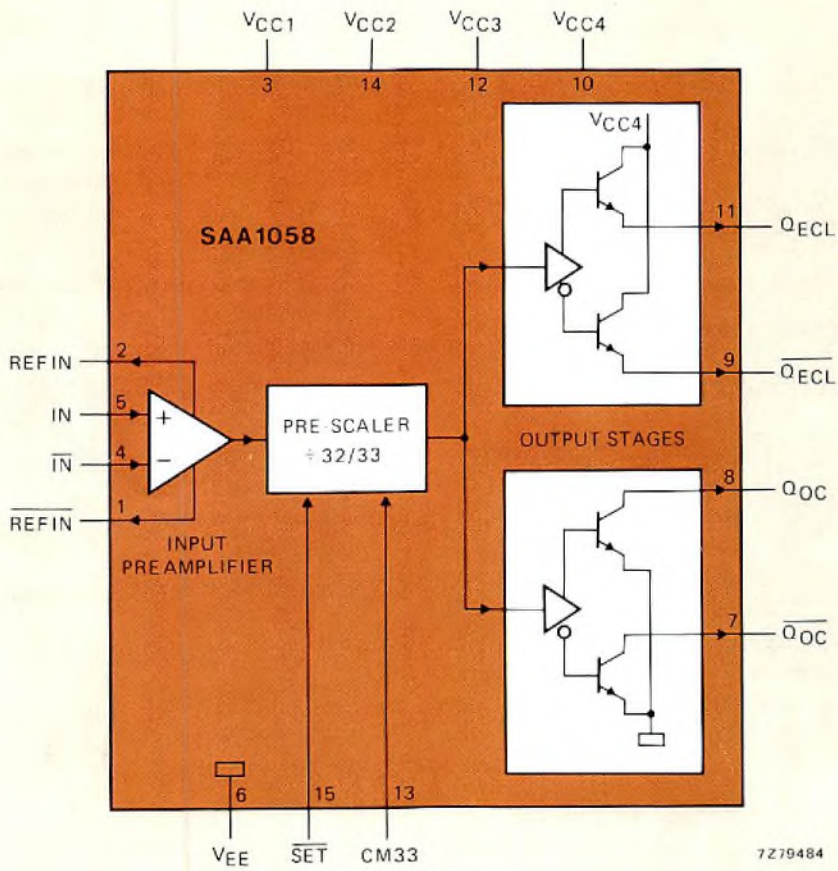

Fig.2 Block diagram of the programmable pre-scaler

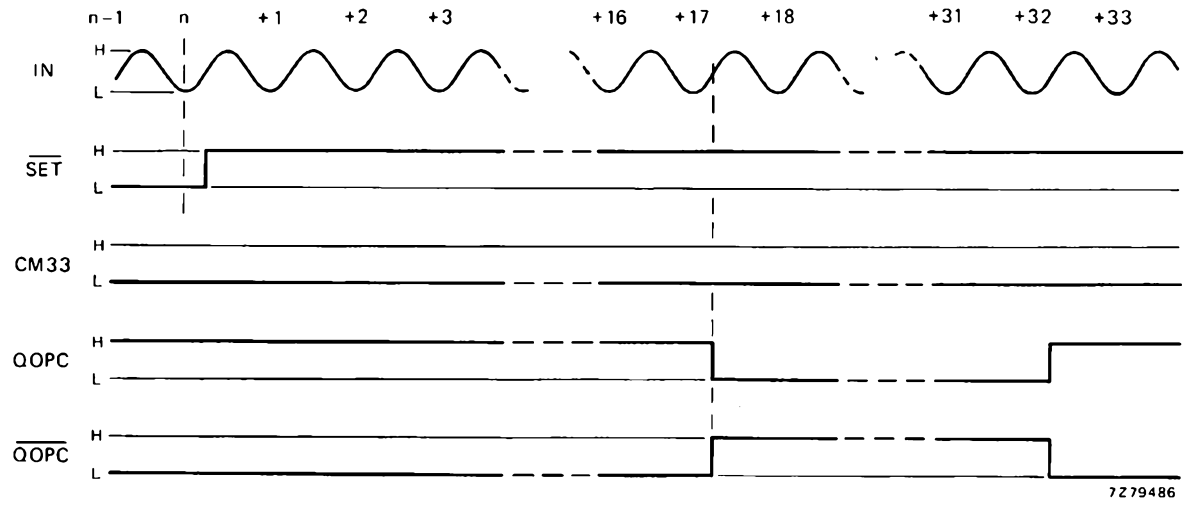

Fig.3 Timing diagram for the programmable pre-scaler

the pre-scaler. The preamplifier ensures a high input sensitivity so that the signals from the local oscillators in the radio can be connected to the system via a passive coupling network. The a.m. and f.m. local oscillators can be simultaneously connected to the symmetrical inputs of the preamplifier without an input filter or a switch, provided that the unused oscillator is switched off in the radio. The pre-scaler incorporates two symmetrical output preamplifiers, each of which drives a different kind of complementary output stage. The outputs are thus made compatible with ECL or MOS inputs and can drive circuits that react to either the falling or rising edges of the drive signal. Each of the four internal functional blocks has its own supply pin; pin 3 for V_{CC1} to the input preamplifier, pin 14 for V_{CC2} to the synchronising stage, pin 12 for V_{CC3} to the divider, and pin 10 for V_{CC4} to the output stages.

Figure 3 is the timing diagram for the pre-scaler. When input CM33 is set low, the division ratio is set to 32:1. If there is phase shift between the measuring period and the transitions at the pre-scaler output, the least significant digit of the display is likely to flicker. To prevent this, the first transition must ideally occur 17 input frequency periods after the start of each counting period. This synchronisation is achieved by applying a low-to-high transition, representing the start of the counting period, to the $\overline{SET}$ input of the pre-scaler.

Display interface and frequency counter

The integrated display interface and frquency counter (SAA1070) is specifically designed for the control of a duplex-driven seven-segment display of the frequency or v.h.f. channel number to which an a.m./f.m. radio is tuned. A simplified block diagram is given in Fig. 4. The main features of the circuit are:

- Output stages capable of directly driving a 4½ digit LED frequency/channel number display with LED lamp indication of kHz and MHz. To minimise the number of output pins, and to reduce radiated interference, the segment drive outputs are driven in duplex mode in synchronism with the zero crossing of the mains-derived supply connected to the display anodes.
- 18-bit frequency counter which can be preset to compensate for a wide range of externally programmed intermediate frequencies for the v.h.f., short-wave and medium-wave/long-wave bands.
- 16-bit comparator for comparing the measured and displayed frequencies and updating a 16-bit display register if there is a discrepancy for three successive measuring periods. This technique prevents display flicker due to short-term drift of the local oscillators in the radio.
- Seven-segment decoder and multiplexer for driving the output stages.
- Internal timing pulse generator controlled by a 4 MHz quartz crystal.
- A display 'freeze' facility which causes the result of the last frequency measurement to be continuously displayed.
- Display test and blanking facilities.

The functions of the display interface and frequency counter will be explained with the aid of the simplified block diagram given in Fig. 4.

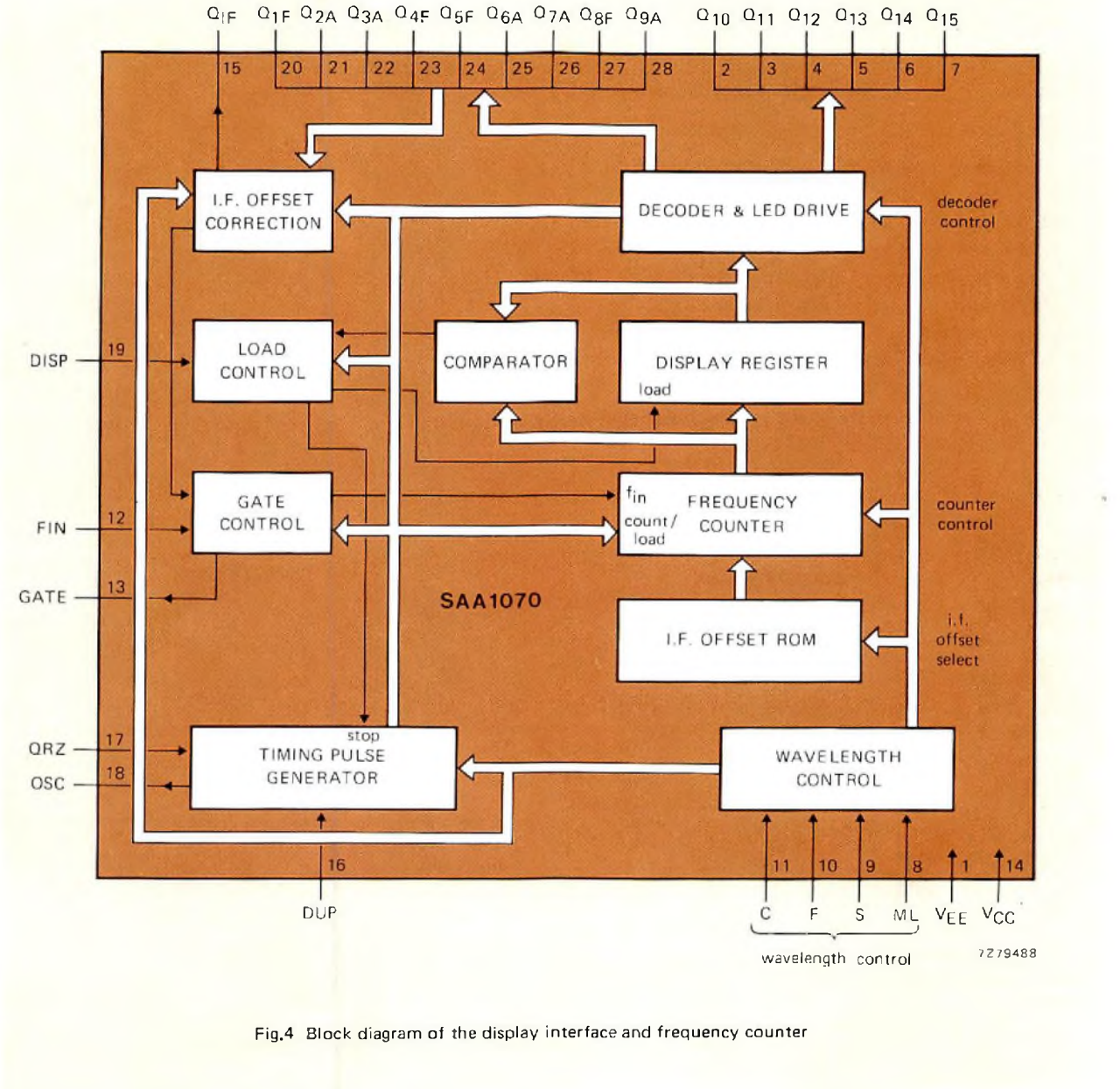

Fig.4 Block diagram of the display interface and frequency counter

After the radio local oscillator signal has been divided by 32 in the pre-scaler, it is fed to input FIN (pin 12). The counter then determines how many pulses have occurred during a measuring period defined by a pulse generator under the control of a 4 MHz quartz crystal connected between pins 17 and 18. Since the counter has been preset with a number corresponding to the i.f. of the radio, the pulse count is proportional to the frequency to which the radio is tuned. The result of the count is compared with the displayed frequency and, if there is a difference for three successive measuring periods, the display register is updated on occurrence of the next synchronising pulse (DUP) at pin 16.

Wavelength selection and i.f. offset

Before the SAA1070 is ready for operation, it must be set up for use in accordance with the operating conditions of the radio and of the display.

Pins 8, 9, 10 and 11 must be programmed in accordance with Table 1 to suit the waveband in use and, in the case of v.h.f., to determine whether the channel

number or the tuned frequency of the radio will be displayed. This program also determines the display resolution as given in Table 2 by presetting the 4 MHz crystal-controlled timing pulse generator to determine a measuring period of the following duration:

v.h.f. and channel no. 256 μs (1024 cycles of 4 MHz)

short-wave 2.56 ms (10 240 cycles of 4 MHz)

medium/long-wave 3.2 ms (12 800 cycles of 4 MHz)

The waveband program also addresses the i.f. offset ROM to preset the frequency counter to compensate for an intermediate frequency of 10.7 MHz for v.h.f. and 460 kHz for short/medium/long-waves. If the required intermediate frequencies differ from these values, the i.f. offset pulse generator must be preset by programming input/output pins 20 to 28 as shown in Tables 3 and 4. These pins change function from segment drive outputs to i.f. offset inputs for a short period coincident with the negative-going edge of the synchronising pulse applied to the DUP input at pin 16.

TABLE 1
Wavelength control inputs

selection	SAA1070 pin no.			
	8	9	10	11
v.h.f. frequency	1	1	0	1
v.h.f. channel	1	1	x	0
short-wave	1	0	1	x
medium/long-wave	0	1	1	x
display test	0	1	0	0
display blanked	x	0	0	x
	0	0	1	x
	0	1	0	1
	1	1	1	1

0 = common return or pin 1.
1 = not connected or connected to pin 14.
x = 0 or 1.

TABLE 2
Display resolution

waveband	resolution	equivalent number of transistors at input of SAA1070
v.h.f. frequency	0.05 MHz	4
v.h.f. channel*	0.1 MHz	8
short-wave	5 kHz	4
medium/long-wave	1 kHz	1

* One channel = 300 kHz
Channel 02 = 87.6 MHz.

TABLE 3
I.F. offset correction inputs for s.w./m.w./l.w.

SAA1070 input pin					i.f.	
21	22	25	26	28	s.w. (kHz)	m.w./l.w. (kHz)
0	0	0	0	0	460.00	460
0	0	0	1	0	448.75	449
1	0	0	1	0	450.00	450
0	1	0	1	0	451.25	451
1	1	0	1	0	452.50	452
0	0	1	1	0	453.75	453
1	0	1	1	0	455.00	454
0	1	1	1	0	456.25	455
1	1	1	1	0	457.50	456
0	0	0	0	1	456.25	457
1	0	0	0	1	457.50	458
0	1	0	0	1	458.75	459
1	1	0	0	1	460.00	460
0	0	1	0	1	461.25	461
1	0	1	0	1	462.50	462
0	1	1	0	1	463.75	463
1	1	1	0	1	465.00	464
0	0	0	1	1	463.75	465
1	0	0	1	1	465.00	466
0	1	0	1	1	466.25	467
1	1	0	1	1	467.50	468
0	0	1	1	1	468.75	469
1	0	1	1	1	470.00	470
0	1	1	1	1	471.25	471
1	1	1	1	1	472.50	472

0 = no connection.
1 = 22 kΩ resistor connected to 2.5 V (see Fig. 6).

Display testing and blanking

Pins 8, 9, 10 and 11 can also be programmed in accordance with Table 1 to either blank the display, or cause all the display segments to glow simultaneously for test purposes.

Synchronising pulse

The start of the frequency measuring and display switching sequence is synchronised with the negative-going edges of pulses applied to the DUP input at pin 16. If mains-derived antiphase half-sinewaves are used to power the LED display, it is convenient to use one of them as a synchronising pulse. This will ensure that radiated interference is reduced by effecting the decoded segment output switching at the instant when the mains waveform crosses zero.

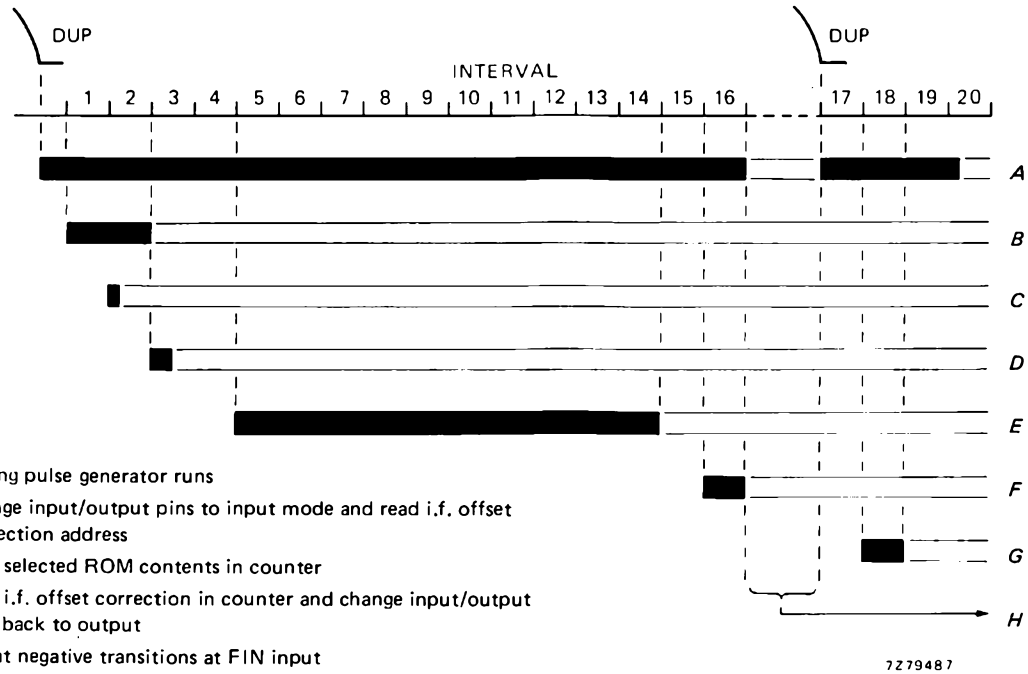

A timing pulse generator runs
B change input/output pins to input mode and read i.f. offset correction address
C load selected ROM contents in counter
D load i.f. offset correction in counter and change input/output pins back to output
E count negative transitions at FIN input
F compare register and counter contents
G load register with counter contents and change display
H halt and re-start timing if contents of register and counter differ for three consecutive measuring periods.

Fig.5 Timing diagram for the frequency measuring and display system

TABLE 4
I.F. offset correction inputs for v.h.f.

SAA1070 input pin				i.f. (MHz)
20	23	24	27	
0	0	0	0	10.70
1	0	0	0	10.60
0	1	0	0	10.6125
1	1	0	0	10.625
0	0	1	0	10.6375
1	0	1	0	10.65
0	1	1	0	10.6625
1	1	1	0	10.675
0	0	0	1	10.6875
1	0	0	1	10.70
0	1	0	1	10.7125
1	1	0	1	10.725
0	0	1	1	10.7375
1	0	1	1	10.75
0	1	1	1	10.7625
1	1	1	1	10.775

0 = no connection.
1 = 22 kΩ resistor connected to 2.5 V (see Fig. 6).

THE SIGNAL PROCESSING SEQUENCE

To clarify the signal processing sequence of the frequency measuring and display system, each of its twenty intervals will be described with the aid of Fig. 5. Each interval lasts for a period determined by the number of 4 MHz cycles demanded by the program at the wavelength control inputs of the SAA1070. The duration of each interval is given in Table 5. The timing sequence is started by the negative-going flank of the mains-derived half-sinewave synchronising pulse (DUP) applied to pin 16 of the SAA1070.

TABLE 5
Duration of timing intervals shown in Fig.5.

Interval	wavelength in use				
	v.h.f.	ch	s.w.	m.w./ l.w.	unit
1 to 3, 15 to 20	256	256	256	320	μs/interval
5 to 14	256	256	2560	3200	μs/interval
measuring period (GATE = high)	2.56	2.56	25.6	32.0	ms

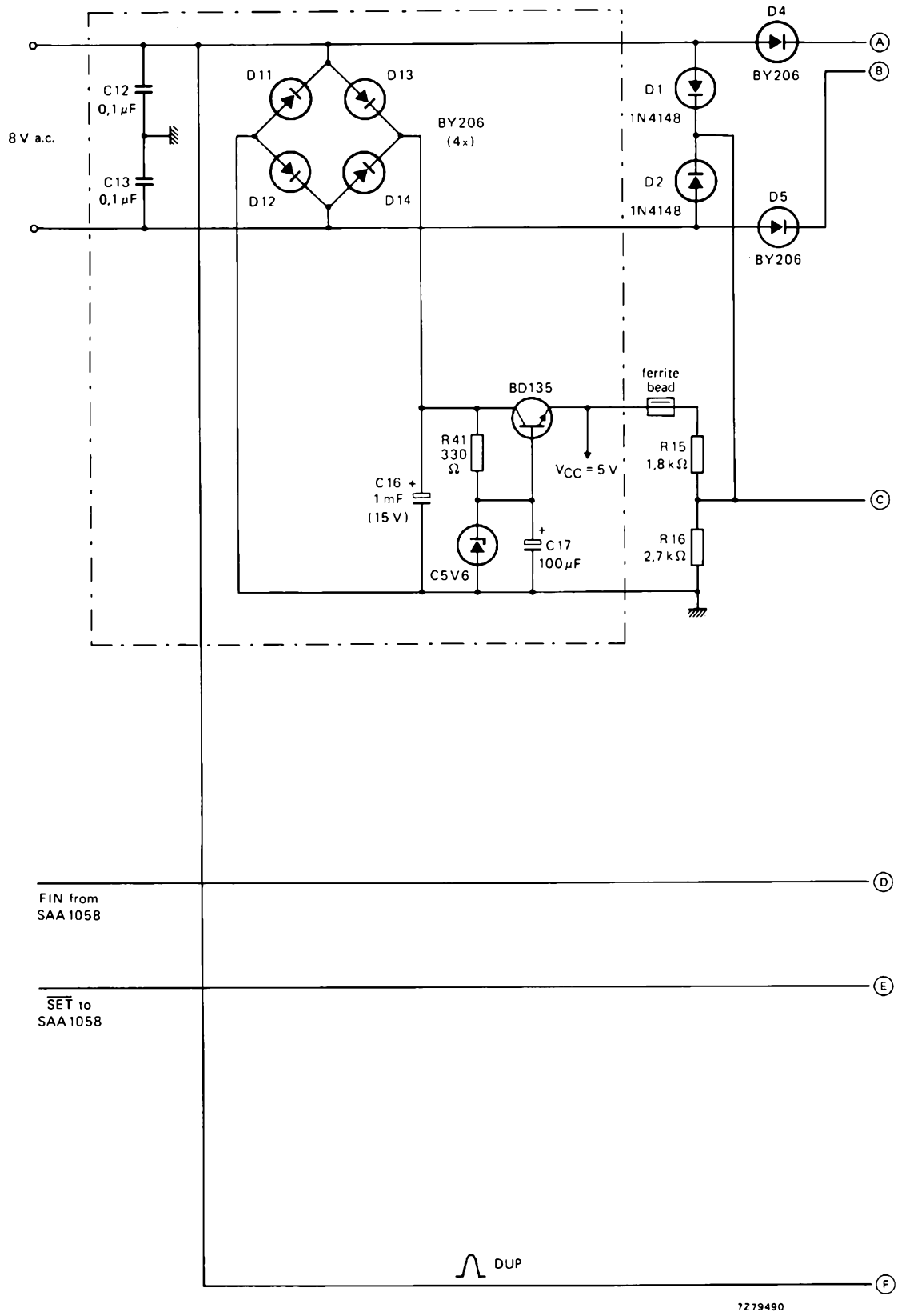

Fig.6(a) Display drive circuit for the frequency measurement system

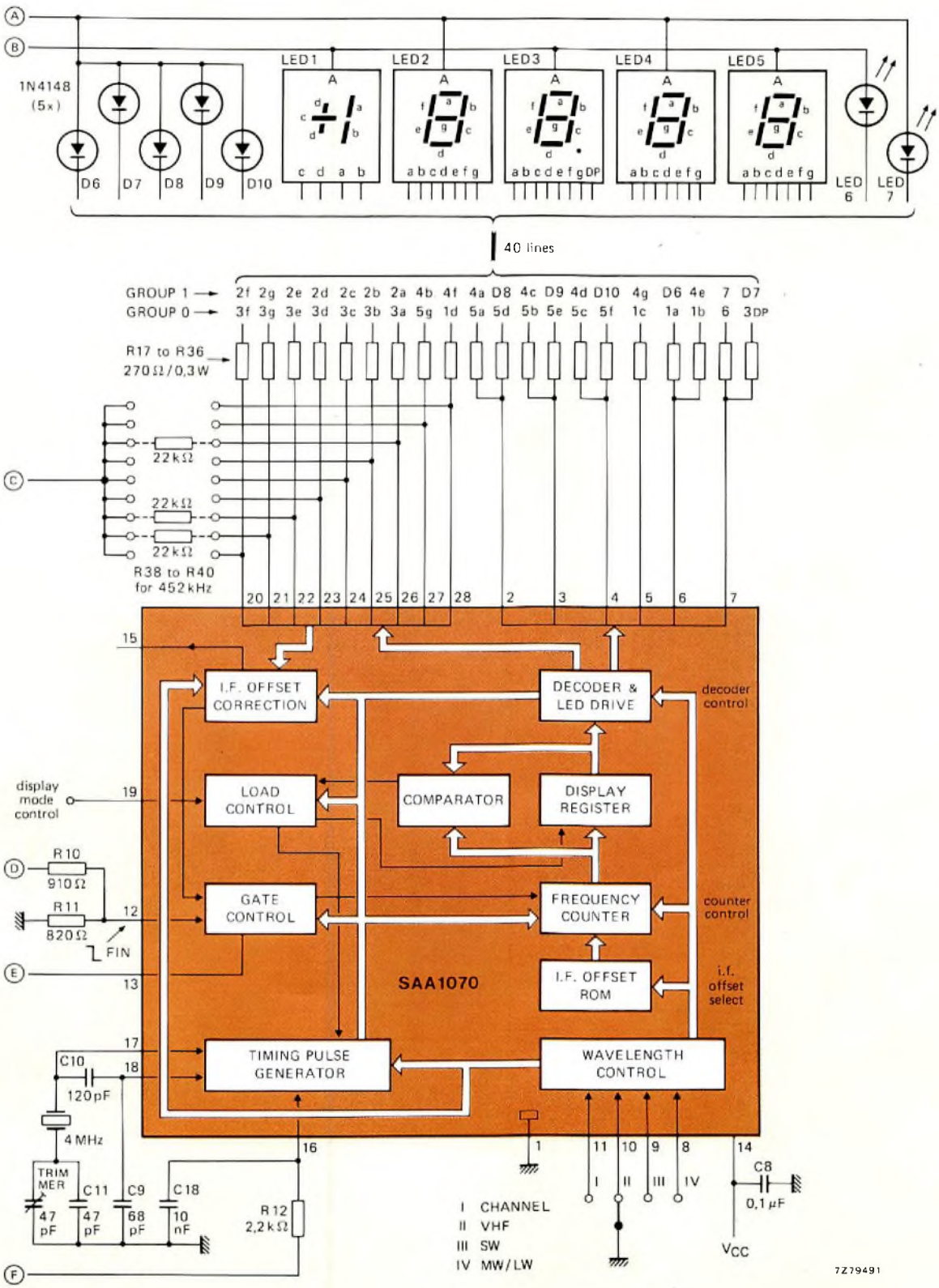
A
B
1N4148
(5x)
D6
D7
D8
D9
D10
LED1
LED2
LED3
LED4
LED5
LED 6
LED 7
c d a b
a b c d e f g
a b c d e f g DP
40 lines
GROUP 1
GROUP 0
2f 2g 2e 2d 2c 2b 2a 4b 4f 4a D8 4c D9 4d D10 4g D6 4e 7 D7
3f 3g 3e 3d 3c 3b 3a 5g 1d 5a 5d 5b 5e 5c 5f 1c 1a 1b 6 3DP
R17 to R36
270Ω/0,3W
22kΩ
22kΩ
22kΩ
R38 to R40
for 452kHz
20 21 22 23 24 25 26 27 28 2 3 4 5 6 7
15
I.F. OFFSET CORRECTION
DECODER & LED DRIVE
decoder control
display mode control
19
LOAD CONTROL
COMPARATOR
DISPLAY REGISTER
R10
910Ω
R11
820Ω
FIN
12
GATE CONTROL
FREQUENCY COUNTER
counter control
13
SAA1070
I.F. OFFSET ROM
i.f. offset select
17
18
C10
120pF
4MHz
TIMING PULSE GENERATOR
WAVELENGTH CONTROL
16
1
11 10 9 8
14
C8
0,1μF
TRIM MER
C11
C9
C18
47 pF
47 pF
68 pF
10 nF
R12
2,2kΩ
I CHANNEL
II VHF
III SW
IV MW/LW
I II III IV
Vcc
7Z79491

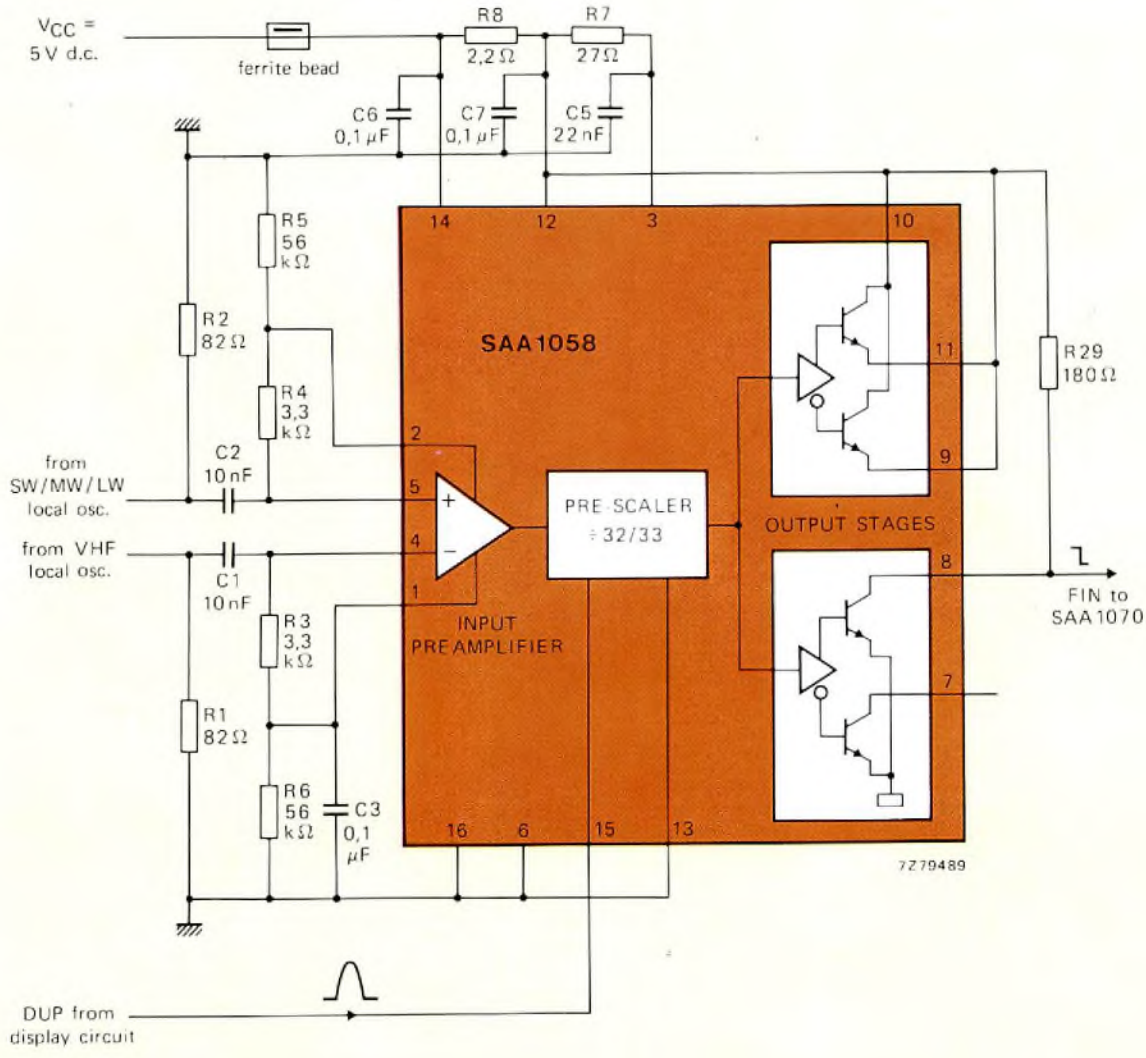

Fig.6(b) Pre-scaler circuit for the frequency measurement system

The timing sequence intervals and the events that occur during each of them are as follows:

Interval 1. Pins 20 to 28 of the frequency counter/display driver are switched over to functions as i.f. offset correction address inputs and the required address is stored in the offset correction circuit.

Interval 2. The i.f. offset ROM contents addressed by the wavelength selection circuit is loaded into the frequency counter.

Interval 3. The required number of i.f. compensation pulses are loaded into the frequency counter. Pins 20 to 28 of the SAA1070 are switched back to their function as display segment drive outputs,

Interval 4. The timing pulse generator is programmed by the waveband selection circuit to generate a measuring period of the appropriate duration.

Interval 5 to 14. At the end of interval 4, the GATE output from the SAA1070 goes high, thereby activating the SET input to the pre-scaler and initiating the output pulse train. These pulses enter the SAA1070 at the FIN input at pin 12. They are then passed through a measuring-period gate and loaded into the frequency counter. At the end of interval 14 the timing pulse generator inhibits further pulse counting by disabling the measuring-period gate.

Interval 16. During this interval, the 16 most significant bits from the 18-bit frequency counter are compared with the contents of the 16-bit display register. If there is a discrepancy, a 2-bit counter in the comparator is incremented by one. If the contents of the 2-bit counter are then less than 3, the sequence proceeds through intervals 17, 18 and 19 without further action. If the contents of the frequency counter and the display register are the same, the 2-bit counter is reset before the sequence proceeds through intervals 17, 18 and 19 without further action. If incrementing the 2-bit counter causes its contents to reach 3 (contents of frequency counter and display register different for three consecutive measuring periods), the timing pulse generator is stopped before the sequence proceeds to interval 17.

Interval 17. If the 2-bit counter has reached a count of 3, the system waits for the negative-going flank of the next half-sinewave to appear at the DUP synchronising input. The timing pulse generator is then re-started and the sequence proceeds to interval 18.

Interval 18. If the timing pulse generator was re-started in interval 17, the contents of the frequency counter are loaded into the display register and the display is thereby changed to the new value during the zero-crossing of the drive voltage.

Interval 19. This interval is free.

Interval 20. The timing pulse generator is stopped and the system waits for the negative-going flank of the next half-sinewave to appear at the DUP synchronising input of the SAA1070. The timing pulse generator is then re-started and the sequence recycles to interval 1.

DISPLAY OPTIONS

The previously described sequence of events applies only as long as the DISP pin (pin 19) of the SAA1070 remains disconnected. Pin 19 then becomes an output at which the i.f. offset correction pulses can be monitored. Pin 19 can be connected to change the mode of operation as follows.

Static display

If pin 19 is connected to the common rail, the sequence is halted at the end of interval 16 because the timing pulse generator is inhibited, the GATE output from the SAA1070 is continuously low and the pre-scaler is therefore held in the SET state. The displayed value is therefore 'frozen' at the least frequency to be measured.

Reduced display response time

If pin 19 is connected to the same supply voltage as pin 14 of the SAA1070, the displayed frequency is changed whenever there is a difference between the contents of the counter and the display register during interval 16, regardless of the contents of the 2-bit counter. In this mode of operation, the flicker reduction facility is lost but the response time of the system is reduced.

THE OVERALL CIRCUIT

In its simplest form, as shown in Fig. 6, the system provides an LED display of the frequency or v.h.f. channel number to which a mains-powered ratio is tuned. Only a single 8 V 50 Hz power supply is then required. The system can, however, be adapted for use with a battery supply of 11 V to 16 V if an additional drive pulse generator is used. Furthermore, other types of display can be accommodated if a more complex power supply and segment drive circuit are used.

Acknowledgement

Much of the information given in this article has been derived from 'Rundfunk-Frequenzmeszsystem mit den integrierten Schaltungen SAA1058 und SAA1070' published as Technische Informationen für die Industrie Nr. 781110 and distributed by Valvo G.m.b.H., Hamburg.

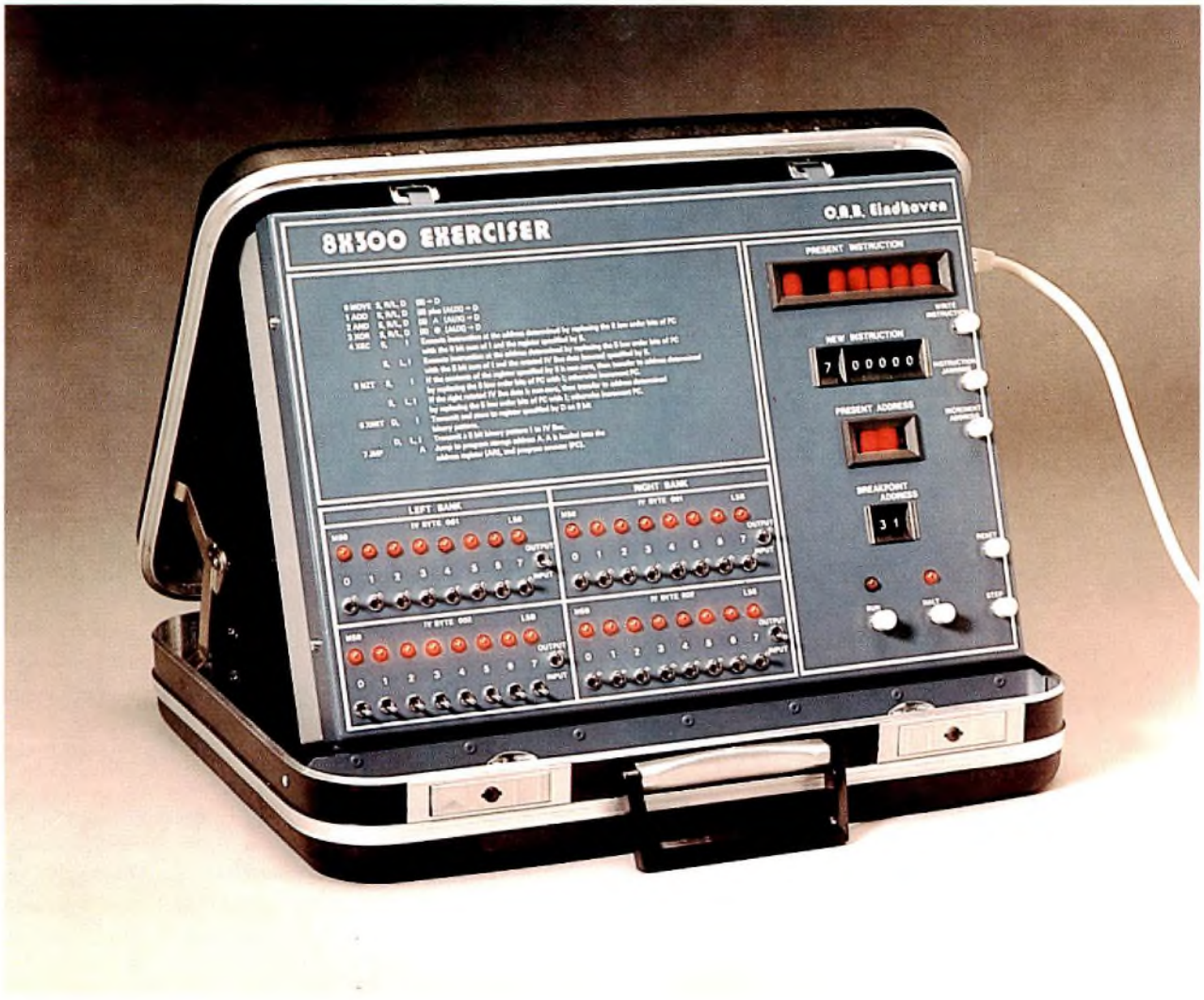
8X300 EXERCISER
PRESENT INSTRUCTION
NEW INSTRUCTION
PRESENT ADDRESS
BREAKPOINT ADDRESS
LEFT BANK
RIGHT BANK

The 8X300 - a high-speed control-oriented microprocessor

E. D. VAN VELDHUIZEN

The 8X300 is a bipolar microprocessor designed for high-speed control application. As the first of a series to be devoted to its applications and support facilities, this article describes the 8X300 architecture and instruction set, paying particular attention to the special I/O system which permits data input, processing, and output within a single 250 ns cycle.

Microprocessors represent the latest step in the evolution of semiconductor technology. In but a few years, the microprocessor has been developed from a slow and simple general purpose device to a wide range of specialised devices. Each application area demands different characteristics, the total of which cannot be supplied by a single device. The fabrication process determines basic characteristics such as speed, power consumption, function density, etc. Bipolar processes allow the construction of high-speed devices at the cost of increased power consumption.

Further divisions in the microprocessor range spring from the internal architecture and instruction set. The 8X300 is a good example: its architecture and instruction set are designed to provide a high data throughput with bit-oriented, rather than word-oriented operations. A bipolar process is used to provide a high data throughput rate and a short cycle time.

CONTROL ENVIRONMENT

The 8X300 is designed for real-time control applications. Typically, this entails such tasks as regular examination of statuses within the system being controlled, monitoring system functions and issuing commands, words, and data to direct the actions of the system. Thus, the microprocessor must be able to select and test individual bits or groups of bits, make calculations and decisions based upon the selected data, and issue appropriate commands to the system. In some applications, high data transfer rates or critical timing so restrict the time available for calculations and decision-making that only a high speed microprocessor will do. The ability of the 8X300 to accept input data, process it, and output new data, all in a cycle time of only 250 ns, makes it particularly suitable for such demanding applications as:

- communication controllers
- data concentrators
- multi-terminal controllers
- magnetic disk controllers
- digital image processing
- high speed industrial control
- I/O control of large memory systems.

8X300 ARCHITECTURE

Figure 1 shows the architecture of the 8X300. The broad lines indicate the various possible paths along which data flows, according to the current instruction. The device uses three separate buses: the interface vector (IV) bus for data input and output; the instruction address bus to the program memory, and the instruction data bus for delivery of the program instructions. (The IV bus is further described under the heading *I/O concept.*)

The instruction address bus is driven from the address

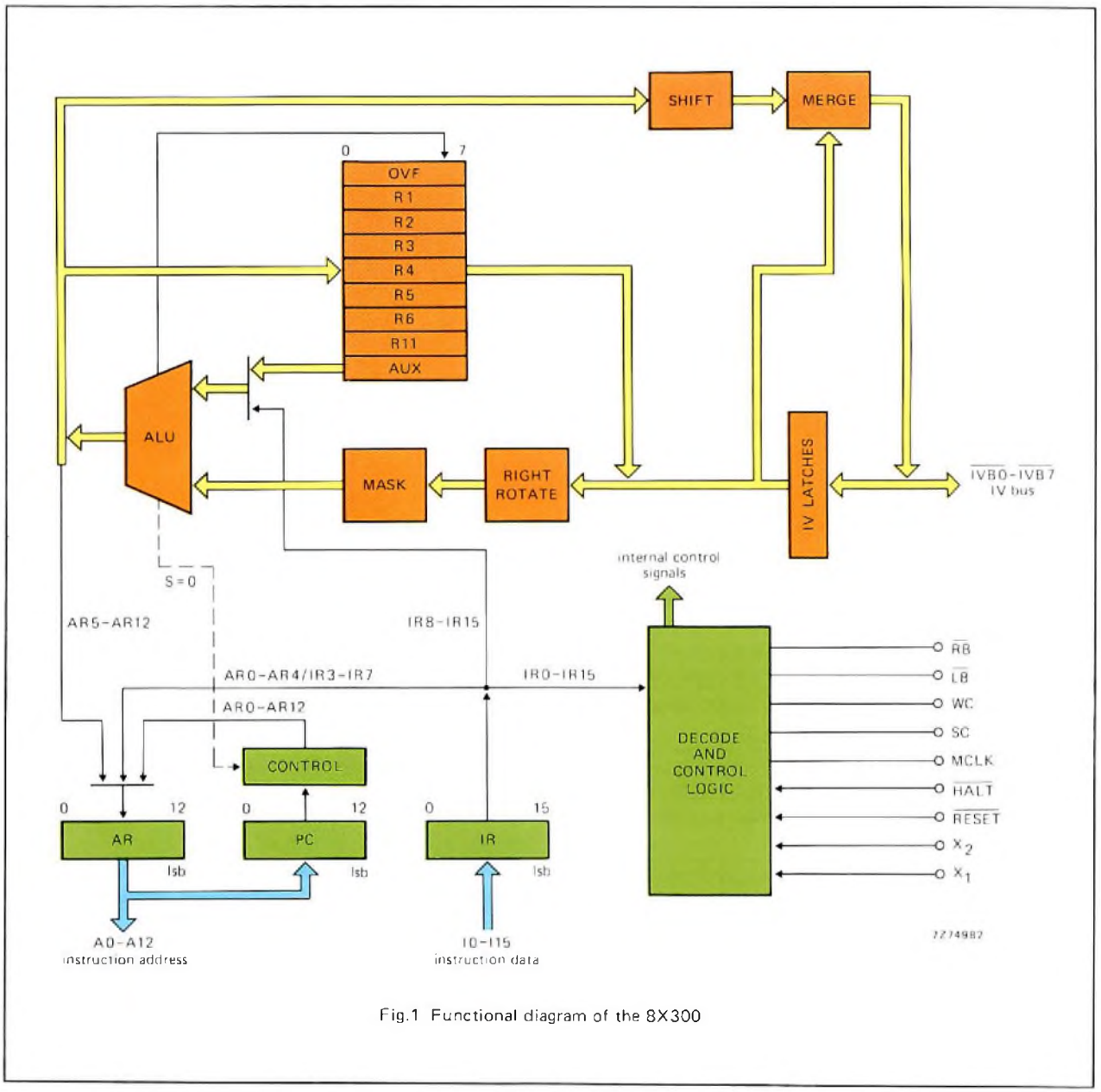

Fig.1 Functional diagram of the 8X300

register, which holds the address of the current or next instruction to be fetched from memory. Both bus and register have 13 bits, giving an addressing range of 8192 locations. The program counter is also driven from the address register. It is used as a temporary store for the current instruction address to allow modification by the control circuitry to generate the next instruction address. Unless influenced by an instruction causing a jump, the instruction address is automatically incremented by one during each cycle.

The instruction addressed in the program memory is passed via the instruction bus to the instruction register. An 8X300 instruction is 16 bits long. The decode and control logic provides the internal and external control signals required by the current instruction and the cycle timing. Note that parts of the instruction word can be passed to the data path or the instruction address register, allowing the programmer a direct influence on data or address. Further inputs to the decode and control logic are:

$X1, X_2$ connections for the crystal to determine the cycle time;

$\overline{\text{HALT}}$ a signal generated within the system to delay processing for reasons defined by the system designer;

$\overline{\text{RESET}}$ to reset the microprocessor.

Five outputs are provided for I/O control.

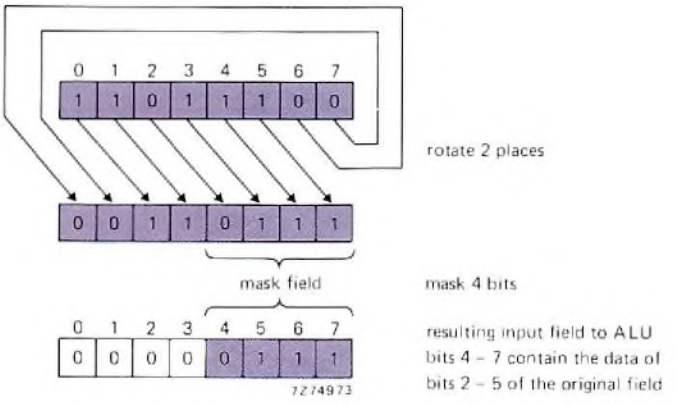

Fig.2 Effect of the right-rotate and mask functions

Data path

Sources of data for processing are: the nine internal registers, the IV bus input latches and instruction data. The internal registers comprise an overflow register, seven general purpose registers (R_1 to R_6 and R_{11}) and an auxiliary register. The overflow register contains all zeros except for bit 7 which is set if overflow occurs during an ADD instruction. The overflow register can only act as the source of data, not the destination. The general purpose registers are each 8 bits wide and can be either the source or destination of data. The auxiliary (AUX) register is somewhat special in that it is used as an implied operand by ADD, AND and XOR instructions. This is indicated by its direct connection to the arithmetic and logic unit (ALU). The AUX register can be treated as a general purpose register although it may not be specified as the source operand when it is also an implied operand. The IV bus input latches are loaded at the beginning of a cycle with the data on the IV bus, when this is specified as the data source. The data in the input latches is available, via the merge function, for whole or partial output to the IV bus.

Data from the IV latches or registers can be pre-formatted by the right-rotate and mask functions before processing in the ALU. The right-rotate function provides an end-around-shift of up to seven places, while the mask function allows selection of only a part of the data byte. The mask function cannot be specified when the data source is a register. Figure 2 shows a typical effect of the rotate and mask functions.

The ALU performs the tasks of addition, logic functions (AND and exclusive-OR), zero testing and some address modification. For addition and logic functions, the operation is performed on the data from the specified source together with the contents of the AUX register. Depending on the instruction, up to eight bits of data can be passed from the instruction register to the ALU. The output of the ALU can be directed to the AUX or general purpose registers, or, via the shift and merge functions, to the IV bus. For non-zero transfer (NZT), execute (XEC) and jump (JMP) instructions, the output of the ALU is passed to the address register.

The shift and merge functions allow selection and repositioning of part of the ALU output before merging this with the existing data in the input latches and presenting the modified data on the IV bus. Figure 3 illustrates a typical shift and merge action. During a left shift, any data passing bit position 0 is lost. After left shifting until the original bit 7 (LSB) is aligned with the specified position, the required number of bits are merged with the data from the input latches.

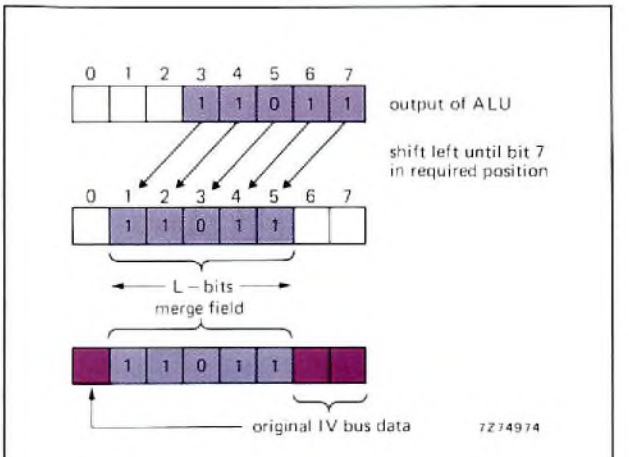

Fig.3 Effect of the shift and merge functions

I/O CONCEPT

The 8X300 uses the IV bus for all data input/output. This is an 8-bit, bidirectional bus that transports both data and the I/O port address. The eight bits of the IV bus are capable of addressing up to 256 latched I/O ports, known as IV bytes in the 8X300 system. The IV bytes are grouped into two sections, known as the left bank and the right bank, by means of two bank enable signals. Use of the left and right bank signals enables the device to address up to 512 IV bytes. These typically take the form of I/O ports or working storage locations. Figure 4 shows a configuration where the I/O ports are all left bank IV bytes and a 256 x 8 RAM forms the IV bytes on the right bank. The size of the working storage is thus limited to 256 bytes per bank. However, this can be increased to 256^2 (65 536) by using two I/O ports as an address buffer. This requires a few extra instructions but, due to the high execution speed of the 8X300, the system performance is rarely degraded.

Control signals are used to specify the instantaneous function of the IV bus:

SC — Select Command: a high level indicates that the data on the IV bus is an address. A low level indicates the presence of data.

WC — Write Command: a high level indicates that data is being output to the bus; a low level indicates data being input to the 8X300.

MCLK — Master Clock: used as a strobe for output data and to provide synchronisation for external logic.

$\overline{LB}$ — $\overline{\text{Left Bank}}$: a low level enables IV bytes on the left bank.

$\overline{RB}$ — $\overline{\text{Right Bank}}$: a low level enables IV bytes on the right bank.

When the 8X300 is required to accept data from or transmit it to a particular IV byte, it must first enable that byte. This is done by an instruction presenting the IV byte address on the IV bus with the SC signal and appropriate bank enable signal. All other IV bytes on that bank will become disabled. The selected IV byte will remain enabled until another IV byte on the same bank is enabled.

The signals $\overline{LB}$ and $\overline{RB}$ are complementary and although they provide the effect of a ninth address bit, their function differs in that they can be changed during the data I/O instruction cycle (the addresses are specified in previous instructions). This means that it is possible to have two IV bytes enabled at the same time, and select one or the other by using the left or right bank signals. In this way, data can be input from an IV byte on one bank, processed and output to another IV byte on the other bank in one instruction.

Clearly, the IV bus system requires special addressable I/O ports to perform the IV byte function. These I/O ports could be designed using separate address decoders and latches. Instead, dedicated IV bytes have been designed which combine both these functions in a single device, resulting in a more efficient and compact system.

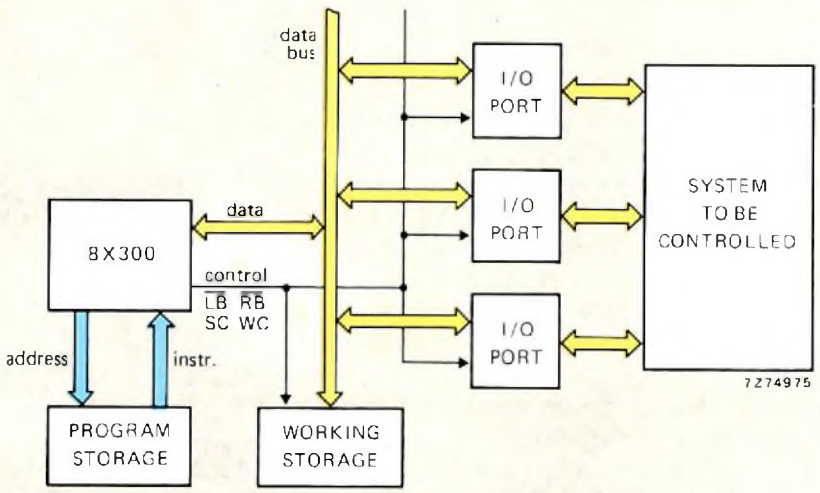

Fig.4 Typical 8X300 system configuration

Figure 5 shows the block diagram of the 8T32, a bi-directional latched I/O port designed to work as an addressable IV byte. The IV byte address can be programmed by the user, or the device can be supplied with a pre-programmed address. The data latches are accessible from either the IV bus or the user's bus. The only constraint upon access to the latches is that data cannot be written in from the IV bus and the user's bus simultaneously. In this case, the user's port has priority.

The control logic holds the port to the IV bus inactive until the address comparator detects its own address and SC signal. The user's port is accessible at all times under control of the signals $\overline{BIC}$ and $\overline{BOC}$. The user system must set $\overline{BIC}$ low when writing to the IV byte, and $\overline{BOC}$ low when reading from the IV byte. The IV byte can be designated as left or right bank by connecting the appropriate bank select signal to the $\overline{ME}$ (Master Enable) input.

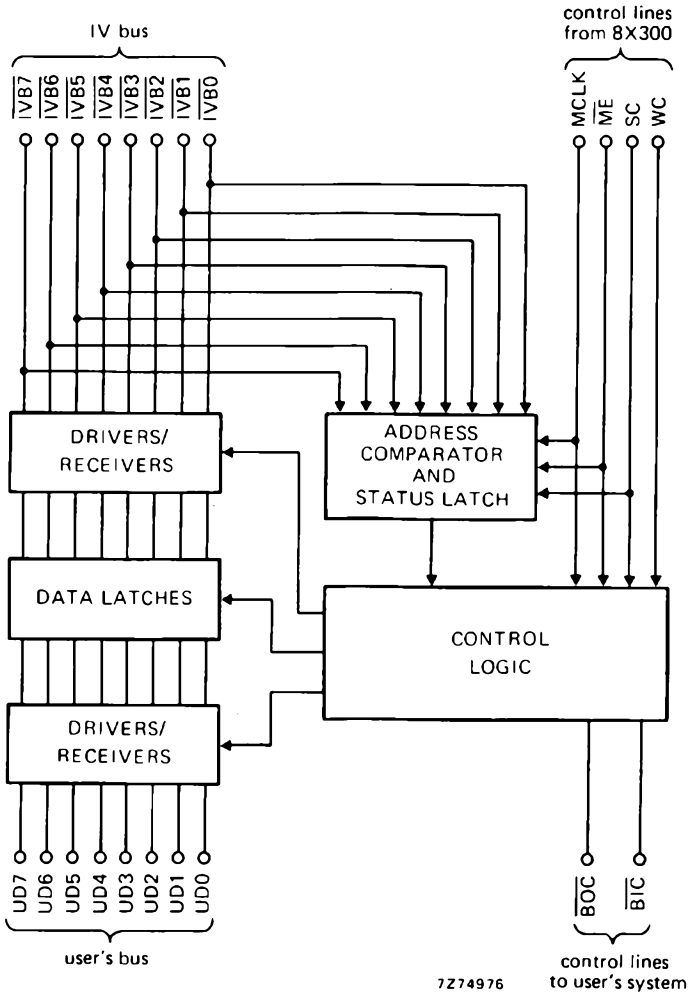

Fig.5 Block diagram of the 8T32 series of addressable bidirectional latches (IV bytes)

INSTRUCTION SET

The 8X300 uses a 16-bit instruction format as shown in Fig. 6. The first three bits are used to define the operation code (OP code), allowing eight broad classes of instruction. The repertory of 32 different instructions is obtained by the widely varying operand specifications.

The operand fields are used to define the data source and destination, the selection of part of an input data word, constants and addresses. Table 1 shows the operands that must be specified for the different instruction classes, the OP codes and a brief explanation of the instruction operation. Each class is identified by a mnemonic. The operand fields are Source (S), Destination (D), Rotate (R), Length (L), Integer constant (I) and Address (A).

TABLE 1
Operand specification per instruction class

OP code	Mnemonic	Operand fields used	Effect
0	MOVE	S, R or L, D	(S) → D
1	ADD	S, R or L, D	(S) plus (AUX) → D
2	AND	S, R or L, D	(S) · (AUX) → D
3	XOR	S, R or L, D	(S) ⊕ (AUX) → D
4	XEC	S, L, I; or, S,I	Execute the instruction at the current address offset by (S) and I.
5	NZT	S, L, I; or, S,I	If (S) ≠ 0, jump to the current address offset by I.
6	XMIT	D, L, I; or, D, I	Transmit the constant I to the destination D.
7	JMP	A	Change contents of program counter to value A, and continue processing at that address.

Operand fields

Source is a 5-bit field that identifies the location of the data which is to be processed. It is divided into two parts S_1 and S_0, of 2 and 3 bits respectively. The source field can thus be specified as an octal number in the range 00 to 37. Table 2 shows the allocation of the source codes to the various source locations: internal registers, left bank IV bytes and right bank IV bytes. IV bytes are identified by the codes 2n and 3n (left and right banks) where n, in the range 0 to 7, specifies the least significant bit of the data from the IV bus. When the source is an internal register, a separate Rotate field is used.

TABLE 2
Coding for source and destination fields

Octal code	Source/ destination	
00	AUX register	
01 to 06	work registers 1 to 6	
07	left bank address register (destination only)	
10	overflow register (source only)	
11	work register R11	
17	right bank address register (destination only)	
2n	left bank IV byte	n specifies the least significant bit of the IV bus data.
3n	right bank IV byte	

Destination is a 5-bit field identifying the location to which the processed data is to be sent. It is divided into parts D_1 and D_0 in the same way as the source field, and the address coding of Table 2 applies except that the overflow register cannot be used. For left and right bank addresses (2n and 3n) n specifies the least significant bit of the data to be output to the IV bus.

Rotate is a 3-bit field specifying the number of places the source data from an internal register is to be right-rotated.

Length is a 3-bit field specifying the number of bits from the IV bus data to be processed by masking or merging operations.

Integer is a 5 or 8-bit field used to introduce constants in the range 0 to 37_8 or 0 to 377_8.

Address is a 13-bit field used to specify the absolute address of the next instruction to be executed.

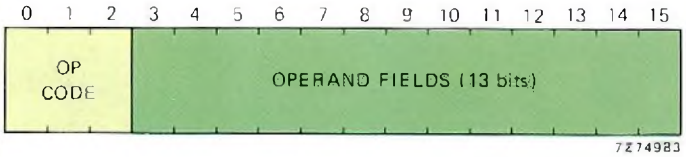

Fig.6 General instruction format for the 8X300

Examples of instruction

Example 1. To add the contents of bits 4 to 7 of the IV byte at the left bank to the contents of the AUX register and move the least significant 4 bits of the sum to the most significant 4 bits of the IV byte at the left bank.

Instruction word

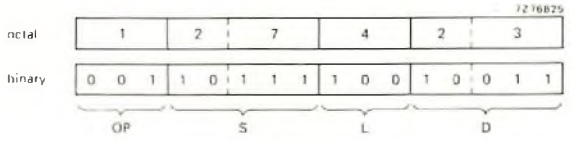

Instruction operation

0 1 1 0 0 1 1 0	IV bus data to input latches
0 1 1 0 0 1 1 0	no right rotate (S_0 = 7)
0 0 0 0 0 1 1 0	mask 4 bits (L = 4)
0 0 1 1 0 0 1 0	contents of AUX
0 0 1 1 1 0 0 0	sum
1 0 0 0	shift left 4 places (D_0 = 3)
1 0 0 0 0 1 1 0	merge with input data and output to IV bus
original values	

Data flow

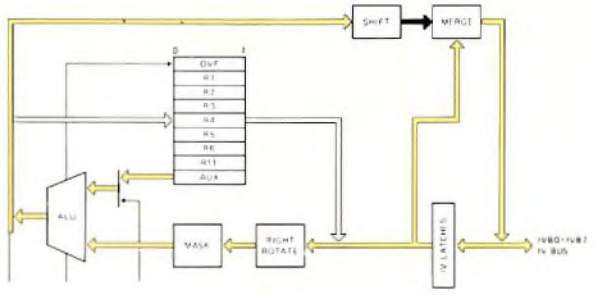

Results

The 4 most significant bits of the IV byte are changed to the values given by the sum of the 4 least significant bits and the contents of the AUX register. The overflow indicator is set to 0.

Example 2. Store the one's complement of the contents of R5 in the IV byte at the right bank. (It is assumed that the AUX register already contains all ones.)

Instruction word

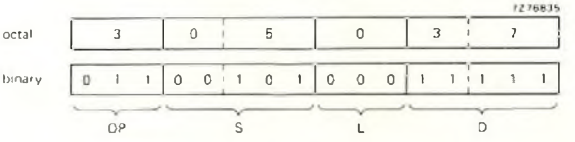

Instruction operation

0 1 1 0 0 1 1 1	copy source register
1 1 1 1 1 1 1 1	contents of AUX
1 0 0 1 1 0 0 0	results of XOR
1 0 0 1 1 0 0 0	no shift (D_0 = 7)
1 0 0 1 1 0 0 0	data to IV bus

Data flow

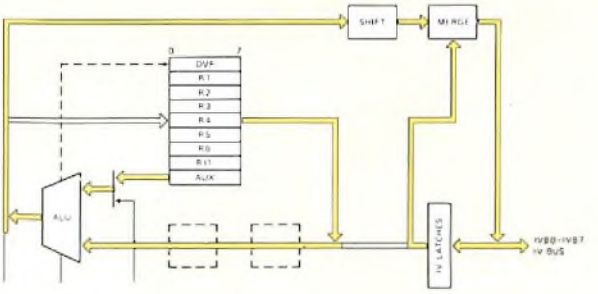

Result

The one's complement of the source register is output to the right bank of the IV bus.

Example 3. Enable the IV byte at the left bank whose address is 468.

Instruction word

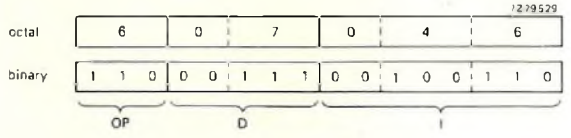

Instruction operation

value of I field (278)	0 0 1 0 0 1 1 0
new I/O address at left bank	0 0 1 0 0 1 1 0

Data flow

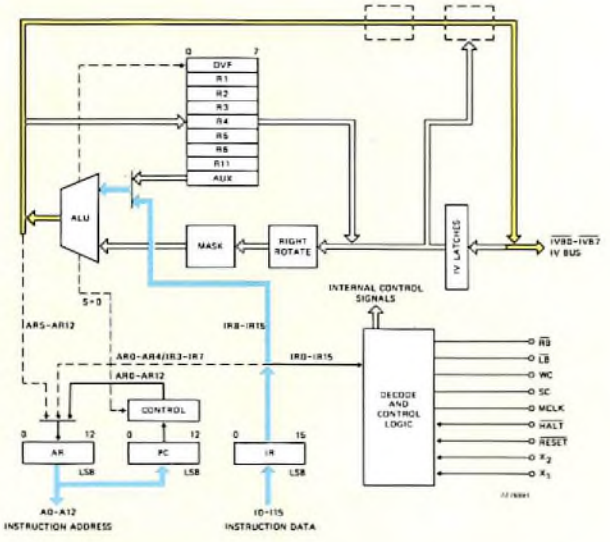

Result

The previously enabled IV byte at the left bank is disabled and the byte at address 468 at the left bank is enabled. The right bank is not affected.

The examples show that, by specifying the least significant bit and the number of bits (length), any group of contiguous bits from an IV byte can be used as source or destination. This is an extremely important feature of the 8X300 which makes it a powerful device in control applications.

TIMING

The timing of the 8X300 is controlled by a crystal oscillator circuit, of which all but the quartz crystal is on the chip. For the minimum cycle time of 250 ns, the crystal frequency must be 8 MHz. Figure 7 shows the instruction cycle divided into four phases. During the first quarter cycle, the instruction word is accepted by the instruction register and the data input latches are enabled to accept data on the IV bus. As processing takes place during the second and third quarter cycles, the input data must be stable by the start of the second quarter cycle. The address for the next instruction becomes available during the third quarter cycle, enabling access to the program memory for the ensuing instruction during the third and fourth quarter cycles. If data is to be output on the IV bus, output drivers are activated during the third quarter cycle to present stable output data during the fourth quarter cycle. Thus, the IV bus works in the input mode during the first two quarter cycles and in the output mode during the last two quarter cycles.

The value of the 8X300's high speed and its ability to perform both an input and an output function within one cycle is illustrated by Fig.8, where a sequence of three instructions addresses an I/O device, adds data from that device to a running total and stores the new total in a register at the right bank. The whole task of addressing I/O device and external register, and adding and storing the data is performed in only 750 ns.

SYSTEM SUPPORT

All microprocessor systems consist of two fundamental parts: the hardware and the software. In general, the software can be written, but not tested until the hardware is complete. With software stored in PROM, small changes and corrections are a lengthy task. Moreover, the hardware cannot be thoroughly tested until the software is complete, further aggravating the problem of software development. Development aids can alleviate these difficulties.

The 8X300 Development and Monitoring System (DMS) has been designed to facilitate speedy and economical development of 8X300 based systems. It provides useful services during both hardware and software development and allows the programmer to use assembly language in place of machine code. The user can store his program in RAM, so that PROMs need not be programmed until the software is fully proven, and changes can be made as they are required. A detailed description of the 8X300 DMS will appear in a later edition of E.C.&A.

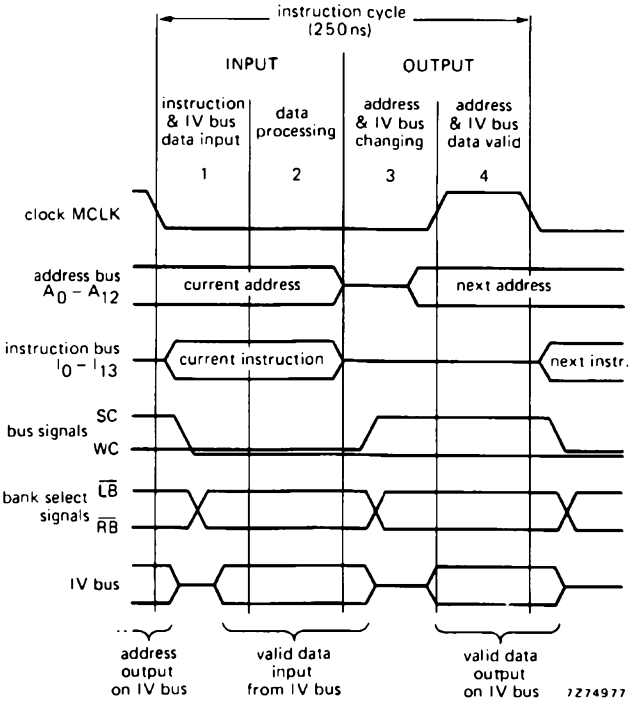

Fig.7 Timing diagram of the 8X300

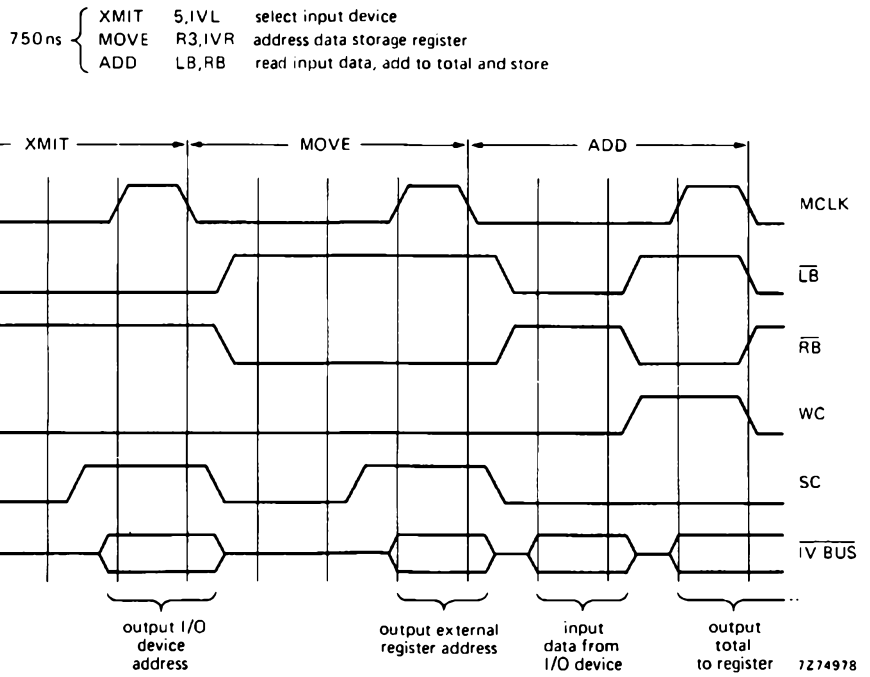

Fig.8 Instruction sequence to read data from an I/O device, add it to a running total and store the result in an external register. Note that data input and output are performed within one instruction cycle

A comprehensive 8X300 system design manual is available, providing information on all facets of 8X300 systems and their components. The photograph on page 90 shows the 8X300 exerciser, a device upon which the novice programmer can become familiar with the instruction set and I/O concept.

TYPICAL APPLICATIONS OF THE 8X300

Bubble memory controller

Magnetic bubble memories provide a compact, non-volatile, solid-state data storage system. However, bubble memory devices cannot be used without a considerable amount of control circuitry to perform such tasks as:

- data formatting
- rotating field control
- major/minor loop control
- redundant loop control
- read and write timing.

The cycle time of the rotating field is typically only 10 μs, within which period many actions must be performed, often with critical timing. A suitable controller could be designed from discrete logic or in a custom LSI chip. However, both these approaches are expensive, and the discrete logic approach results in a bulky controller. The 8X300 is ideally suited to this sort of application: its 250 ns cycle time allows execution of 40 instructions for each cycle of the rotating field. Moreover, its instruction set is tailored for the high-speed, flexible data manipulation that is required here. Figure 9 shows the block diagram of a bubble memory system, using the 8X300 as the controller. For evaluation purposes, the microcomputer was programmed to operate the system as an intelligent typewriter with the bubble memory as main storage. The 8X300 has ample processing power and speed for such an application.

Text reader

Figure 10 shows the block diagram of a system to recognise printed character patterns. The printed characters are transported past a row of photo-cells which provide an 8-bit word corresponding to the presence of blank paper or ink adjacent to a photo-cell. The character is thus read in a number of columns of 8 bits.

The patterns of all valid characters are stored in memory (e.g. working storage 1) and the 8X300 compares the photo-cell input with these patterns. Obviously the likelihood of the photo-cell output corresponding exactly with one of the stored patterns is not very great: the microcomputer must thus search for the pattern that is closest, by comparing each of the columns representing a character with those of the stored patterns. This comparison entails considerable processing and thus a microcomputer with the speed of the 8X300 is required to maintain a reasonable reading rate.

Disk controller

A magnetic disk controller is another example of the suitability of the 8X300 to high-speed control systems. Typical tasks are:

- track and sector control,
- sector identification,
- preamble and postamble processing,
- error recovery.

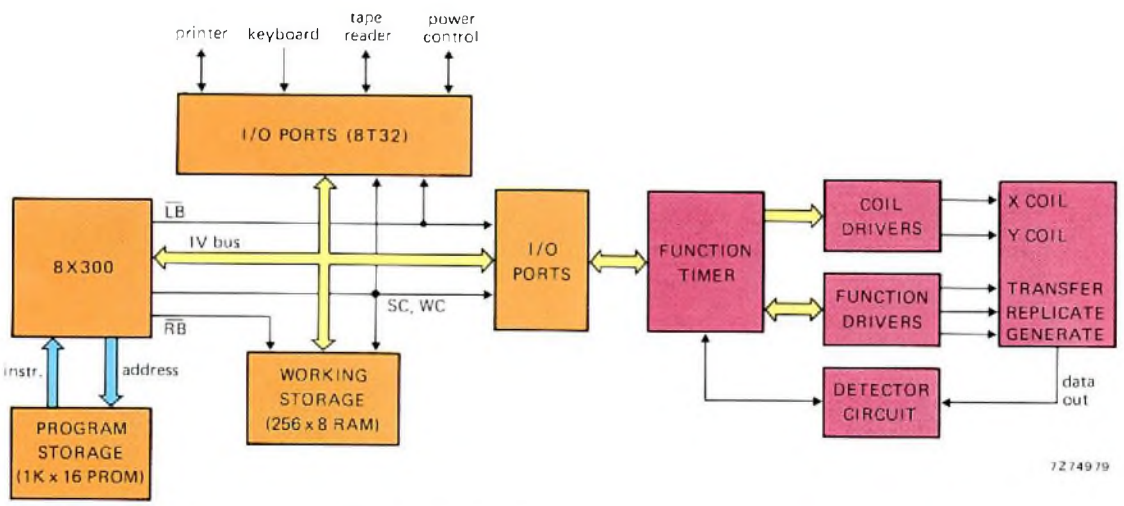

Fig.9 Block diagram of bubble memory controller system

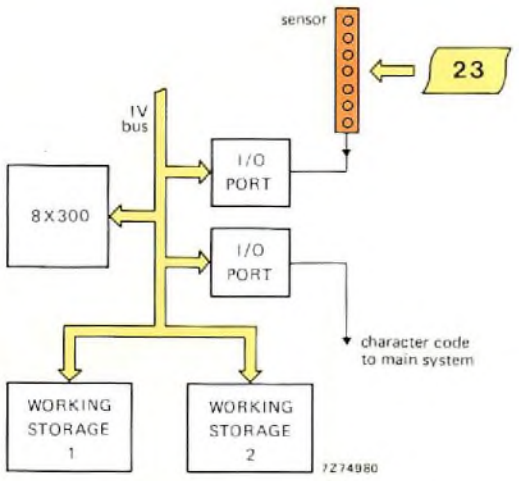

Fig.10 Block diagram of text recognition system

The high speed of the 8X300 and the efficiency of its data I/O functions mean that its use can result in a compact and economic design for a disk controller. Details of such a design will appear in a later issue of E.C.&A.

Interface between CAMAC and PDV bus

CAMAC, Computer Application for Measurement And Control (Ref. 1), is a parallel data handling system common in Europe. The PDV bus, Prozesslenkung mit Daten Verarbeitungsanlagen (Ref. 2), is a bit-serial data transmission system for process control. Both systems are designed for similar applications and environments; clearly, an interface between the two will extend the capabilities of either. Such an interface, using the 8X300, is described in Ref. 3.

One of the most important features of such an interface is its ability to pass data/messages from one bus system to the other with a minimum of delay. This delay is dependent on the cycle time of the microprocessor and the suitability of its instruction set to the tasks that must be performed. The 250 ns cycle time and bit-oriented instruction set of the 8X300 mean that many tasks otherwise accomplished by hardware can be accomplished by software without degrading the performance of the interface. The suitability of the 8X300 system is also reflected in the I/O concept and the design of the addressable IV bytes. These provide a flexible and compact set of I/O ports connecting both bus systems. Figure 11 shows a block diagram of such an interface.

REFERENCES

1. Commission of the European Communities, CAMAC – a modular system for data handling, EUR 4100E, Luxembourg, August 1972; IEC Recommendation 516.
2. PDV-Arbeitskreis TP30, KFK-PDV70 Serielles Bussystem für industrielle Anwendung unter Echtzeitbedingungen (PDV Bus), Gesellschaft für Kernforschung m.b.H., 75 Karlsruhe 1, Postfach 3640, May 1976.
3. Microprocessor based flexible interface between CAMAC and PDV bus, by Sauer and Zwoll, published in H. W. Lawson Jr., Large Scale Integration, North-Holland Publishing Company, pp. 210-220.

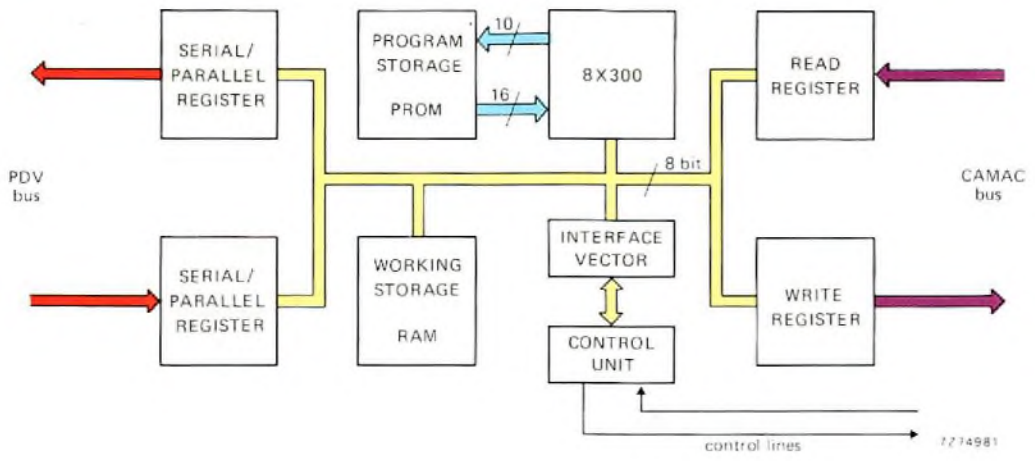

Fig.11 Block diagram of interface between CAMAC and PDV bus

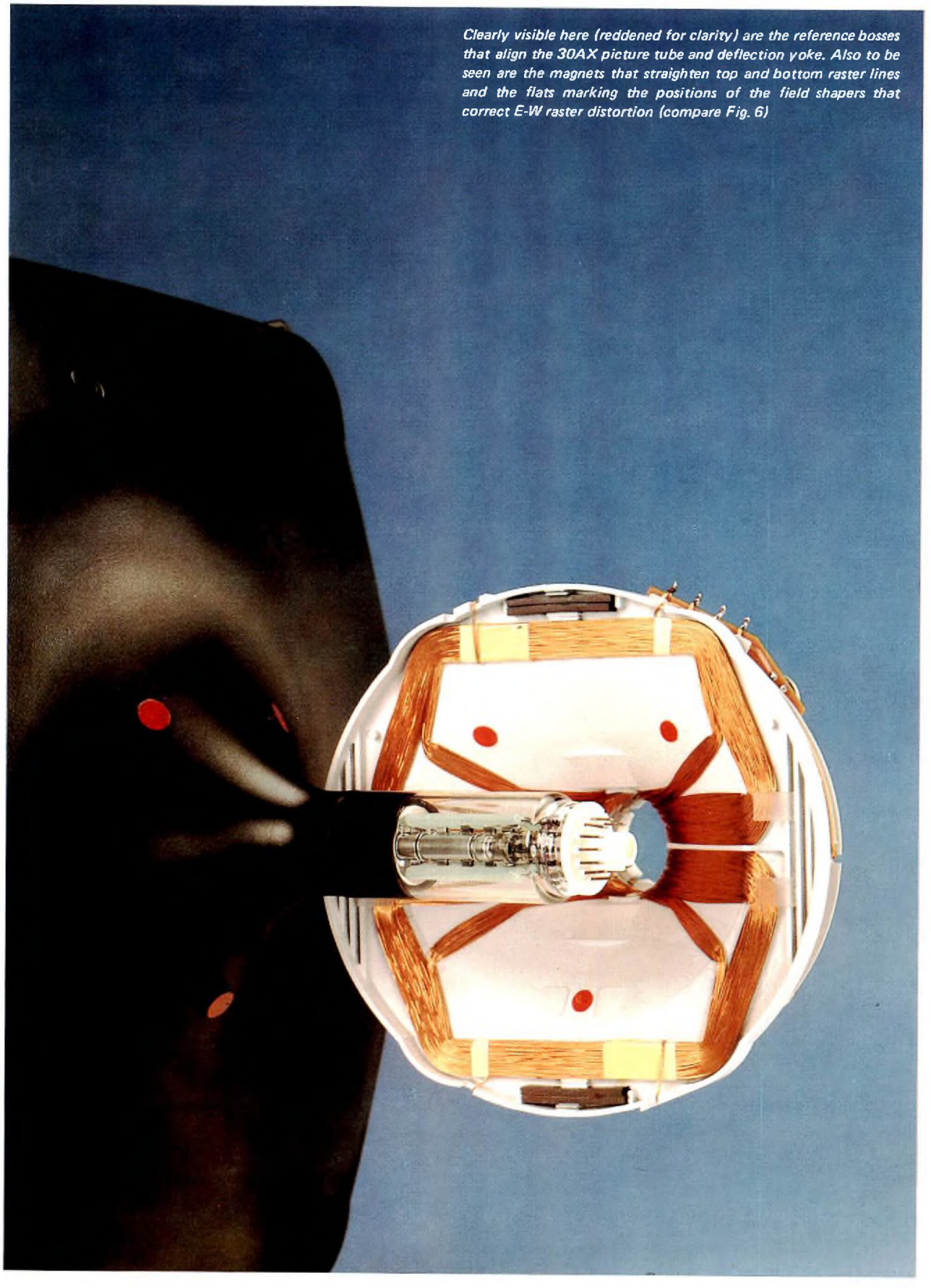

Clearly visible here (reddened for clarity) are the reference bosses that align the 30AX picture tube and deflection yoke. Also to be seen are the magnets that straighten top and bottom raster lines and the flats marking the positions of the field shapers that correct E-W raster distortion (compare Fig. 6)

30AX self-aligning 110° in-line colour TV display

P. G. J. BARTEN AND J. KAASHOEK

Mechanical and electromagnetic improvements combine to obviate the need for convergence, colour-purity and raster orientation adjustments in the 30AX display system. Closer mechanical tolerances and a set of positioning bosses make it possible to align the tube and deflection unit merely by pushing them together. A permanent magnet ring in the electron gun compensates for variations within the tolerance limits. Control of the deflection field, aided by field shapers embedded in the coil windings, eliminates coma. A weaker main lens in the electron gun and a quadrupole deformation of the lens field in front of the cathode reduce the spot size and improve the focus uniformity, especially at high beam currents.

30AX is a new in-line 110° colour tv system requiring no mechanical adjustments and the minimum of electrical adjustments. It uses fully interchangeable picture tubes and deflection yokes and is truly self-aligning and self-converging; each 30AX deflection yoke will automatically match any 30AX tube of the appropriate size. The system is based on the production experience gained with 20AX (Refs. 1 to 3), introduced in 1974, and on the results of further research in picture tube technology and deflection yoke design. Notable features of 30AX are:

- a great reduction in the number of adjustments; none are required for dynamic convergence, static convergence, colour purity, or raster orientation.

This article is based on that previously published in IEEE Transactions on Consumer Electronics, August 1978, Vol. CE-24, No. 3, pp. 481-488.

- a new design of deflection yoke, giving increased deflection sensitivity, reduced E-W raster distortion, and a straight N-S raster.
- a new design of electron gun, giving improved spot sharpness and focus uniformity.

The technological advances which have made these improvements possible are outlined below.

ELIMINATION OF DYNAMIC CONVERGENCE CORRECTIONS

One of the design objectives of the 30AX system was to eliminate all dynamic convergence corrections. Replacing these corrections by mechanical tilt and shift adjustments of the yoke with respect to the tube would only correct one error by introducing another. The only fully satisfactory way of eliminating dynamic convergence corrections is to further reduce the manufacturing tolerances; this has been achieved as follows.

First, the alignment of tube and yoke has been improved. For this purpose, a new reference system has been introduced in which the cone of the tube is provided with three bosses which mate with the inside of the deflection unit (see Fig. 1). These define three reference points whose centre, together with the centre of the clamping ring at the rear of the deflection yoke, determines the common axis of tube and yoke. Throughout tube manufacture, care is taken to ensure that this axis coincides with the screen axis determined by the exposure process and the gun axis. Special measures are taken to control neck-to-cone sealing, screen-to-cone fritting, gun sealing and other mechanical operations (see Fig. 2).

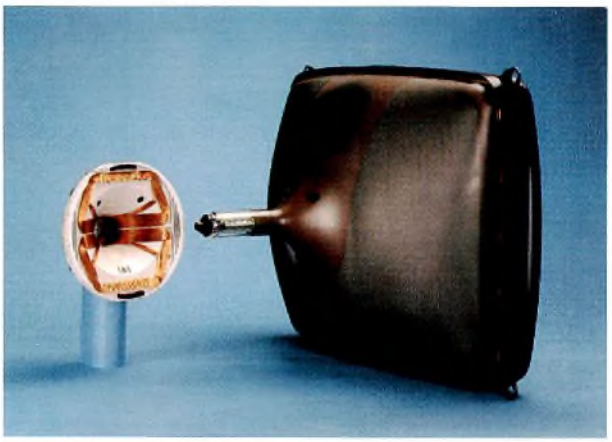

Fig.1 Reference bosses on cone of tube for aligning tube with yoke

In this regard, an important processing step is grinding the cone edge perpendicular to the tube axis.

In the deflection unit the introduction of new 'flangeless' windings (see Fig. 3) not only enables improvements to be made in the design of the deflection yoke but also contributes to the reduction of tolerances. Elimination of the flanges makes it practical to apply the multi-section winding technique at the gun side of the coils: previously, as in the 20AX coils, it could be applied only at the screen side. It also allows the use of a one-piece ferrite ring and a one-piece insulation cap of rigid construction which serves as an accurate carrier for the coils.

Together, these measures improve the precision to such an extent that, with any combination of tube and yoke, dynamic convergence is obtained automatically, without correction. In this way full freedom of interchangeability is ensured.

AXIAL COLOUR PURITY POSITIONING

A second step on the way to simplification was to make use of the bosses on the cone to establish the axial colour purity position of the deflection coil on the tube axis. Normally, axial shift of the yoke is necessary to bring the deflection point into coincidence with the position occupied by the light-source during exposure of the screen (see Fig. 2). It was found that the usual variation in colour purity position of the yoke with respect to the cone is due mainly to tolerances on the length of the cones. By grinding the cones to exact length, the tolerances on the axial colour purity position of the yoke are reduced to such an extent that the yoke has only to be pushed against the reference bosses of the tube to ensure a colour-pure picture.

RASTER ORIENTATION

A third simplification was also to make use of the bosses on the cone as a reference for the angular position of the yoke with respect to the screen axes. Small locating ridges moulded on either side of one of the boss locations in the yoke lock it in the required position for correct raster orientation. Thus, assembly of tube and yoke is even simpler than for a black-and-white combination.

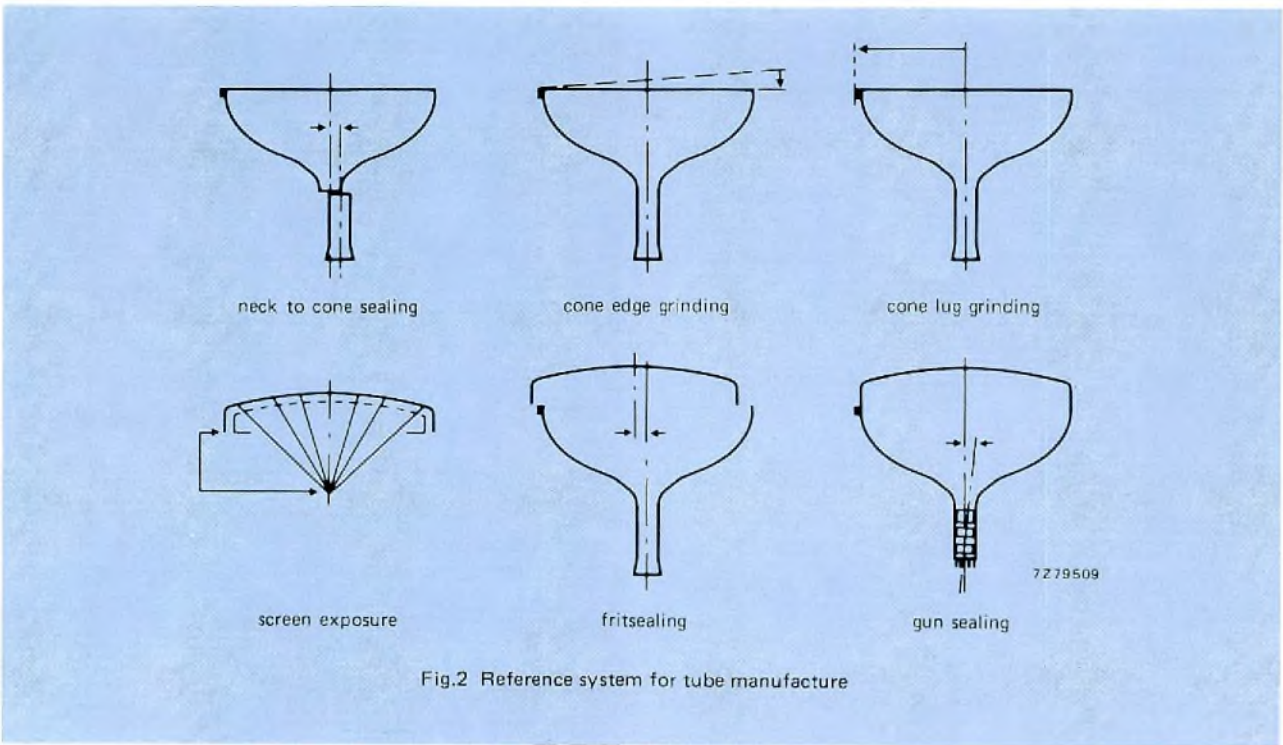

Fig.2 Reference system for tube manufacture

Fig.3 Saddle coils with flanges (left) and without flanges (right)

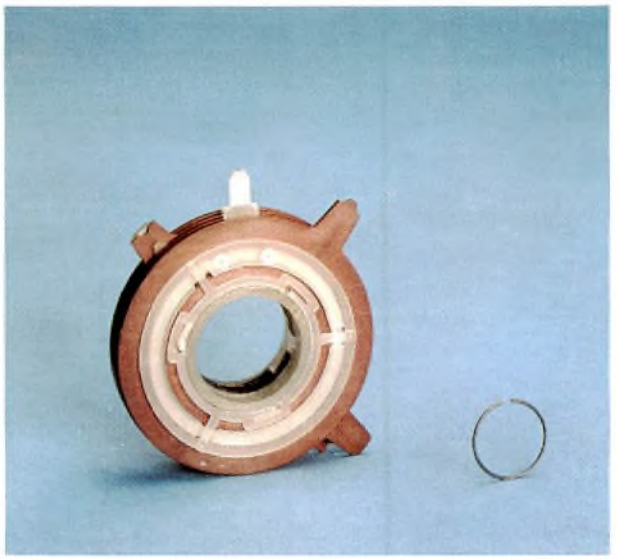

Fig.4 Internal magnetic ring in comparison with multipole unit

INTERNAL MAGNETIC CORRECTION RING

A fourth simplification has to do with the static beam corrections. One of the few remaining differences between the use of a colour-tube and a black-and-white tube is the need to correct the directions of the beams leaving the guns. They must pass exactly through the exposure points of the screen and meet in a single point at the centre of the screen. In in-line tubes, these corrections are normally carried out with the aid of a multipole unit, a set of magnet rings on the neck of the tube which provides adjustable 2, 4, and 6-pole fields. An important innovation in 30AX is the introduction of an internal correction system, consisting of a thin magnetic wire ring incorporated in the electron gun, which corrects any deviations of the beams and replaces the usual multipole unit (see Fig. 4). This ring is magnetised with the required combination of 2, 4, and 6-pole fields during a late stage of manufacture so that when the tube is delivered it needs no static convergence or colour purity adjustments.

DESIGN OF THE DEFLECTION UNIT

The flangeless construction of the coils has opened new possibilities for the design of the deflection unit to obtain the required self convergence. An important error that has to be avoided is coma. Coma can cause misconvergence of the centre beam (green) with respect to the side beams (red and blue), together with defocusing of the side beams. As in 20AX, preference has been given to correcting coma in the deflection yoke itself rather than by means of field-shapers in the gun. The latter correct only the coma effect on the convergence of the beams, not the effect on the focusing of the beams. This results in an asymmetric deflection defocusing of the side beams.

To avoid coma errors, the character of the field distribution at the gun side of the yoke has to be opposite to that at the screen side (see Ref. 2). This can be effected by using an opposite winding distribution at the front and rear ends of the coils, as has been realised for the horizontal deflection field in the line deflection coils (see Fig. 5). For the vertical deflection field, field

Fig.5 30AX line and frame coils

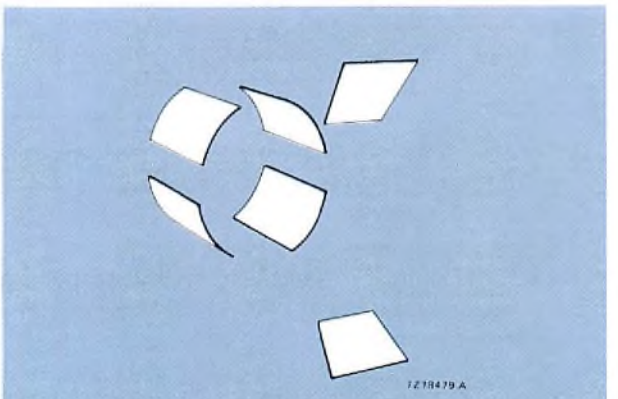

Fig.6 Positions of field shapers in deflection yoke; the curved ones are for coma correction of the frame deflection fields; the plane ones reduce E-W raster distortion

shapers embedded in the deflection coil itself are used (see Fig. 6). These do not cause a variation of the field between the beams but generate a totally coma-free field surrounding the three beams. In this way, not only the influence of coma on the convergence of the beams is corrected but also its influence on deflection defocusing.

RASTER SHAPE

Introduction of a second pair of field shapers embedded in the deflection coils has made it possible to reduce E-W raster distortion so that the required modulation of the scan current has been decreased from 13% to only 8%.

In the N-S direction the distortion is zero. Horizontal lines at the top and bottom of the picture are straightened by changing the shape of the windings at the screen side of the line deflection coil from circular to hexagonal, and by introducing two permanent magnets of fixed value at top and bottom of the unit (see Fig. 7).

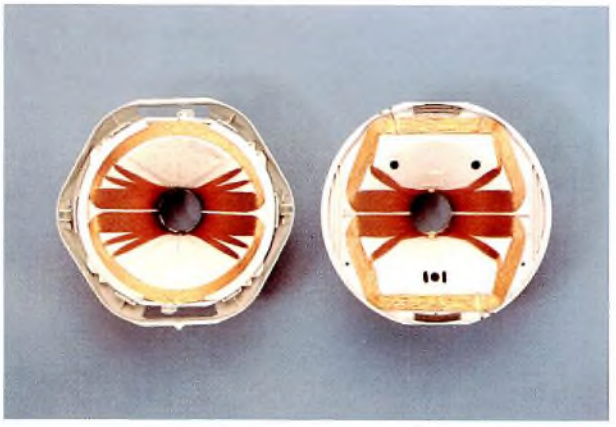

Fig.7 30AX deflection unit (right) compared with 20AX unit (left)

INCREASE OF DEFLECTION SENSITIVITY

Exact positioning of the deflection yoke with respect to the cone of the tube has made it possible to extend the length of the deflection field without risk of neck-shadowing. This results in an increase of deflection sensitivity. To avoid loss of sensitivity, care has been taken to adapt the shape of the neck-funnel contour optimally to the electron trajectories in the longer deflection field. Other factors contributing to increased sensitivity are omission of the cut-outs that characterised the core used in the 20AX deflection unit, and an increase in the copper content of the frame coil windings. These measures result not only in a saving of the required deflection power but also in a reduction of the temperature of the yoke, which contributes to the reliability of the yoke itself and the receiver as a whole. Table 1 lists the most important data of the deflection coils for a 26 in picture tube. Coil specifications for other sizes are set so that a single chassis design can be used for all sizes.

In a complete receiver, 30AX gives a total saving of 20 W compared with 20AX. As Table 2 shows, this brings the difference in power consumption between a wide-neck 110° receiver and a narrow-neck 90° receiver with comparable circuitry down to 12 W.

TABLE 1
Data for 30AX deflection coils in comparison with 20AX (26 in tubes)

	20AX	30AX
horizontal deflection:		
inductance	1.1 mH	1.5 mH
resistance (at 25 °C)	1.2 Ω	1.35 Ω
peak-to-peak current*	6.4 A	5.1 A
energy ($1/8\ LI^2_{pp}$)*	5.6 mJ	4.7 mJ
vertical deflection:		
inductance	3.5 mH	10.0 mH
resistance (at 25 °C)	3.0 Ω	6.3 Ω
peak-to-peak current*	3.4 A	2.05 A
power ($1/12\ RI^2_{pp}$)*	2.9 W	1.8 W

* At 25 kV e.h.t.

TABLE 2
Power consumption of mains-isolated CTV receivers with in-line picture tubes: 110° wide-neck with double-saddle coil compared with 90° narrow-neck with hybrid coil.

	110°		90°
	20AX	30AX	
Power consumption at 1.2 mA beam current, 25 kV e.h.t., and 1 W average audio output	120 W	100 W	88 W

COMPACT CONSTRUCTION OF DEFLECTION UNIT

The simplified positioning of the yoke has made it feasible to do away with the cage that was previously required to facilitate axial and angular adjustment. Together with elimination of the multipole unit, this has led to a considerable saving of room around the neck of the tube (see Fig. 8).

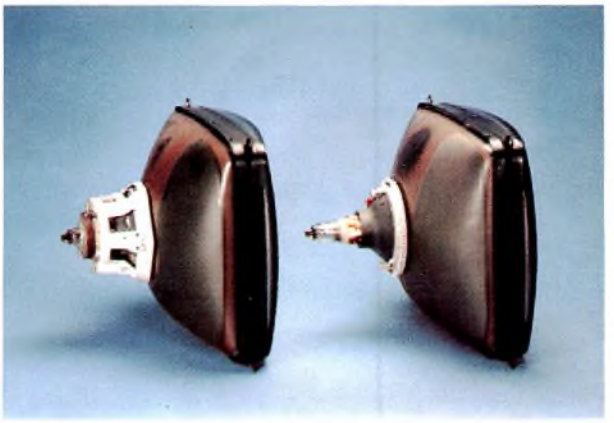

Fig.8 Mounted 20AX deflection unit with cage and multipole unit (left) compared with mounted 30AX unit (right)

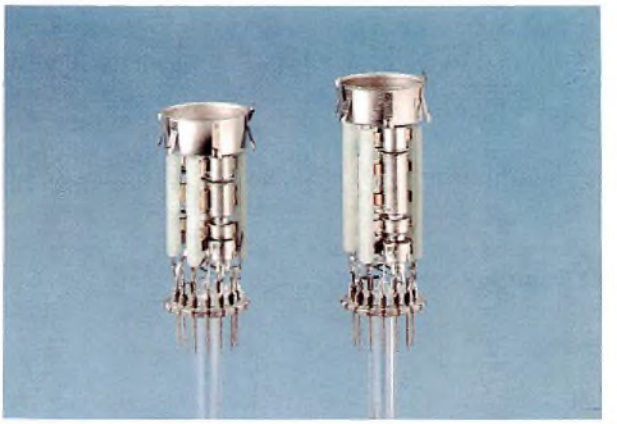

Fig.9 30AX gun (right) compared with 20AX gun (left)

ELECTRON GUN

To meet the demand for improved spot sharpness that is imposed by the introduction of teletext and viewdata systems in Europe, a new electron gun assembly has been designed. In the interests of optimum spot quality and maximum drive flexibility, separate gun construction is maintained. Use of a wide neck is also maintained to allow maximum room for the main lens of the gun to focus the beams with reduced spherical aberration.

The spherical aberration of the main lens has been further reduced by using a weaker lens with lower magnification, which necessitates increasing the focusing voltage to 28%, instead of 18%, of the e.h.t. This focus voltage can still be applied via the normal base without a change in the pinning. Because of the lower magnification, the gun is 10 mm longer (see Fig.9); the resulting increase in the overall length of the tube is 9 mm.

As the spot on the screen is the image of the crossover formed in the lower part of the gun (see Fig. 10), the spot size depends not only on the spherical aberration of the main lens but also on that occurring during formation of the crossover. Because of the high current density and the low velocity of the electrons in the crossover, space-charge repulsion in this part of the gun accounts for an extra contribution to spot size. In the design of the 30AX gun, both effects are reduced by the introduction of a quadrupole disturbance of the rotationally symmetric lens field in front of the cathode. The field is formed by replacing the normal circular-aperture first grid by an assembly of two flat plates welded together, one having a horizontal slit and the other a vertical slit (see Fig. 11). The square aperture where the two slits overlap focuses the electron beam into two focal lines. Spherical aberration in these focal lines is less than in a conventional crossover due to the fundamentally better focusing action of a quadrupole lens. Moreover, the lower current density in the line crossovers, compared with that in a point crossover, reduces the influence of space-charge repulsion.

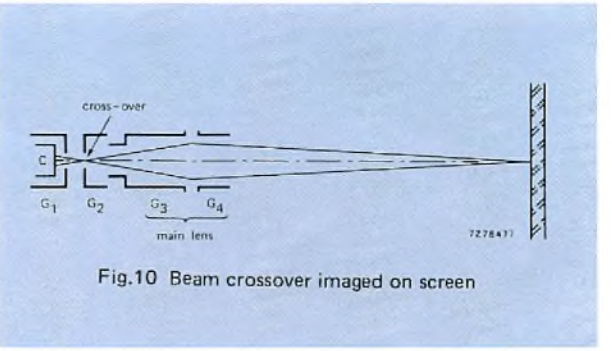

Fig.10 Beam crossover imaged on screen

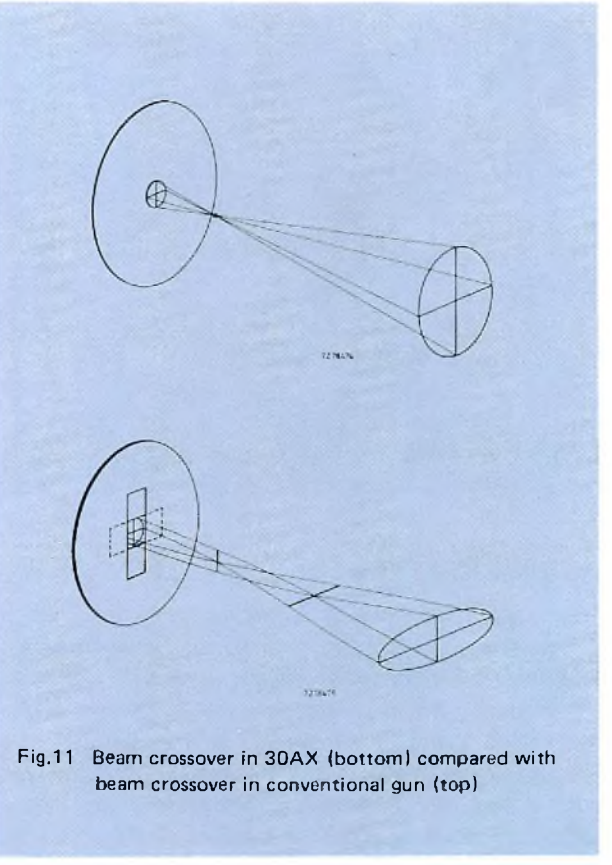

Fig.11 Beam crossover in 30AX (bottom) compared with beam crossover in conventional gun (top)

The astigmatism of the crossover is not objectionable but is used for minimising deflection defocusing. In self-converging in-line systems, the horizontal cross-section of the beam is automatically focused by the self-converging action of the deflection field, at least if this field is coma-free. However, the vertical cross-section will suffer from strong over-focusing at deflection, unless the undeflected beam is slightly underfocused in the vertical direction and the vertical dimensions are kept as small as possible. Both conditions are fulfilled at the same time by the astigmatism of the quadrupole lens.

The total effect of these measures is a considerable decrease in spot size and improvement in focus uniformity over the entire screen, especially noticeable at high beam currents (see Fig. 12).

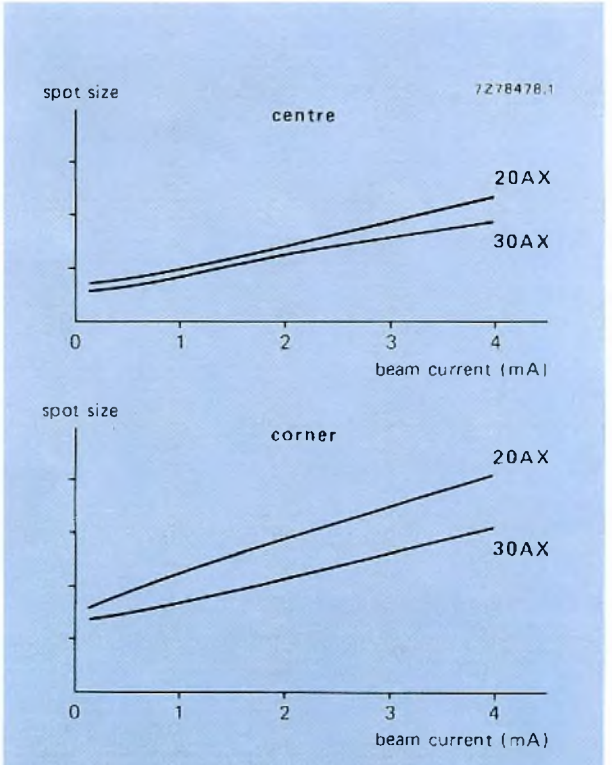

Fig.12 Spot size reduction in 30AX compared with 20AX, in centre and corner of screen.

HIGH BRIGHTNESS

The tubes have the 30% increased mask transmission that has recently been introduced in Europe for High Brightness tubes. Increase of mask transmission without compromising beam landing is possible because of the wide neck diameter (36.5 mm) which permits wide beam-to-beam spacing. This is favourable for colour selection and prevents external interference fields from having a noticeable effect on landing. The contrast has been improved by the introduction of pigmented phosphors. A fine uniform mask pitch, equal to that of the existing tube, supports the effect of the improved resolution of the gun.

30AX is produced in 26 in, 22 in and 20 in sizes, and the tubes are of the Soft-flash type with Quick-heating cathodes.

CONCLUSIONS

In the 30AX system the following design objectives have been realised:

- Interchangeability of tubes and yokes
  - compact construction
  - easy assembly
- No adjustments required for
  - dynamic convergence
  - static convergence
  - colour purity
  - raster orientation
- No multipole unit
- Reduced deflection energy
- Improved raster shape
- Improved spot sharpness

REFERENCES

1. BARTEN, P. G. J., 'The 20AX System and Picture Tube', IEEE Trans. on Broadcast and TV receivers, Vol. 20, no. 4, 286-292, Nov. 1974.
2. KAASHOEK, J., 'Deflection in the 20AX system', IEEE Trans. on Broadcast and TV receivers, Vol. 20, no. 4, 293-298, Nov. 1974.
3. BARTEN, P. G. J. and KAASHOEK, J., 'Large-screen colour television with intrinsically convergent 110° deflection', Electronic Applications Bulletin, Vol. 33, no. 2, 75-87, Oct. 1975.

ACKNOWLEDGEMENT

The authors wish to thank all the engineers and technicians who participated in the 30AX development and whose dedicated interest made so invaluable a contribution to its success.

Solar panels for terrestrial applications

C. FRANX

In some applications, solar energy is now becoming a viable economic alternative to conventional energy sources. This article describes the operation and construction of photo-voltaic solar cells and solar panels, and their use in terrestrial applications. It also discusses the factors affecting the design of practical cost-effective solar generators, and gives details of suitable storage accumulators, charge regulators, and motor-drive circuits.

INTRODUCTION

The use of solar power sources is now firmly established as a method of generating power in areas of the world where mains electricity is not available and where the cost of maintaining conventionally-powered equipment would be prohibitive. Such solar generators consist of series or parallel arrays of solar cells, large-area (~25 cm^2) photodiodes optimised for the direct photovoltaic conversion of solar energy into electrical power. Typically, each cell can produce an open-circuit voltage of up to 0.6 V, or a short-circuit current of up to about 690 mA. In arrays with accumulator back-up to span sunless periods, continuous powers of up to several hundred watts can already be generated.

The number of solar array applications is growing steadily. Already they are being used to power remote meteorological stations; emergency telephones on motorways and in National Parks; pumps for irrigation in arid regions; telecommunications repeater stations; beacons and navigational buoys; and navigational and anti-corrosive equipment on small craft. The scale of application is growing also. For example, between Alice Springs and Tennant Creek in Australia, there is a 580 km microwave link where 13 solar-powered repeater stations provide power for a total of 3000 telephone circuits. In Chile, a solar-powered plant for the electrolytic refinement of copper has been in operation since 1961.

In the future, solar power may well come to rival conventional power sources in many applications since the cost of energy is generally rising whereas solar cells are becoming less expensive as production increases and manufacturing techniques improve. It is possible to foresee a time when solar installations will help power whole rural communities, existing side-by-side with central generating systems.

In this article, the operation, construction, and characteristics of solar cells and solar arrays are discussed, with particular reference to BPX47A series solar panels. This is followed by detailed consideration of the operation and performance of cells and panels connected in series, in parallel, and in series-parallel combinations. Finally, the design of practical cost-effective solar generators is described, and detailed information on charge regulator circuits, accumulator characteristics, and motor drive circuits is given.

SOLAR RADIATION AND THE ENERGY BALANCE

It has been estimated that the earth receives energy from the sun at the rate of 1.73×10^{17} W, some 20 000 times the world's current rate of energy consumption. Since the temperature of the earth is comparatively stable, all the energy received must eventually be re-radiated. In

fact about 30% of the energy received is directly reflected by the atmosphere, while a further 47% is converted into heat and radiated at much longer wavelengths during the night. Most of the remaining 23% is consumed in evaporating water, producing vapour which later condenses and releases the energy for subsequent radiation. A small fraction, less than 0.2%, sustains wind, wave, and convection motion. An even smaller amount, about 0.025%, is stored by photosynthesis in plants.

Apart from wind and water power, the main source of energy since the earliest times has been the 0.025% of solar energy stored in vegetation (wood) and in the form of the fossil fuels – coal and oil. However, since it has been estimated that six-months supply of coal requires 10^6 years to replace, there is obviously a limit to these traditional sources of energy. Less than 10% of the potential energy in the rain cycle has been exploited but because the majority of suitable hydroelectric sites are remote from the industrialised parts of the world, the remaining 90% of this source of energy is not of practical interest at present.

Thus, hydroelectric power, fossil fuel replenishment, and wind and wave power account for less than 2% of the total energy received from the sun, leaving about 70% of the intercepted energy still to be exploited.

USING SOLAR ENERGY

Two methods of exploiting solar energy are currently under development: photothermal conversion and photovoltaic conversion. In photothermal conversion, solar radiation is used to heat a working fluid, either directly or through a heat pump. The heated working fluid is used in some form of heat engine to provide power. In photovoltaic conversion, solar radiation is converted directly into electricity. Electricity is, of course, readily conveyed to the point of use, where it can be converted easily into any other form of energy. Solar cells are photovoltaic converters.

PHOTOVOLTAIC CONVERSION USING SOLAR CELLS

A solar cell can be considered as a large-area silicon diode. In an open-circuited (unconnected) cell shielded from radiation, the charge inhomogeneity at the pn junction causes some of the electrons supplied by the Group V donor atoms on the n-side of the junction to diffuse across the junction into the region of low electron density on the p-side. This diffusion leaves ionised donor atoms which create a positive space charge in the n-region close to the junction. The electrons which diffuse into the p-region fill valence levels created by Group III acceptor atoms and are immobilised, creating a negative space charge near the junction. Under equilibrium conditions, this charge separation produces a barrier (diffusion) potential V_B across the junction.

Voltage V_B can be thought of as a contact potential. However, if contacts are made to the p-region and n-region with the same metal, and a circuit is made via a high-resistance voltmeter (Fig.1a), no voltage will be measured because the contact potentials cancel. For instance, typical values might be $V_B = -0.7$ V, $V_{C1} = +0.5$ V, and $V_{C2} = +0.2$ V.

If the cell is now irradiated with solar energy, electron-hole pairs will be generated in the junction region and separated by the field associated with V_B, the holes being forced to the p-side and the electrons to the n-side. Consequently $|V_B|$ will fall sharply, to say 0.1 V. However, the p-contact will then be at a potential +0.6 V above that of the n-contact. This voltage can be measured (since the diffusion potential in the reverse junction formed in the external circuit is unaffected) and, with sufficient irradiation, can sustain current flow from the p-region to the n-region.

When a diode is used for rectification (Fig.1b), a voltage source with its positive terminal connected to the p-contact will cause current to flow from the p-region to the n-region inside the diode. This gives the normal diode characteristic passing through the origin, with normal conduction taking place in the first quadrant (Fig.1d).

Fig.1c represents an irradiated solar cell. In this case, current flows from the n-region to the p-region inside the cell. This is termed the photovoltaic current. The generation of photovoltaic current (or voltage) occurs in the fourth quadrant of Fig.1d, the maximum current obtainable being approximately proportional to the level of irradiance.

The conversion efficiency of a solar cell is about 12% under a standard solar irradiance of 1 kW/m^2. It is limited in the main by three factors: first, only that part of the spectrum between 0.4 and 1.1 μm out of the total spectral interval of 0.2 to 4 μm is used: second, the absorbed photons have an unused excess of energy; third, some electron-hole pairs are created outside the region of the junction and recombination occurs before charge separation can take place.

BPX47A-SERIES SOLAR PANELS

In practice, solar cells are rarely used singly but are used in arrays or solar panels (sometimes referred to as solar batteries). Fig.2 shows the construction of a BPX47A solar panel which comprises 34 series-connected silicon photovoltaic cells sandwiched between glass plates.

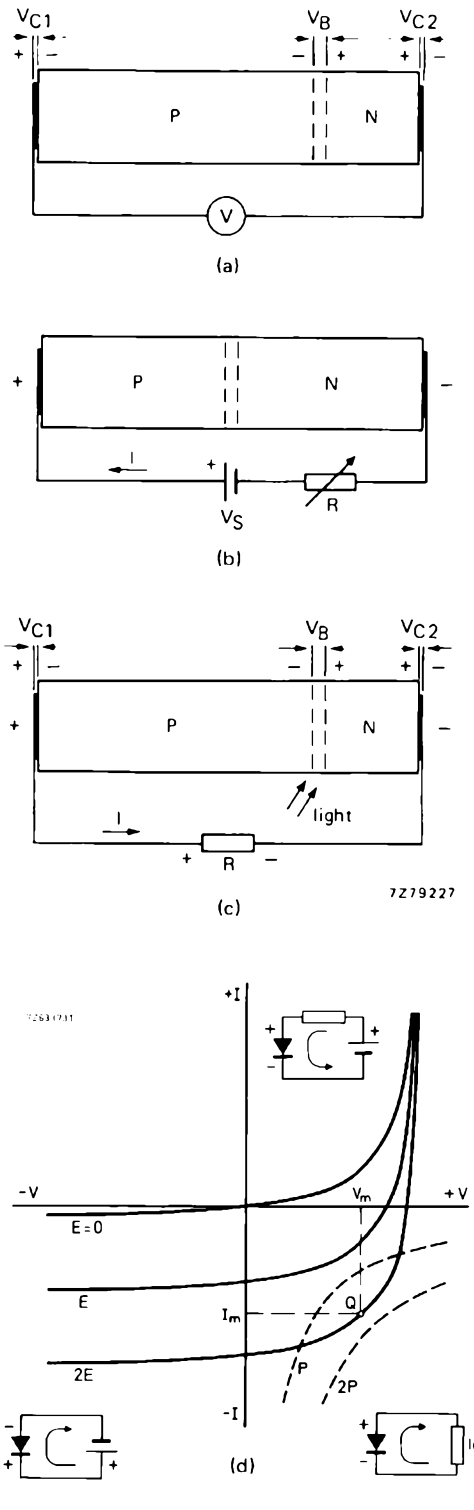

Fig.1 Operation of solar cell:
(a) barrier potential and contact potentials in non-irradiated solar cell
(b) normal diode conduction
(c) production of photovoltaic current in an irradiated solar cell
(d) diode characteristics

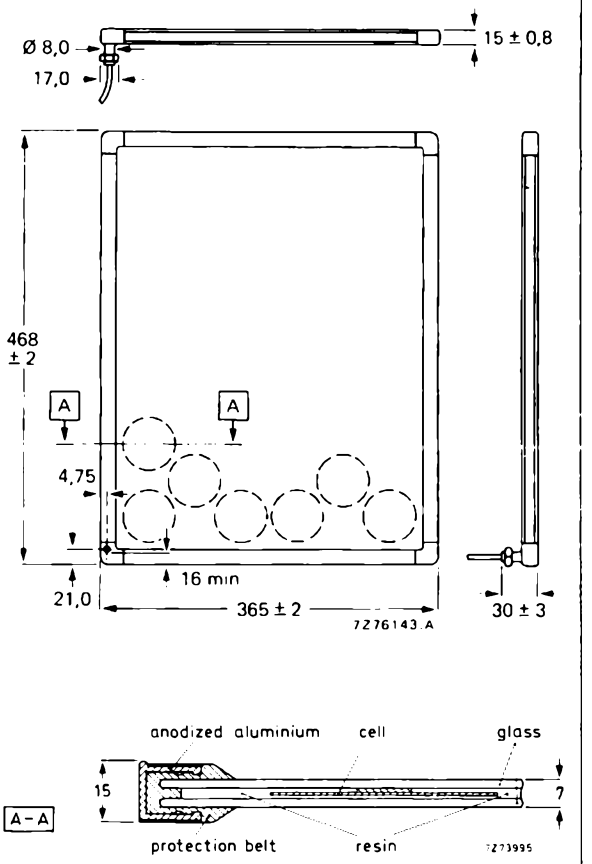

Fig.2 Mechanical details of BPX47A solar panel

Panel construction

The cells are encapsulated in silicone resin and mounted between 2 mm glass plates; this ensures that the assembly is moisture-proof. The glass is chemically hardened to improve its abrasive resistance by about 30% and increase its strength by a factor of 5. The surfaces of the plates are made very smooth to inhibit the accumulation of dust and snow.

The robust construction of the panels enables them to withstand winds of up to 280 km/h. They are proof against the deleterious effects of ultraviolet radiation. Since the conversion efficiency of the panels is about 14% at 0 °C, more than 80% of the incident radiation is converted into heat. This heat is conducted through the silicone resin encapsulant and glass sheets and convected away by the surrounding air. At an irradiance of 1 kW/m^2, the temperature rise is only about 15 °C.

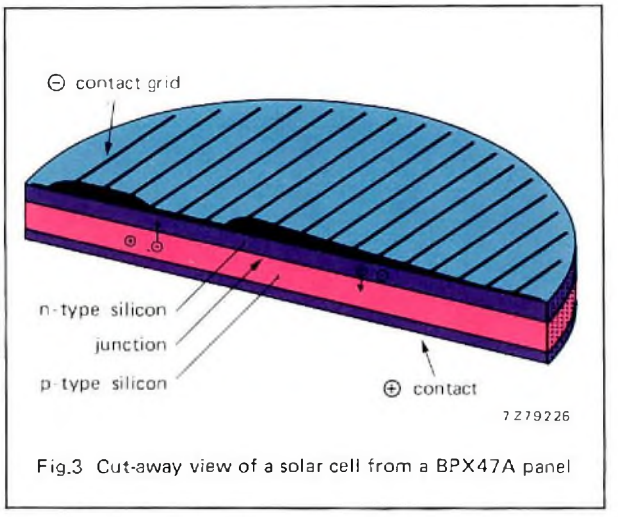

Fig.3 Cut-away view of a solar cell from a BPX47A panel

Cell construction

Individual cells are formed from silicon slices cut from a 57 mm diameter ingot. The ingot is doped with boron (a Group III element) to make it a p-type semicondictor. Phosphorous (a Group V element) is then diffused into one surface of each slice to form a shallow n-type region, with a pn junction a few tenths of a micrometre below the surface. Contact with the top surface of the slice is made through a metal grid that covers about 7% of the surface. The complete n-type surface is covered by a TiO_2 anti-reflection coating. The p-type side of the slice is completely metallised to reflect unabsorbed photons and to provide the second contact. A cell of this construction is shown in Fig.3.

Characteristics

As stated above, solar cells are operated in quadrant IV of the diode characteristic and therefore only this quadrant is considered. The voltage-current characteristics of the BPX47 solar panel as a function of irradiance is shown in Fig.4 for a junction temperature of 60 °C. Power output contours are also shown.

Insolation

The response of any solar cell depends on the spectral distribution of the radiation falling on it. For this reason, it is not sufficient to use the power per unit area as a measure of the irradiation falling on a solar cell: the spectral distribution of the power must also be specified. The term *insolation* is used here to mean 'solar irradiance', thus specifying in one term both the power and its spectral distribution.

Optimum load

As Fig.4 shows, the maximum power obtainable from a BPX47A solar panel at an insolation of 1 kW/m² is 9.7 W at 60 °C. This power output occurs at levels of current and voltage equivalent to a load of 20 Ω. This 20 Ω load-line is shown in the figure, and it can be seen that the maximum available current is roughly proportional to the insolation.

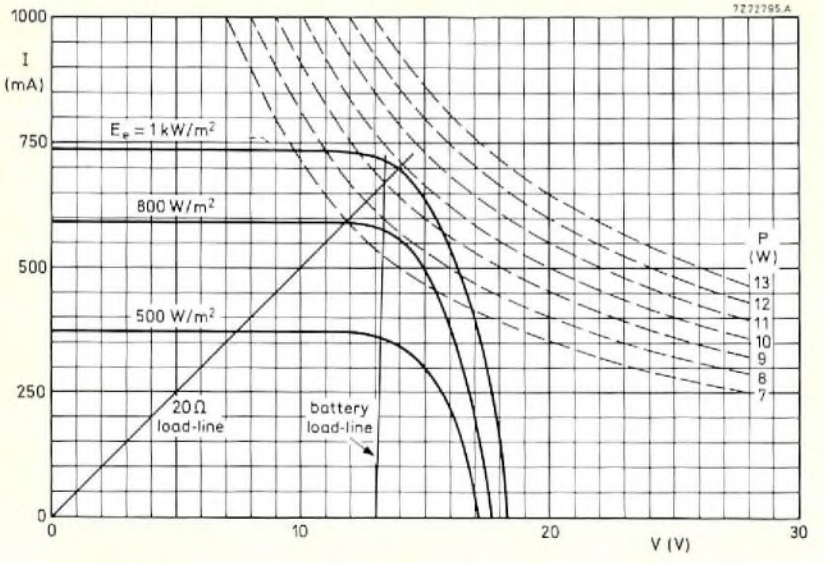

Fig.4 Generating quadrant of a BPX47A solar panel (T_j = 60 °C)

Operation with a fixed load resistance is not ideal since, at different levels of insolation, the voltage/current coordinates of the maximum power point vary, so the optimum load resistance also varies. However, if a secondary battery (accumulator) is used as the load, this problem is largely overcome. Whereas the power output into a 20 Ω load falls to 2.9 W at 500 W/m^2 insolation, the output into a 12 V accumulator only falls to 4.8 W.

The use of a secondary battery as the load is normal practice. It enables peak demands to be met and periods of darkness and overcast skies to be bridged, and the solar cells generally work under near-optimum conditions. For this reason, the number of cells in a panel has been chosen to match the nominal voltage of a 12 V accumulator (six lead-acid cells) in series with a protection diode and a charge regulator.

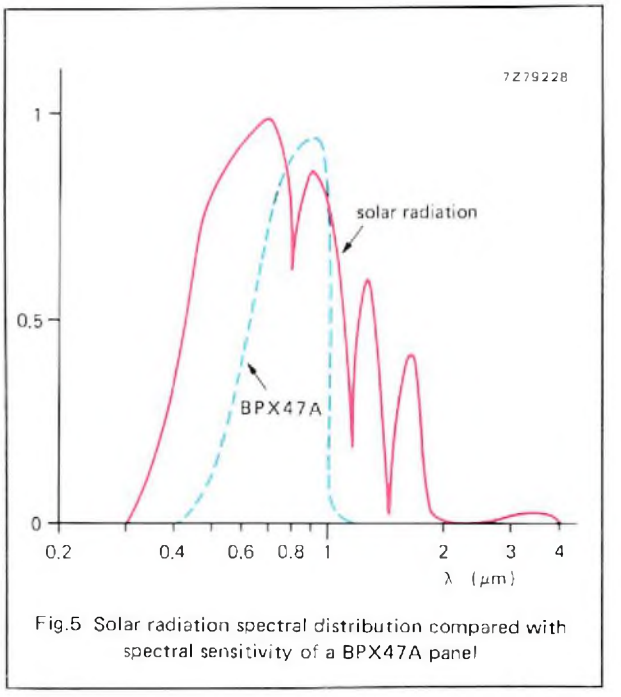

Fig.5 Solar radiation spectral distribution compared with spectral sensitivity of a BPX47A panel

Efficiency

The conversion efficiency of the BPX47A solar panel is about 12% at an insolation of 1 kW/m^2. It is limited partly by the mismatch between the spectral distribution of sunlight and the spectral sensitivity of the cells (Fig.5), and partly by the unused excess of energy of the absorbed photons.

Temperature

Fig.6 shows the effect of temperature on the operation of the BPX47A solar panel. At an insolation of 1 kW/m^2, the temperature coefficient of the short-circuit current is about +0.64 mA/K (mA/°C), and that of the open-circuit voltage is about −74 mV/K(mV/°C). When the junction temperature in the cells increases from 0 to 60°C, the maximum output power only falls to 9.7 W from 12 W.

The load-line shown in Fig.6 represents a fully charged battery. The solar panel has been designed to minimise the effect of temperature variations. Since the temperature coefficient of the voltage of a lead-acid accumulator is also negative, this will somewhat reduce the effect of temperature on power matching.

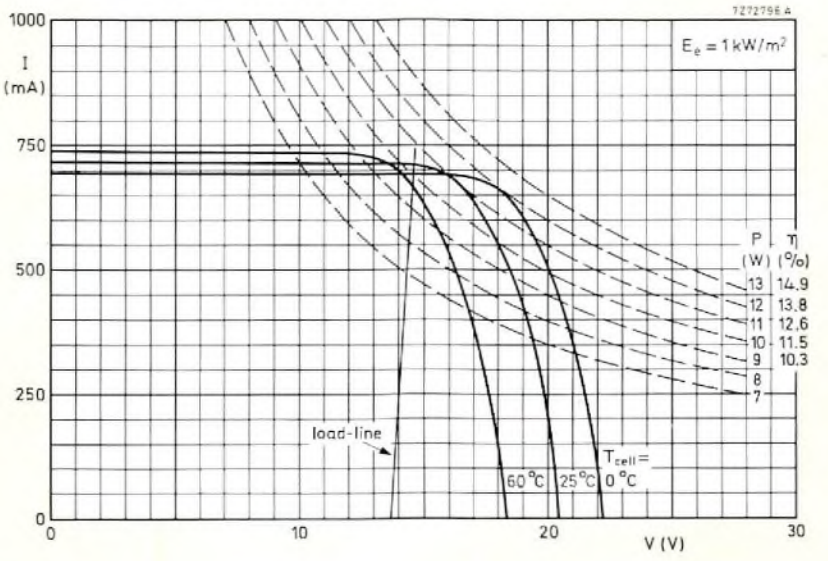

Fig.6 Effect of temperature on the generating characteristics of a BPX47A solar panel

SAFE OPERATING AREA

As with other semiconductor devices, it is possible to define for solar cells and panels an area bounded by the combined device characteristics and operating characteristics within which the devices can be safely operated. Outside the boundary of this Safe Operating Area (SOAR), operation may damage or destroy the device.

To define the SOAR, the Absolute Maximum Ratings for the individual cells and panels and the worst-case operating conditions must be known. As usual, the most important parameter is temperature.

The junction temperature of an individual cell can be quite high before its structure is damaged. The junction temperature, however, is not the limiting factor in the case of a solar panel. If the temperature of a cell exceeds 85 °C, or differs greatly from that of its neighbours, the silicone-resin potting material may be strained or partially decomposed. Thermally-induced strains may cause the resin to part from the sensitive surface of cells, and decomposition will discolour the resin. Both result in attenuation of the light reaching the cell, thermal strain increasing reflection, and discolouration increasing absorption. Both phenomena are irreversible.

An otherwise normal cell will heat up when current is forced through it, causing a reverse voltage across it (see later). This will happen when one cell in an irradiated panel is put partially into shadow. A partially-shadowed cell is subject to maximum dissipation when:

- it is part of a series-connected chain of irradiated cells in a short-circuited panel, or array of panels;
- it is in a panel connected in parallel with other panels but with no load.

The SOAR must be determined so that a partially-shadowed cell is protected under both circumstances.

Short-circuit series connection

The operation of n cells in series into a short-circuit is shown in Fig.7; the total voltage V_{tot} is given by:

$$V_{tot} = \sum_{i=1}^{0} V_i = 0.$$

A current I, which is proportional to the irradiance, flows through the cells. Since the internal resistance of the cells can be ignored (see Figs.4 and 6), the dissipation in cell i will be $P_i = V_i I$. Assuming that the cells are identical and equally irradiated:

$$V_i = \frac{V_{tot}}{n} = 0,$$

and the dissipation in cell i will therefore be zero.

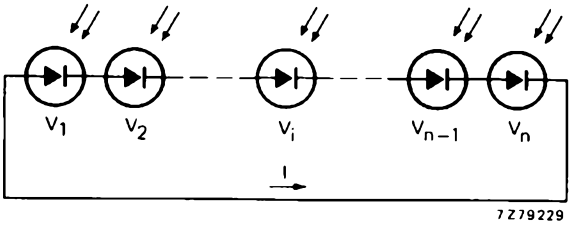

Fig.7 Solar cells in series

These ideal circumstances, however, seldom apply. If a given cell produces a short-circuit current $I_{sc} > I$, then $V_i > 0$. If $I_{sc} < I$, then $V_i < 0$; this occurs when a cell is partly shadowed. Thus, when $V_i < 0$ (voltage inversion), $P_i > 0$ and the cell will heat up.

The condition $V_i > 0$ cannot lead to overheating. In the worst case when all cells except one are in shadow, the cell being irradiated will be unable to force a significant current through the shadowed cells.

It is essential, however, that the system is protected against the condition when $V_i < 0$, which is most severe when one cell only is partially shadowed. This condition is analysed using Fig.8 in which the right-hand curves are the voltage-current characteristics of 33 and 34 cells respectively from a BPX47A panel, and the left-hand curves are the reverse characteristics of a single cell (from the same panel) under varying degrees of shadowing. The reverse characteristic passing through the origin is for the cell completely shadowed. Note that in accordance with the convention normally adopted for solar cells, the currents are shown positive.

The combined voltages of the 33 irradiated cells will force current through the shadowed cell, producing a reverse voltage across it. The current through the cell, and the power dissipated, depends on the degree of shadowing. In a completely shadowed cell, the maximum allowable current is 120 mA at V_R = 17 V and the dissipation is 2.04 W.

If now the amount of radiation falling on the shadowed cell is increased, the current passing through it will increase and so will the dissipation. With the other 33 cells receiving an insolation of 1 kW/m², V_{F33} = 13.5 V and I = 670 mA. Thus, if the shadowed cell is irradiated to a level where it is capable of supplying 570 mA, an extra 100 mA will be driven through it by the other cells, resulting in a dissipation of 9 W. This exceeds the maximum permissible dissipation for one cell which is taken to be the power received at an insolation of 1 kW/m². In a BPX47A panel, each cell has an area of 26 cm² and at 1 kW/m², receives a maximum of 2.6 W, which is a safe value. This power curve is shown in Fig.8. (note that if more than one cell is shadowed, the voltage produced by

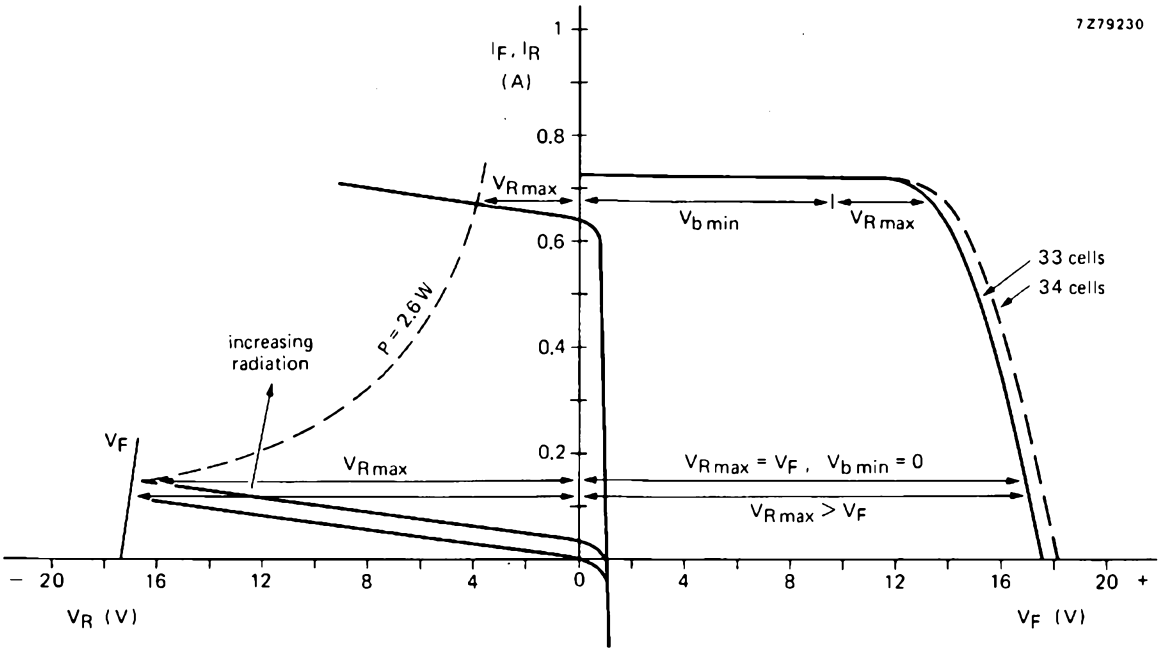

Fig.8 Generating characteristics of 33 and 34 cells in a BPX47A panel and the reverse characteristics of a single cell from the same panel

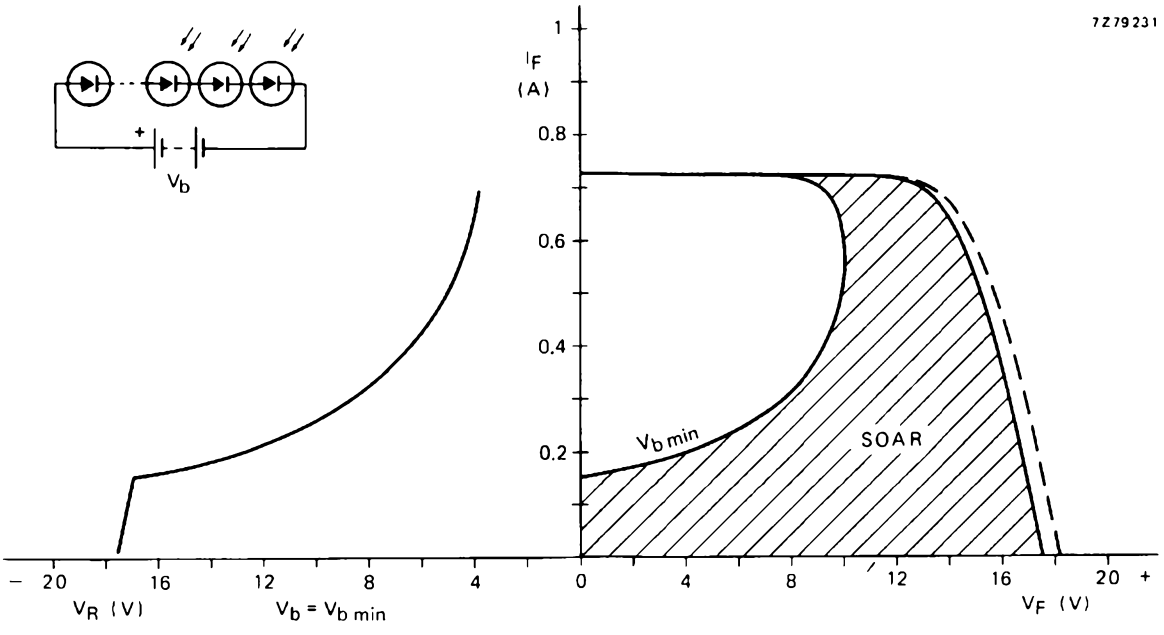

Fig.9 SOAR for a BPX47A solar panel at an insolation of 1 kW/m²

the irradiated cells will be divided between them, and consequently the power will be reduced and the dissipation will be less.)

A way must therefore be found for limiting the dissipation in a shadowed cell. One obvious method is to shunt each cell with a protection diode. This, however, is a rather expensive solution. A better solution is to ensure that the panel is always in parallel with a voltage source, thus reducing the voltage available to drive current through shadowed cells.

When solar panels are used to charge a secondary battery, some degree of protection is automatically provided, the accumulator acting as an effective voltage source. Complete protection requires a certain minimum battery voltage V_b which depends on the insolation and the degree of shadowing of a cell. When a maximum insolation of 1 kW/m^2 is available, the worst-case condition will occur for the power and voltage available at this value. Only the degree of shadowing therefore needs to be considered.

In the example given earlier where I = 670 mA, V_R must be reduced to 2.6/0.67 or 3.9 V, to avoid excess dissipation. This means that V_b needs to be at least 13.5 − 3.9 = 9.6 V (see Fig.8). Obviously when I < 154 mA, P < 16.9 x 0.154 = 2.6 W, and no voltage source is required. By constructing intermediate V_b points on Fig.8, the curve for $V_b$min shown in Fig.9 can be derived. The SOAR lies between the panel characteristic and this V_b min curve.

From Fig.9 it is clear that where $V_b > 10$ V, damage cannot occur for any shadowed arrangement. Where a number of panels are connected in series, a protection diode must be connected across each panel.

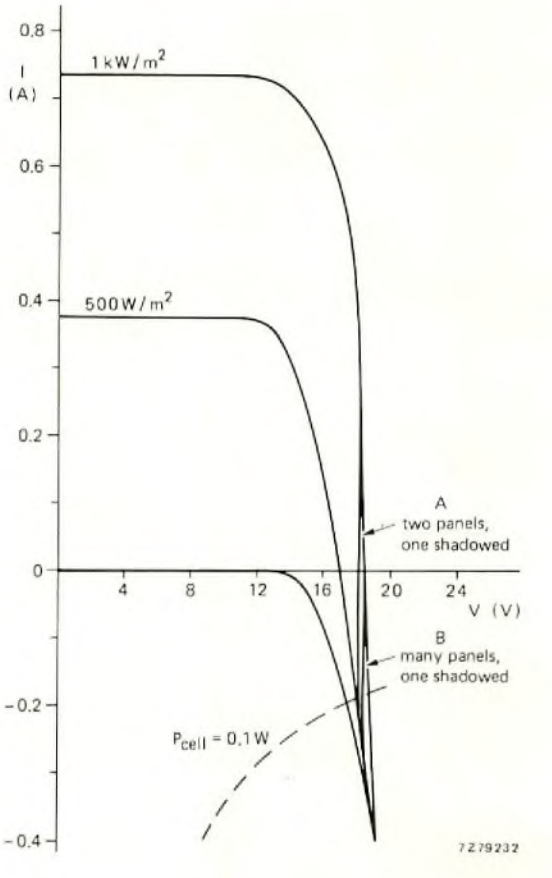

Fig.10 Generating and diode forward characteristics, showing the effect of unequal insolation on parallel operation

Open-circuit parallel connection

When two panels connected in parallel with no load receive differing levels of insolation, the panel receiving the lower level will be driven into the forward region of its diode characteristic. Fig.10 shows the generating and forward quadrants of a BPX47A panel. Where one panel receives 500 W/m^2 and the other 1 kW/m^2, the operation will lie on the intersection of line A with the relevant characteristics. The voltages across the panels are, of course, equal, and the currents through the panels are also equal but of opposite sign.

Where one of many panels in parallel receives 500 W/m^2 and the rest 1 kW/m^2, the current will be higher. In the worst case, all energy produced by the panels receiving 1 kW/m^2 will be dissipated in the panel receiving only 500 W/m^2. This dissipation will be equally divided over all 34 cells. Therefore, the temperature rise is limited and allows shunting of 12 solar panels.

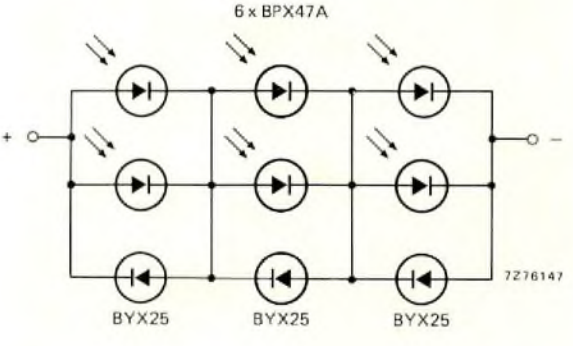

Fig.11 Matrix of six BPX47A panels protected by three BYX25 rectifier diodes

Panels in series/parallel

An array of n panels in series by m panels in parallel requires only n protection diodes. However, the array must be connected as a matrix, as shown in the example of Fig.11 where n = 3 and m = 2. Further information is given in the published data for the BPX47A panel. With such an arrangement, panels cannot be damaged by excess dissiaption, although a series voltage source is still necessary to protect individual cells.

SYSTEM DESIGN CONSIDERATIONS

A solar power installation must be able to supply power as and when required. However, its power input is variable, the level depending not only on the dimensions of the panel, but also on the amount of sunlight falling on it. That, in turn, depends on the site of the installation, the time of day, the season, and the weather. There are times when no power input is available, so some form of energy storage must usually be considered.

It is already evident that the design of a cost-effective solar power system is extremely difficult. A large amount of information is required and a number of compromises must be made. For this reason, a computer-aided design routine has been developed which indicates the most efficient system parameters for a given set of conditions. Some of the inputs required by the program are discussed below.

Quality of sunlight

The daily amount of sunlight depends on the latitude of the site and the time of year. During daylight hours, sunlight reaches a solar panel in two ways: directly, the light being modified only by atmospheric absorption and scattering; and indirectly, the light diffused by clouds, scattered by the atmosphere, or reflected from adjacent surfaces. Even the darkest shadows are illuminated to some extent by indirect radiation.

The radiation I incident on a panel normal to the direction of the sun is given by:

$$I = I_0 \exp(-ax)$$

where I_0 is the radiant flux density external to the atmosphere, x is the distance travelled by the sunlight through the atmosphere, and a is the extinction coefficient (the abosorption coefficient added to the scattering coefficient). Obviously, the value of x depends on the elevation of the sun above the horizon and the altitude of the site above sea level.

Where indirect radiation is of importance, the nature of surrounding surfaces must be considered; snow, in particular, reflects light very efficiently.

Fig.12 shows the general distribution of solar energy falling on the earth's surface, integrated over a year. The values given are for a horizontal surface. Note that 1 kJ/cm^2 corresponds to a day-and-night average insolation of 0.32 W/m^2.

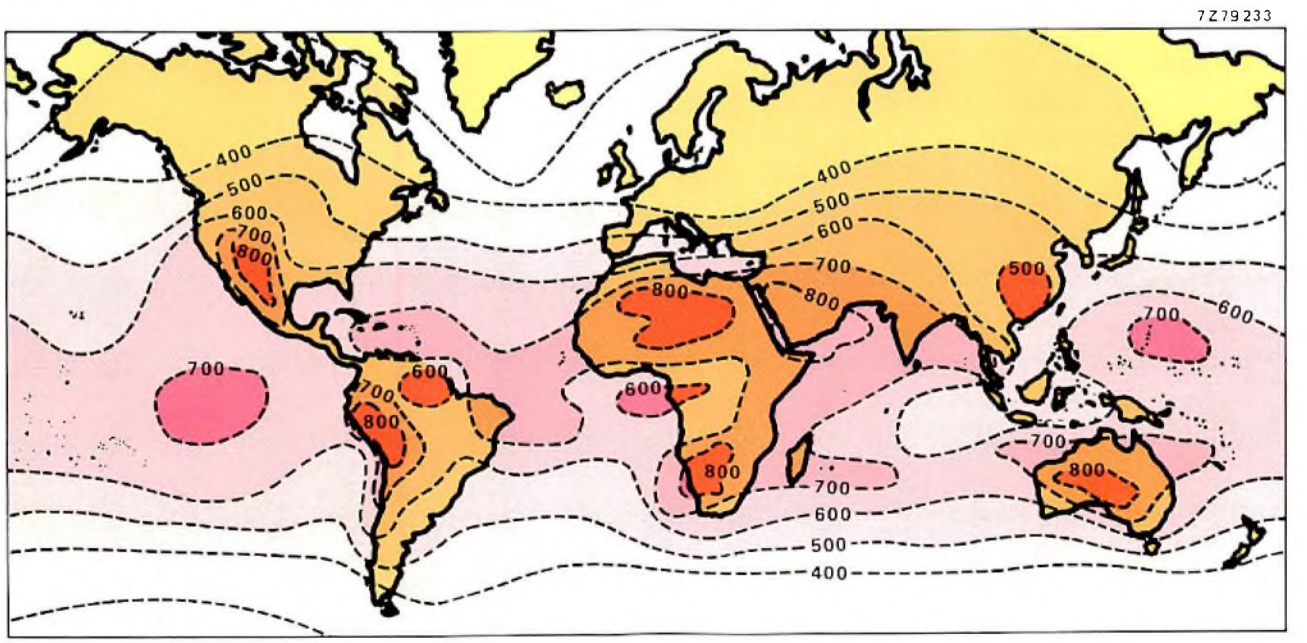

Fig.12 Annual average distribution of solar energy in kJ/cm^2 at the earth's surface

Fig.13 shows the effect of inclining an array of panels at an angle equal to the latitude of the site. It can be seen that the effect is to reduce the variation in energy received through the year.

Other climatic effects

For various reasons, it may be desirable to incline solar panels at an angle other than that equal to the latitude. Thus, to prevent snow accumulating, a panel slope of 90° is required. To prevent acumulation of sand in desert regions, a slope of 45° is necessary. For self-cleaning in rainy tropical regions, the slope should be at least 30°.

These factors will often dictate the design of an array of panels so that energy collection efficiency becomes secondary. For example, a solar array for use near the equator might comprise an equal number of panels inclined 30° north-to-south.

Power demand

Both the nature and the pattern of the power demand must be established, together with likely maxima. It is evident that the power available will vary considerably in both the long and the short term. Thus, some form of energy storage will usually be required. From the pattern of power demand and a knowledge of conditions at the site, the type and capacity of the storage accumulator can be specified.

If very long dark periods are to be bridged, an accumulator with a low self-discharge rate (pure lead) will be needed. In the tropics, where dark periods are short and well defined, a higher self-discharge rate can be tolerated and a lead-antimony accumulator might be selected.

Site conditions

It is obviously important to know as much as possible about the actual weather at the site. Meteorological records are often sketchy for remotes sites, so measurement of the solar radiation and its variation will be unavoidable. Although computer models can be used to simulate some conditions, they are, at best, approximations. The more information that can be made available about the proposed site of a solar power installation, the more cost-effective the installation will be.

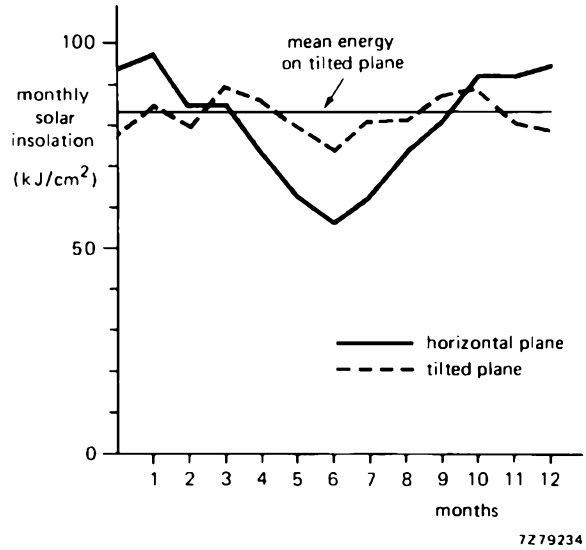

Fig.13 Comparison of the solar energy collected monthly by a solar array at an angle equal to the site latitude with the mean energy received and the energy falling on a horizontal surface (based on the measured performance of a solar power installation at Alice Springs, Australia)

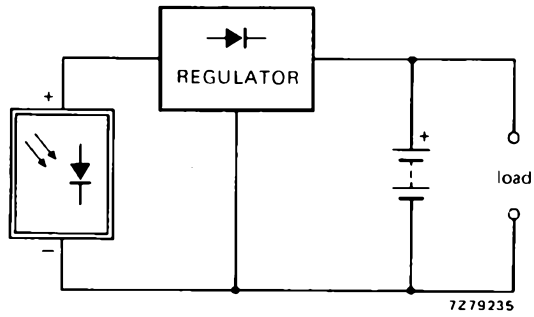

Fig.14 Essential elements of a solar power installation, in this case with a series charge regulator

SOLAR POWER SYSTEMS

Fig.14 shows the basic elements of a solar power system (in this case with a series regulator). They are: the solar panel array, a reverse protection diode to prevent the battery draining through the solar panels, a charge regulator, and storage accumulators. Any necessary protection diodes are incorporated in the solar panel array; the reverse-protection function may be included in the regulator.

Where the only load is a motor, the accumulator and regulator may be replaced by an electronic motor-control circuit.

TABLE 1
Representative characteristics of storage accumulators

Characteristic	Unit	Nickel-cadmium		Lead-acid		
		sealed	open	sealed	Pb-Sb	Sb-free
Unit capacities:						
minimum	Ah	0.01	10	1	10	20
maximum	Ah	15	1500	10	200	2000
Discharge rate	h	10	5	20	20	10
Charge/discharge cycles*		>500	>1000	>250	>250	>1000
Maintenance interval	months	–	6	–	6	12
Working life	years	10	10 to 25	4	5	20 to 25
Charge retention	%/month	35	35	3	10 to 30	1.5 to 3
Operating temperature:						
minimum	°C	−20	−20	−20	−20	−20
maximum	°C	+45	+45	+45	+60	+50

* Discharging to not less than specified minimum percentage of capacity.

Storage accumulators

Besides supplying power during dark periods, a storage accumulator can have other advantages to a solar power system. One has already been discussed: the use of a battery as a voltage source to protect panels from excess dissipation. Other functions include:

- allowing the use of a high-power motor or pump where this would be more efficient than a low-power or low-current alternative;
- averaging the power available – excess energy collected around noon can be stored until available power falls off later in the day.

Selecting the correct storage battery for a solar power installation involves a number of options and trade-offs. The battery selected should be suitable for the available array current and the load demand current, and its capacity must be sufficient to bridge the maximum dark period. A generous margin in advisable. High current capacity may be obtained only at the expense of poor charge retention. Maintenance is, of course, a major consideration in many applications.

Another factor that influences the choice of battery is climate. Climate determines not only the operating environment but also the maximum dark period to be bridged.

Two main types of secondary battery are suitable for this application: nickel-cadmium batteries and lead-acid accumulators. There are several versions of each type, each with its own particular advantages. The properties of the principal versions are shown in Table 1. Characteristic values are averaged from manufacturers' data, which should be consulted before a final choice is made.

Nickel-cadmium

Sealed

Sealed nickel-cadmium (Ni-Cd) batteries are suitable for small installations. They have a long useful life of many charge-discharge cycles and are reliable. Being sealed, they are particularly suitable for applications where battery attitude varies, such as in mobile equipment. On the debit side, their charge retention is poor especially when fully charged, and unit capacities are small.

Unsealed

Unsealed Ni-Cd batteries are made for very high unit capacities. Although they require some maintenance, they have a long working life – up to 20 or 25 years. They will tolerate complete discharge without damage and very many charge-discharge cycles. Their energy density is high, making for compact installations. As with the sealed type, charge retention is not good.

Lead-acid

There are many varieties of the lead-acid accumulator, but for solar applications they can be reduced to three main versions.

Solid electrolyte

These are small-capacity units intended for applications in which charge and discharge are well balanced. Either a gelled electrolyte is used or the electrolyte is combined with some absorbent material so that the disadvantages of a liquid electrolyte are avoided. Thus they are suitable for mobile installations. Maintenance is not required and charge retention is good. However, discharge to less than 50% of capacity can reduce their life.

Antimony-free

Antimony-free or low-antimony accumulators are used for high-capacity units that are required to store energy for long periods. They retain their charge well, have a long working life, tolerate many charge-discharge cycles, and are efficient in operation. Their maintenance requirements are moderate, and, in consequence, they are very suitable for use in conjunction with solar power installations. For some applications their low energy density may be found a disadvantage.

Lead-antimony

Addition of about 15% of antimony to the lead plates of a liquid-electrolyte lead-acid accumulator hardens the plates and permits higher peak discharge currents. Unfortunately, the presence of antimony causes poor charge retention, reduces the number of charge-discharge cycles, and shortens life. The maintenance required depends on type and manufacturer. They are principally used for starter batteries.

Charge regulator

The charge regulator protects the battery, which is particularly important where remote maintenance-free operation is required. It also helps match the panel to the load, improving efficiency and reducing capital cost.

There are two basic types of regulator: one shunts the output of the panels through a resistor when the end-of-charge voltage of the accumulator is reached; the other open-circuits the panels when charging is complete. Most shunt regulators keep the battery voltage constant in the end-of-charge state by dissipating the excess of energy. This is troublesome in high ambient temperatures. Shunt regulators are therefore preferred only for low-power systems (less than 80 W). For higher-power systems the on-off switching series regulator is preferred because of the low resulting dissipation. The single example of a charge regulator given here is a simple shunt regulator for small installations using one or two BPX47A panels. It has been designed to protect cells and panels.

Simple shunt regulator

Fig.15 shows a simple shunt regulator for one-panel or two-panel arrays. It is based on an op-amp comparator circuit, and uses a switched darlington transistor to avoid the complications associated with shunt thyristor operation.

When the accumulator end-of-charge voltage is reached, the solar panels P are shunted through R_{10} by darlington TR_2 which is switched by the op-amp U_1 connected as a comparator. Accumulator voltage V_b is fed to the positive input of the op-amp through the potential divider R_4 R_5; the actual operating voltage is set by adjustment of R_6. Reference voltage V_{ref} for the comparator is obtained from voltage regulator diode D_1 and resistor R_3 decoupled by C_1. The current through the reference circuit is stabilised by current source TR_1; its value is set by adjustment of R_2 to give $V_{ref} = 3$ V.

The value of V_{ref} is chosen in conjunction with the temperature coefficient of D_1 to match the temperature coefficient of the accumulator used. A BZX75-C2V8 voltage regulator diode has a temperature coefficient of -8 mV/°C. The accumulator has a temperature coefficient of -6 mV/°C per cell at a voltage of 2.25 V per cell. Thus:

$$V_{ref} = 2.25 \times (8/6),$$
$$= 3 \text{ V}.$$

The values for the input potential divider for the op-amp are chosen so that the output goes HIGH at the end-of-charge voltage of the accumulator. That value for the accumulator used is 13.5 V; thus:

$$\frac{R_5 + R_6}{R_4 + R_5 + R_6} = \frac{3}{13.5}$$

Transistor TR_2 must be switched cleanly to minimise the dissipation. To achieve this, there must be some hysteresis in the value of V_b for which switching occurs. The circuit of Fig.15 has been designed for a hysteresis of 1.2 V. The output voltage swing of the op-amp is internally limited to about 9 V. Using this value, together with the allowed hysteresis, the value of feedback resistor R_7 can be calculated from:

$$R_7 = R_4(9/1.2).$$

With $R_4 = 10.7$ kΩ, a value of 80.25 kΩ is obtained for R_7; the nearest standard (E48 series) value of 78.7 kΩ is taken.

Darlington transistor type BDX65 is used for TR_2: its current gain (>1000) is sufficient to allow direct drive by the op-amp. Complete switch-off is ensured by the connection of regulator diode D_2 in the base circuit. A

heatsink of thermal resistance 10 °C/W is adequate for TR_2 up to an ambient temperature of 70 °C. The recommended mounting accessories should be used. The full current from two BPX47A panels can be shunted with this arrangement.

The reverse-current protection function is provided by D_3 which is mounted on the same heatsink as TR_2.

As discussed in the section on SOAR, the voltage across each panel should remain above 10 V. For this reason, the value of R_{10} should be kept has high as possible. However, there is a maximum value which will satisfy the relationship:

$$V_{CE(sat)TR2} + I_{S(max)}R_{10} < V_{b(min)} + V_{F(D3)}.$$

For a resistance tolerance for R_{10} of 5%:

$$R_{10(nom)} = \frac{V_{b(min)} + V_{F(D3)} - V_{CE(sat)TR2}}{1.05 I_{S(max)}}$$

Now,

$$V_{b(min)} = V_{b(max)} - \text{hysteresis}.$$

Allowing 0.3 V for tolerances in the sensing circuit:

$$V_{b(min)} = 13.5 - 1.2 - 0.3,$$
$$= 12\,V.$$

For each panel, $V_{F(D3)} = 0.6$ V, $V_{CE(sat)TR2} = 1.7$ V, and $I_{S(max)} = 0.75$ A. Therefore, for one panel, a 13Ω 10 W wirewound resister is required, and for two panels, two 13Ω 5 W wirewound resistors in parallel.

Note that in the design calculation above, it is necessary to know the end-of-charge voltage, the on-load voltages, and their temperature dependence, for the particular accumulator being used.

A parts list for the circuit in Fig.15 is given in the Appendix.

Motor drive circuits

Where a solar array is used to power a motor which must develop a large proportion of its maximum power to be able to start, the motor will require a corresponding minimum current. An example is where the array is driving a water pump, where a certain load of water must be

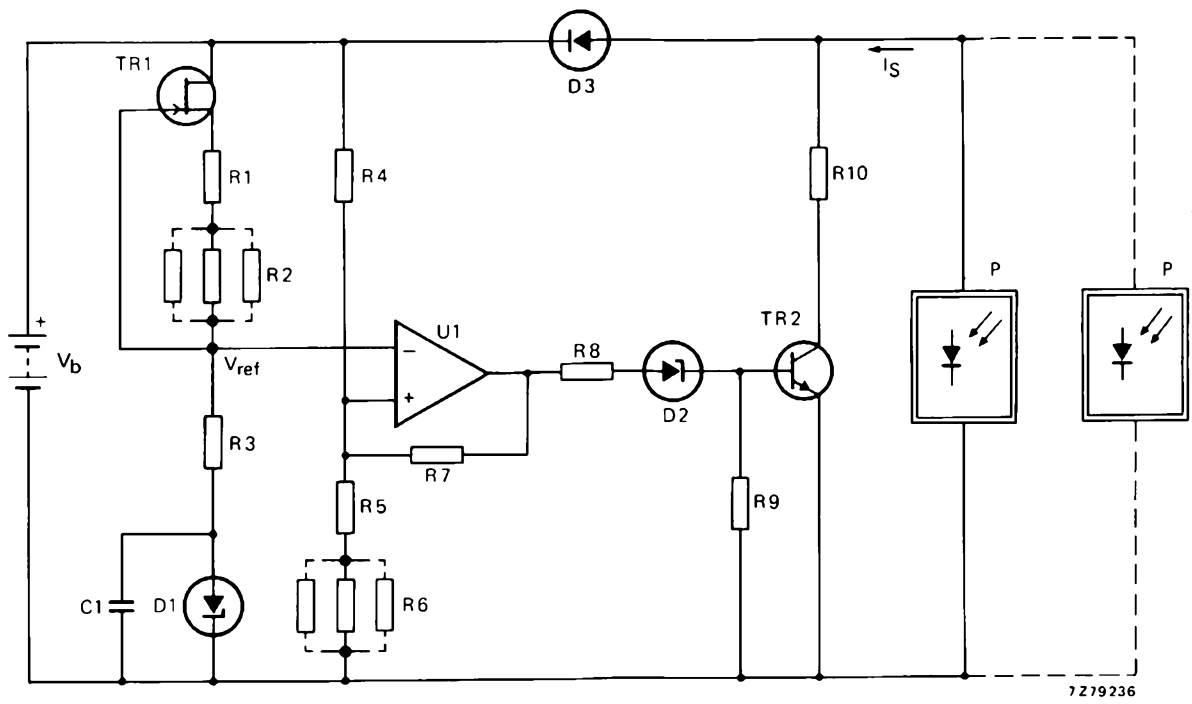

Fig.15 Simple shunt regulator for the output of one or two BPX47A panels

generated before delivery can commence. Under such circumstances, the motor can only operate when virtually the whole output of the array is available. However, this maximum output is only available for a short period during the day.

To overcome this problem, an electric motor drive circuit must be incorporated to ensure that the motor receives sufficient current to develop its starting torque, even when the solar array output is low. Without such provision, either the motor will operate only at around noon, or the array will need to be prohibitively large.

The drive circuit uses the energy from the array to charge a capacitor. The capacitor is discharged through the motor in pulses of current sufficient to provide the starting torque. The duration of the pulses depends on the rate at which the capacitor is recharged by the array. When the output of the array is low, the current pulses will be of short duration and the motor will turn slowly. As the array output increases, so the pulse duration increases and the motor accelerates. The minimum current can easily be calculated once the load, transmission, and motor characteristics are known.

Note that when a solar array is used to power a water pump, the energy storage function is provided by the liquid reservoir, and the accumulator and associated charge regulator are not required.

Drive circuit for d.c. motors

Fig.16 shows a d.c. motor drive circuit built around one half of a LOCMOS HEF4583B dual Schmitt trigger IC. Together with TR_4, TR_5, and C_2, U_1 forms a triangular waveform generator. When the output pin 4 of U_1 is LOW, C_2 is charged through TR_4. When the voltage across C_2, sensed by pin 9, exceeds a preset level, pin 4 goes LOW, and C_2 is discharged through TR_5. When the voltage at pin 9 falls below a second lower set level, U_1 switches again, pin 4 goes LOW, and the cycle repeats. The upper and lower threshold voltages are set by R_{16} and R_{17}. The mean level of the waveform is half the voltage across D_6 (= 8.1/2 V). Its repetition frequency is determined by C_2, R_{12}, and R_{13}.

The voltage across C_2 is fed to the base of TR_3 which forms a long-tailed pair with TR_2. The base of TR_2 is fed from the potentiometer across C_1, which, in turn, is connected across the solar array. When the instantaneous value of the sawtooth waveform across C_2 exceeds the voltage applied to the base of TR_2, only TR_3 conducts and TR_1 is cut off. Conversely, when the level of the sawtooth is below the voltage on the base of TR_2, only TR_2 conducts and hence TR_1 is switched on. Note that whether TR_1 is on or off depends on the relationship between the voltages applied to the bases of TR_2 and TR_3, and not on their absolute values.

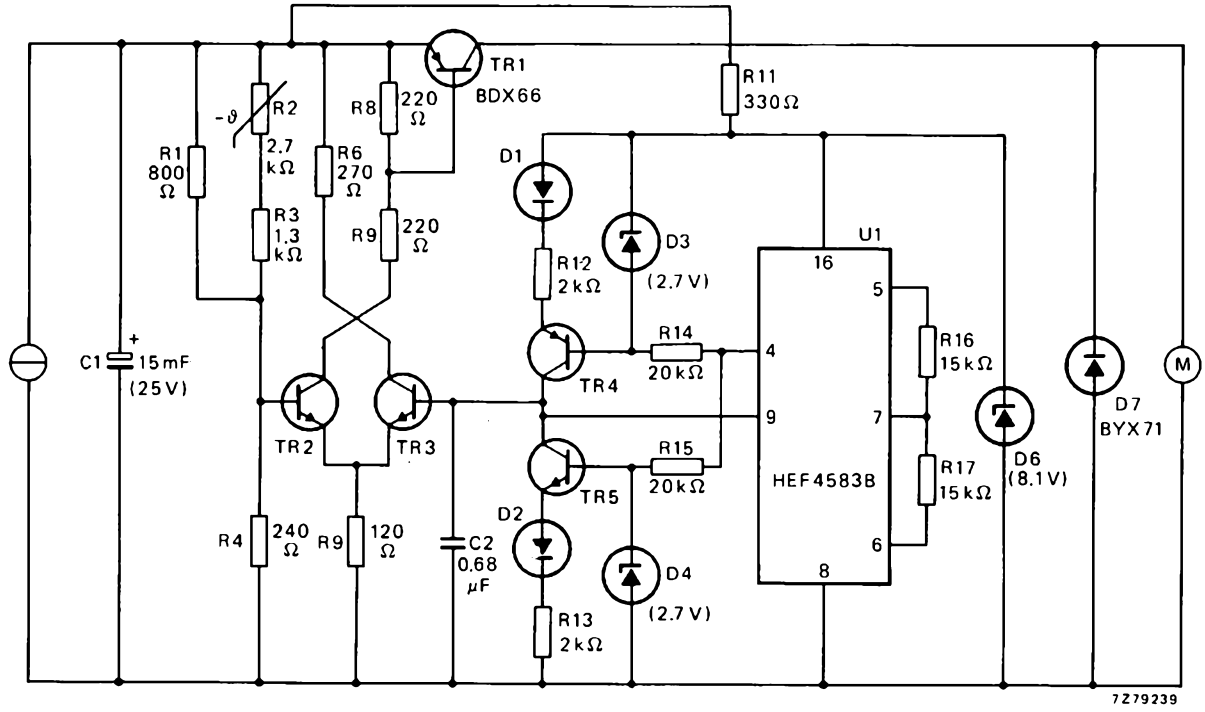

Fig.16 Drive circuit for d.c. motor

The control voltage range on C_1 is about 1.5 V, centred about the panel optimum operating voltage. Because this optimum voltage is temperature dependent, the potential divider that feeds the base of TR_2 includes NTC resistor R_2. This ensures that optimum operation is maintained over a wide temperature range.

At high levels of insolation, the drain on C_1 will be less than the rate of supply from the array: TR_1 then conducts continuously. As the radiation falls so that the voltage on C_1 falls to within the control range, TR_1 starts to switch, and the motor runs at reduced speed.

Drive circuit for a.c. motors

Three-phase squirrel-cage induction motors have a number of advantages over d.c. motors. They require no maintenance, their construction is simpler and, thus, cheaper, a large range of sizes is available from stock, and, finally, their power densities and power-to-weight ratios are generally better. These properties make them more suitable for use in inaccessible places, such as in submerged pump units.

As with d.c. motors, a.c. squirrel-cage motors require a large proportion of their nominal running current to be able to start. Thus, to power these motors efficiently from a solar array requires not only the production of three-phase power, but also full-current pulses at low levels of radiation. In this way, the torque of the motor is maintained down to low speeds and low levels of insolation.

Fig.17 shows the elements of a drive circuit that generates constant-frequency variable-pulse-width three-phase power. Capacitor C_1 is charged by the solar array. A switched-mode power supply (light, efficient, reliable) converts part of the array output into 28 V d.c. to supply the control unit circuitry. Resistor R_1 loads the array until the output is sufficient to start the motor; it is then switched out of circuit. Thus the motor is prevented from starting until the array output is greater than the thyristor holding current. This also prevents the triggering of catastrophic thyristor combinations. An NTC resistor in the control unit ensures that the solar array operating point is kept close to the optimum over a wide temperature range. The array output, close to 300 V, is applied to the control unit which detects the available power level.

THE FUTURE FOR SOLAR ARRAYS

Solar energy is getting cheaper: particularly solar-cell energy. The familiar trends – improved production, increased production, improving performance – are all contributing to the steady decline in installed cost. Installation size is increasing; from watts, through tens

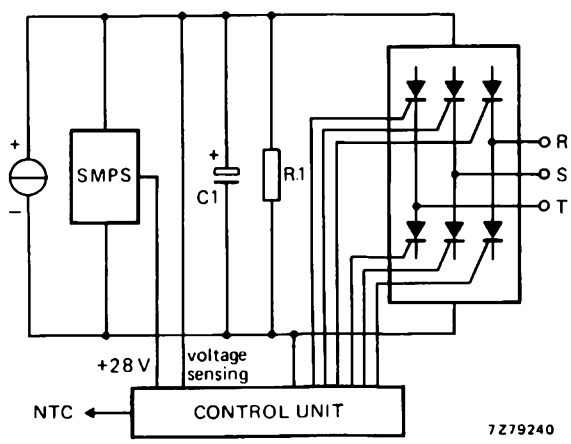

Fig.17 Outline of a drive circuit for an a.c. three-phase squirrel-cage induction motor

of watts and hundreds of watts, solar power capacities are now entering the kilowatt range.

Modern techniques enable the output of solar arrays to be converted into power at any voltage or frequency, cheaply and efficiently. The power produced can, of course, be converted into other forms, mechanical or thermal.

Despite the improvements, solar power is nowhere as cheap as mains electricity from a national distribution system. There are, however, many places where power is needed but where the national distribution systems do not reach. Some activities, such as mining and refining, that take place in remote areas consume large quantities of energy. If power can be provided cheaply enough, it may become attractive to process ores at the mine and transport (another energy-consuming process) only the refined metal. Solar power could be attractive in such cases, even now.

Clearly, the situation is changing rapidly. Even without the almost inevitable development of new device technology, the normal industrial progress from small to large quantity manufacture will certainly erode cost at an accelerating rate. Thus, solar energy cannot be ignored: it is already important, and may become vital.

APPENDIX

Components, Fig.15

U_1	μA741T
TR_1	BFW10
TR_2	BDX65 (with 56201 mounting accessories)
D_1	BZX75-C2V8
D_2	BZX75-C2V8
D_3	BYX25
C_1	100 nF
R_1	1 kΩ
R_2	adjust for V_{ref} = 3 V
R_3	332 Ω
R_4	10.7 kΩ
R_5	2.1 kΩ
R_6	adjust to switch on TR_2 at V_b = 13.5 V
R_7	78.7 kΩ
R_8	1.1 kΩ
R_9	750 Ω
R_{10}	see text

All resistors MR25 E-96 series metal film

Application note

BZW10 transient suppression bridge for telephones

The electromagnetic components of subscriber telephone apparatus are being progressively replaced by active solid-state devices which can provide the many new facilities, extended services and high reliability demanded by the subscribing public. However, since semiconductors cannot function if the polarity of their supply voltage is incorrect, a bridge rectifier must be interposed between the solid-state circuits and the telephone lines. The semiconductors will then receive a constant polarity supply voltage regardless of which way round the lines are connected to the apparatus.

Subscriber telephone apparatus must also be protected against high-voltage transients resulting from induced current surges (possibly secondary lightning effects) flowing through the lines. Some protection can be provided by a passive component with a non-linear voltage/current characteristic such as a voltage-regulator diode, voltage-dependent resistor, spark gap, or even a gas-discharge lamp. Even better protection can be achieved by using transient suppressor diodes which have been designed specifically for this purpose.

The two protection functions are now combined in one inexpensive, compact component. This new component, the BZW10, contains four bridge-connected transient suppressor diodes which function as a polarity guard during normal operation. In the event of line current surges, the BZW10 effectively protects the apparatus by absorbing most of the excess energy and providing a limited voltage output.

This note is based on a laboratory report. Requests for additional data should mention the title of the note, the issue of E.C.&A. in which it appeared, and the nature of the applicant's interest.

TRANSIENT SUPPRESSOR DIODE CHARACTERISTICS

Figure 1 shows that, when a transient suppressor diode is forward biased, it behaves as a normal diode. When the polarity of the applied voltage is reversed however, only a small leakage current flows through the diode. This leakage current remains almost constant over a wide range of applied voltage. If the applied reverse voltage increases sufficiently to reach the breakdown voltage, the current through the diode rapidly increases to a high value.

In Fig. 2 two of the diodes are forward-biased and the other two are reverse-biased. Which diodes are in which state, depends on the polarity of the input voltage. If the input voltage increases from its steady-state value (stand-off voltage = 12 V for the BZW10) to the breakdown voltage, breakdown occurs in the two reverse-biased diodes. The output voltage from the bridge is then limited to the clamping voltage. Four bridge-connected transient suppressor diodes therefore behave differently to a conventional bridge rectifier because they provide a limited voltage output.

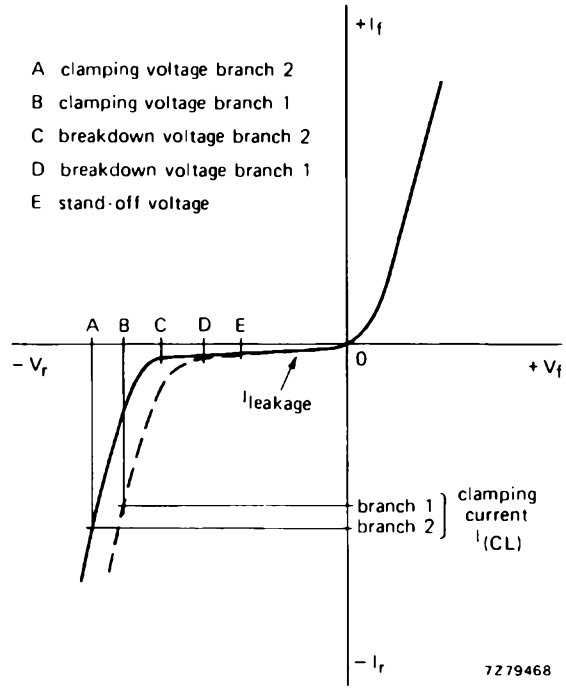

Fig.1 Transient suppressor diode characteristic

POLARITY-GUARD FUNCTION

Figure 3 shows the BZW10 transient suppressor bridge connected to a telephone set. During normal operation, the bridge provides a constant-polarity supply voltage regardless of the polarity of the line voltage. The bridge imposes little additional load on the telephone lines because the leakage current through the reverse-biased pair of diodes (<80 μA) is negligible compared with the current consumption of a telephone set (≈10 mA to 100 mA).

TRANSIENT SUPPRESSOR FUNCTIONS

The transient suppressor function of the BZW10 is somewhat more difficult to define. If an induced current surge passes through the impedance of the lines and the BZW10, a high-voltage spike will occur across the input pins of the BZW10. Under these conditions, although the surge current will be divided between the two parallel branches of the bridge, the two currents will not necessarily be equal because of the difference between the breakdown voltages of the individual diodes as shown in Fig. 1. However, the lower of the two breakdown voltages must not be sufficient to cause damage to the solid-state circuits of the telephone set. To determine the actual voltage level that will occur under these conditions, it is first necessary to define the secondary effects of a lightning strike on the telephone lines.

Figure 4(b) shows that, when the BZW10 is subjected to this test, the peak current through the bridge just reaches the specified peak clamping current ($I_{(CL)SM}$) of 50 A. Under these conditions, the output from the BZW10 is clamped at less than 30 V.

The BZW10 has a stand-off voltage of 12 V, a non-repetitive peak clamping current of 50 A and a maximum output clamping voltage of 30 V. These characteristics make the BZW10 compatible with our two-tone dialling integrated circuit, type TDA1077, described in E.C. & A. 1 no. 1. It is of course possible to manufacture transient suppressor diodes with different characteristics. If the stand-off voltage is increased, the non-repetitive peak clamping current is reduced.

Several standard test circuits for simulating secondary lightning effects are at present being discussed internationally in an attempt to define the requirements for protection devices. One of these test circuits, originating in Germany and published in FTZ specification 10/700, is shown in Fig. 4(a). In this circuit, a 10 μF capacitor is charged to 2 kV and discharged, via a spark gap and RC network, into the device being tested. The test must be repeated six times at one minute intervals. After the third test, the connections to the device being tested must be reversed.

If a purely resistive 600 Ω load (simulated telephone set) is connected to this circuit, the voltage across the load peaks at 1875 V.

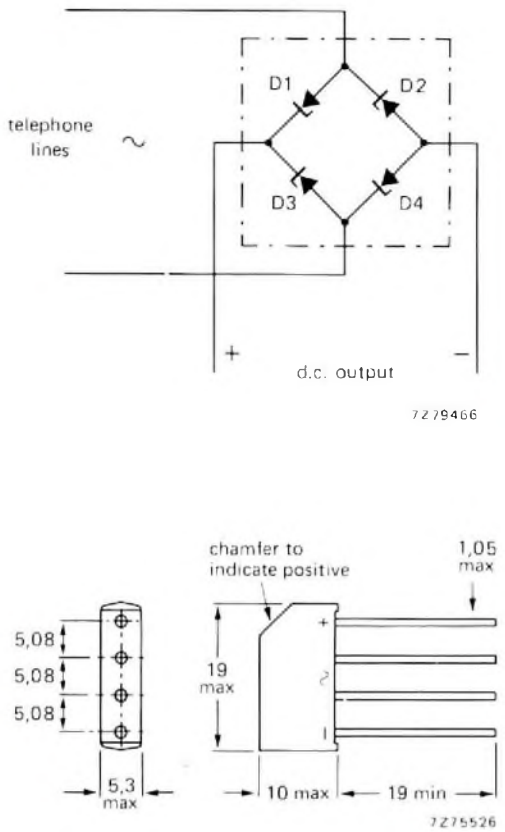

Fig.2 The BZW10 transient suppressor bridge

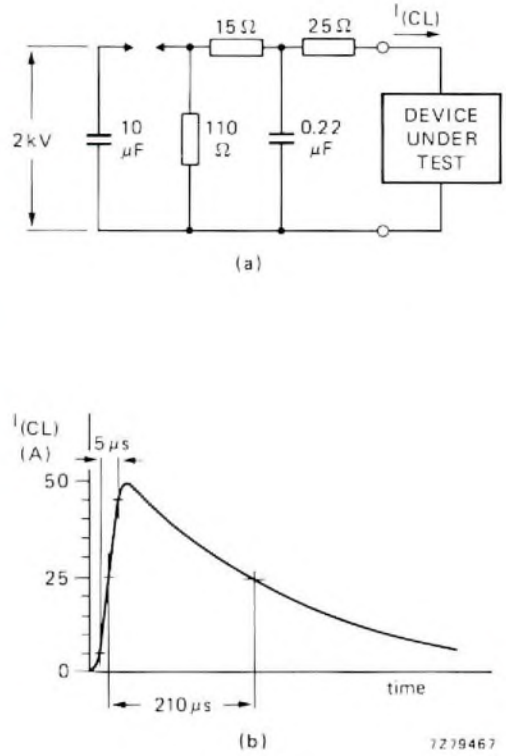

Fig.4 Simulating the secondary effects of a lightning strike.
(a) test circuit in accordance with FTZ10/700
(b) bridge rectifier clamping current as a function of time

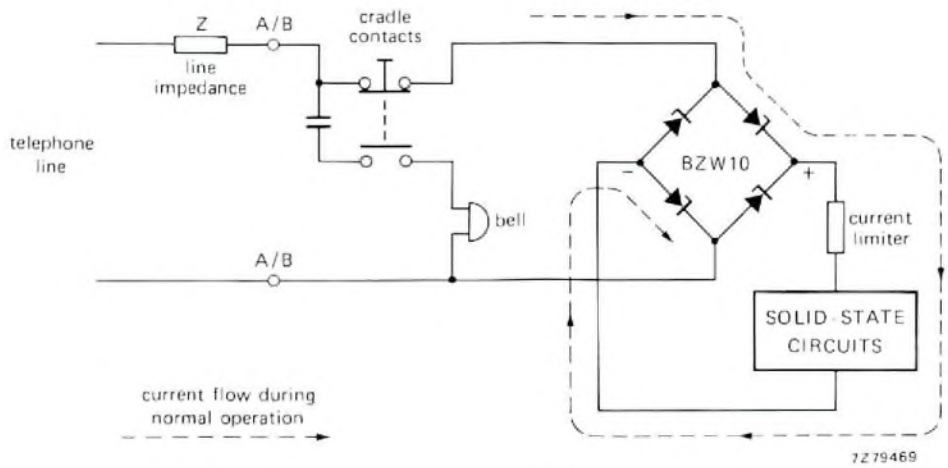

Fig.3 The BZW10 connected to a telephone set

Research news

WORLD'S FIRST DIODE LASER OPTICAL RECORDING SYSTEM

An ultra-compact diode laser optical recording system, the world's first, has recently been introduced by Philips. It allows high-density recording and retrieval of up to 10^{10} bits of data, equivalent to about 500 000 type-written pages, on a pre-grooved 30 cm disk. This capacity represents an improvement of ten times compared with the most advanced magnetic disk pack systems currently available. The system offers direct read-after-write with random access; any address can be reached in a mean time of 250 ms, providing virtually instant access to 5×10^9 bits (the capacity of one side of the disk).

The system uses similar techniques to those developed for VLP (Video Long Play). The real breakthrough, however, has come with the development of a suitable miniature diode laser and matching recording material. The laser used is of the AlGaAs DH type and employs a 0.1 mm square semiconductor chip housed in a transistor-sized encapsulation. Despite its small size, the device develops a pulsed light output power equivalent to that of a large gas laser and its associated modulator. The complete optical system, weighing only 40 g, is shown in Fig. 1.

Reading and writing

The laser light is focused onto the tellurium-based recording material of the disk and data is written, or 'burnt' in, by melting a series of micron-sized holes (Fig. 2). Data produced in this way is read by detecting the difference in intensity between the high light level reflected from the surface of the disk and the low light level reflected from the hole, where most of the light escapes. These high and low detected light levels are converted into electronic binary signals and represent data bits.

The disks used in the system have a 45 000 track pre-grooved spiral, divided into 128 sectors per track. Each sector is identified by an address heading, formed in relief using VLP mastering and replicating techniques. The optical system tracks along the pre-groove, whether or not it contains data, and at the same time it finds and reads sector address headings. Thus data can be posted virtually anywhere on the useful recording area, thereby providing random access for both recording and writing. Up to 1 K user bits of data can be written into each of the 45 000 x 128 sectors. At a disk rotation speed of 2.5 revolutions per second, this gives a mean access time of 250 ms. The writing speed is 300 K user bits per second, but no difficulties are envisaged in running the system at much higher speeds.

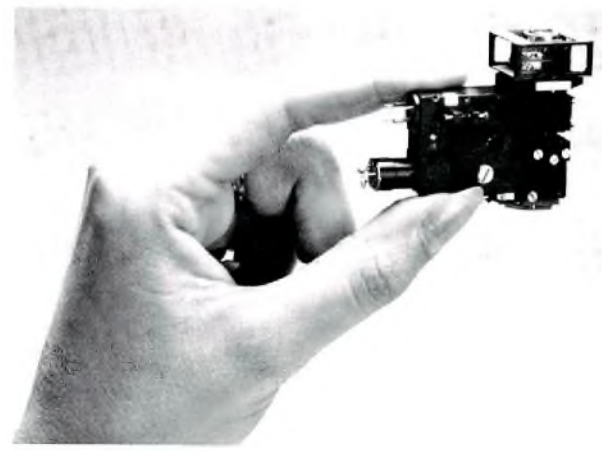

Fig.1 Diode laser optical read/write head

These notes report activities of Philips research laboratories and do not imply commercial availability of any product embodying the described results. For further information, written application should be made to the Publicity Department, Philips Research Laboratory, Eindhoven, The Netherlands.

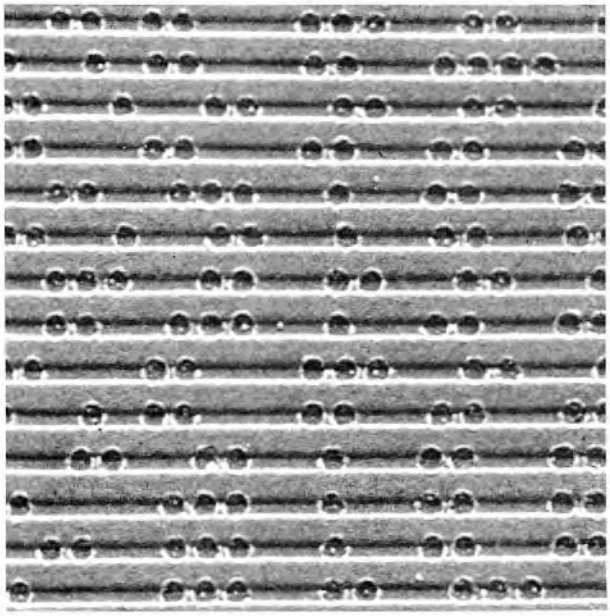

Fig.2 Electron micrograph of pre-groove with data written in

Applications

Two main applications areas are foreseen, one being the storage of alphanumeric information, and the other the storage of images. The latter demands a high bit storage, which is now practical with the 10^{10} bit capacity of the new system. Therefore, since both words and images can be recorded and retrieved with fast random access, this new recording medium may well become the electronic equivalent of paper and microfilm. For example, optical systems will certainly be integrated into word processing systems for electronic filing of all documents including images received through facsimile devices.

SEMICONDUCTOR LASER CREATES ITS OWN LENS

Scientists at the Philips Research Laboratories of the North American Philips Corporation in the U.S.A. are developing a new technique in which a semiconductor laser is made to create a suitable lens for itself during manufacture. This can eliminate the need for separate miniature lenses which, because of their size, are difficult to fabricate using conventional methods. Such lenses are required in many semiconductor laser applications, such as in optical communications and video long play disk systems, to achieve the desired narrow beamwidths. For example, in a conventional semiconductor laser, the active layer emits a beam with a divergence of greater than 40°. If such a laser is coupled directly to an optical fibre, there is a considerable loss of intensity because of the dispersion of the beam. It is necessary therefore to mount a lens between the laser and the optical fibre to adapt the beam to the acceptance angle of the fibre.

The new method of creating an inbuilt lens is as follows. A layer of negative photoresist (that is, one that hardens on exposure to light), a few micrometres thick, is applied to that surface of the laser where the beam is to be emitted. This layer is then irradiated with ultraviolet and the photoresist hardens. A second layer of photoresist is then applied and the laser is switched on. After a few hours exposure to the laser light, this second layer is developed in the usual way. The parts not irradiated by the laser light are removed, and a small lens remains at the spot where light is emitted (see Fig.3). Fig.4 shows that the divergence of the beam is approximately halved.

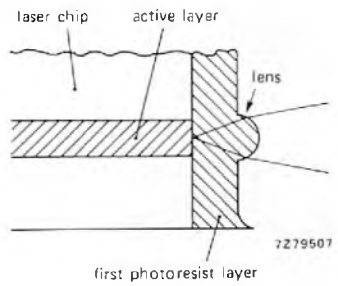

Fig.3 Laser and lens

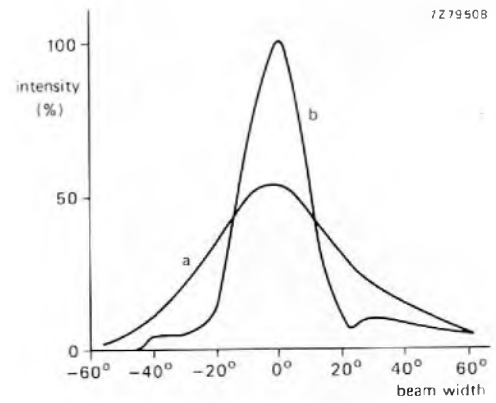

Fig.4 Intensity plotted against beamwidth for (a) an untreated laser and (b) a laser with a lens made from photoresist

Abstracts

2/3"-Plumbicon-Röhre mit erhöhter Leistungsfähigkeit

Bei einer neu konzipierten 2/3"-Plumbicon® Röhre wird die Auflösung verbessert und die Trägheit verringert: durch den Einsatz einer dünneren Fotoschicht in Verbindung mit einem neuen Dioden-Elektronenstrahlsystem sowie durch die Möglichkeit, zusätzliches Auflicht anzuwenden.

Dies hat zu einer sehr hochentwickelten Kameraröhre geführt, die für die elektronische Berichterstattung (EB) und für bestimmte Studio- oder Aussenanwendungen (EFP; Electronic Field Production) geeignet ist.

Frequenzmeszsystem für AM/FM-Empfänger

Das beschriebene System mit nur zwei integrierten Schaltungen ermöglicht eine digitale Frequenzanzeige in den Wellenbereichen UKW, KW, MW und LW; im UKW-Bereich kann zwischen Frequenz- und Kanalanzeige umgeschaltet werden. Das Frequenzmeszsystem kann durch externe Beschaltung im weiten Bereichen auf die im Gerät verwendeten AM- und FM-Zwischenfrequenzen programmiert werden. Da das System in sich abgeschlossen ist, läszt es sich leicht in netzbetriebener Empfänger nachrüsten; auch kann es an Batteriegeräte adaptiert werden. Frequenz bzw. UKW-Kanalnummer werden auf einer 4½-stelligen LED-Anzeige wiedergegeben.

8X300 – ein schneller Mikroprozessor für Steueranwendungen

Die Schaltung 8X300 ist ein bipolarer Mikroprozessor für schnelle Steueraufgaben. Als erster Beitrag einer Serie, die den Anwendungsmöglichkeiten dieses Mikroprozessors und den verfügbaren Entwicklungshilfen gewidmet ist, beschreibt der vorliegende Aufsatz den internen Aufbau und den Befehlsvorrat des Mikroprozessors 8X300. Hierbei wird dem speziellen Ein-/Ausgabesystem, das in einem einzigen Befehlszyklus von 250 ns Dauer eine komplette Datenverarbeitung – von der Dateneingabe über die Verarbeitung bis zur Datenausgabe – erlaubt, besondere Beachtung geschenkt.

30AX – ein selbstkonvergierendes 110° in-line Farbbildsystem

Mechanische und elektromechanische Verbesserungen machen jegliche Form von Konvergenz-, Farbreinheits- oder Rasterkorrekturen bei dem aus Bildröhre und Ablenkeinheit bestehenden 30AX-System überflüssig.

Engere mechanische Toleranzen und die Passauflagepunkte auf dem einteiligen Kunststoffträger der Ablenkeinheit ermöglichen es, Bildröhre und Ablenkeinheit durch einfaches Zusammenschieben auszurichten. Ein in das Elektronenstrahlsystem eingesetzter, speziell aufmagnetisierter Drahtring kompensiert die Streuungen im System. Die genaue Verteilung des Ablenkfeldes durch Doppel-Strangwickeltechnik und durch in die Ablenkspulen eingelegte Feldformer bewirkt ein komafreies Ablenkfeld. Ein kleinerer Vergrösserungsfaktor der Fokuslinse und eine Quadrupol-Verformung des Linsenfeldes in der Nähe der Katode führt zu kleinerem Punktdurchmesser und einer gleichmässigeren Fokusqualität besonders bei hohen Strahlströmen.

Solarbatterien für terrestrische Anwendungen

Für eine Reihe von Anwendungen stellt die Solarenergie schon jetzt eine zukunftsichere, wirtschaftliche Alternative zu den herkömmlichen Energiequellen dar.

Dieses Artikel beschreibt den Aufbau und die Wirkungsweise fotovoltaischer Solarzellen und Solarbatterien sowie ihren Einsatz in terrestrischen Anwendungen. Auszerdem werden Gesichtspunkte diskutiert, die für den Entwurf praxisgerechter, preisgünstiger Solargeneratoren von Bedeutung sind. Detaillierte Angaben bezüglich geeigneter Akkumulatoren, Ladestromregler sowie Motorantriebschaltungen beschlieszen die Ausführungen.

Tube Plumbicon 2/3 inch à performances améliorées

Dans une nouvelle version du tube Plumbicon 2/3 d'inch, le trainage est minimisé et la résolution est perfectionnée par l'emploi d'une couche photoconductive plus mince, associée à un nouveau canon à diode et par polarisation lumineuse de cible. Le résultat est un tube de prise de vues aux possibilités variées, convenant au reportage et à l'utilisation générale en studio.

Commande électronique d'équipements radio et audio

Le système décrit, basé sur deux circuits intégrés, peut être employé en très haute fréquence (FM), ondes courtes, ondes moyennes et ondes longues, et peut être programmé pour compenser une large gamme de fréquences intermédiaires. Etant autonome, il peut aisément être ajouté à des récepteurs existants, fonctionnant sur secteur, et peut également être adapté à des récepteurs fonctionnant sur piles. Un affichage LED à 4½ digits indique la fréquence ou le numéro du canal.

Le 8X300, un microprocesseur de commande ultra-rapide

Le 8X300 est un microprocesseur bipolaire conçu pour des applications de commande ultra-rapide. Cet article, qui est le premier d'une série qui sera consacrée à ses applications et à sa fabrication, décrit l'architecture et le jeu d'instructions du 8X300; une attention particulière est consacrée au système spécial d'entrée/sortie, qui permet l'entrée, le traitement et la sortie des données en un cycle unique de 250 ns.

Le système 30AX tube reproducteur de télévision couleur 110° en ligne à auto-alignement

Les améliorations de conception mécanique et électromagnétique que réuni l'ensemble tube-déviateur 30AX rendent inutile tout réglage de la convergence, de la pureté des couleurs ou de l'orientation de la trame. Grâce à des tolérances mécaniques plus serrées et à la présence de bossages de positionnement sur le porte-bobine monobloc, il suffit de rapprocher l'un de l'autre le tube et le déviateur pour les aligner. Une bague fixe, à aimantation permanente, située dans le canon à électrons compense les tolérances d'alignement des canons individuels. Un réglage précis de la répartition du champ de déviation par des conformateurs de champ incorporés à des bobinages "flangeless" (sans rebord), à enroulement du type "pin-indexed" aux deux extrémités, assure l'absence de coma. Dans le canon électronique, une lentille principale plus faible et une déformation quadripôle du champ de la lentille à l'avant de la cathode assurent une diminution de la dimension du spot et une augmentation de l'uniformité de la concentration, en particulier aux courants de faisceau élevés.

Panneaux solaires pour applications terrestres

Dans certaines applications, l'énergie solaire devient une solution économique viable, capable de remplacer les sources classiques d'énergie. Le présent article décrit le fonctionnement et la construction de piles solaires et de panneaux solaires photovoltaïques et leur emploi dans les applications terrestres. Il discute également des facteurs qui jouent un rôle dans la conception de générateurs solaires rentables et utilisables en pratique et donne des détails sur les accumulateurs, régulateurs de charge et circuits d'entrainement de moteur appropriés.

Tubo Plumbicón de 2/3 pulgadas con rendimiento mejorado

En una nueva versión del tubo Plumbicón de 2/3 pulgadas, el retardo es minimizado y la resolución mejorada mediante el empleo de una capa fotoconductora más delgada en combinación con un nuevo cañón diodo, y la posibilidad de polarización de iluminación. Así se obtiene un tubo de cámara altamente versátil adecuado para ENG, EFP y aplicaciones generales de estudio.

Control electrónico de equipos de radio y audio

El sistema descrito se basa en dos circuitos integrados que pueden emplearse con v.h.f. (f.m.), onda media y onda larga, y pueden ser programados para compensar en un amplio margen de frecuencias intermedias. Siendo autónomo, puede añadirse fácilmente a receptores alimentados por red y también puede ser adaptado para aparatos de radio alimentados por batería. Un visualizador LED de 4½ dígitos indica frecuencia o número de canal.

El 8X300 un microprocesador orientado para control y elevada velocidad

El 8X300 es un microprocesador diseñado para aplicaciones de control de elevada velocidad. Como primero de una serie que ha de ser dedicada a sus aplicaciones y posibilidades de soporte, este artículo describe la arquitectura e instrucciones del 8X300, dedicando particular atención al sistema I/O especial que permite la entrada, el proceso y la salida de datos dentro de un solo ciclo de 250 ns.

Sistema de TV color en linea de 110° con autoposicionado 30AX

Mejoras mecánicas y electromagnéticas se combinan para evitar la necesidad de cualquier clase de ajuste de convergencia, pureza de color, orientación de trama en la combinación tubo-unidad de desviación 30AX. Tolerancias mecánicas más estrechas, junto con salientes de posicionado en el soporte de la bobina de una sola pieza, hacen posible alinear el tubo y la unidad de desviación mediante simple presión. Un anillo fijo imantado permanentemente en el conjunto de cañones electrónicos compensa tolerancias en el posicionado de cada cañón. Un preciso control en la distribución del campo de desviación, mediante formadores de campo alojados en el soporte de los bobinados sin pestaña posterior y con multisección en ambos extremos, elimina la aberración de coma. En el cañón electrónico una lente principal más débil y una deformación de cuadripolo del campo de la lente delante del cátodo contribuyen a una disminución del tamaño del punto luminoso y a un aumento de la uniformidad del foco, especialmente para elevadas corrientes de haz.

Paneles solares para aplicaciones terrestres

En algunas aplicaciones, la energía solar se convierte ahora en una alternativa económica viable como fuente de energía convencional. Este artículo describe el funcionamiento y la contrucción de paneles solares y células solares fotovoltaicas, y su empleo en aplicaciones terrestres. También analiza factores que afectan el diseño de generadores solares con buena relación coste/rendimiento, y da detalles de acumuladores, reguladores de carga y circuitos excitación de motor adecuados.

Authors

P. G. J. Barten graduated in physics at the Technical University at Delft in 1953. After military service in the Royal Dutch Air Force he joined the Research Laboratory of N.V. Philips' Gloeilampenfabrieken in 1956 where he was engaged in development of storage and pickup tubes. In 1961 he transferred to the Electron Tubes Division; since 1969 he has been responsible for television picture tube development. He is a member of the Dutch Physical Society and the Royal Institute of Engineers. He is author of four technical papers and holds 33 patents.

A. A. J. Franken was born in Roosendaal, The Netherlands, in March 1941. He studied physics and electronics at the University of Amsterdam from 1959 and obtained a doctorate in 1965. Two years later he joined Philips, working in the Development and Applications group of the Medical Systems Division, and specialised in X-ray image intensifier tv systems. Since 1976 he has worked in the Applications Group, tv tubes, Elcoma.

C. Franx was born in Rotterdam in 1925 and graduated from the Technical University at Delft in 1951. Joining Philips in 1952, he was first involved in the development of quartz crystal elements and, later, of ultrasonic delay lines. From 1969 to 1977 he was concerned with hybrid integrated circuits and interconnection technologies. Since then, as a member of the Energy Systems group, he has been primarily concerned with solar energy systems.

J. Kaashoek graduated in electronics at the Technical University at Delft in 1954. He then joined the Research Laboratory of N.V. Philips' Gloeilampenfabrieken where he began the studies of the electron-optics of cathode-ray tube deflection that later formed the basis for his doctoral dissertation at the Technical University of Eindhoven. He is now chief engineer in charge of the components design laboratory of Philips' Television Division. A member of the Royal Institute of Engineers and the Netherlands Radio and Electronics Society, he is author of seven technical papers and holds seven patents.

J. van Straaten was born in Haarlem, the Netherlands, in 1943. He completed his studies at the Technical High School at Utrecht in 1965 and joined Philips Research Laboratories where he investigated the high-frequency behaviour of tuner transistors. After military service in 1966 and 1967 he joined the IC Development Centre of Philips Elcoma Division at Nijmegen. Until 1975 he was concerned with the design of integrated circuits for television applications. He is now chief engineer of the bipolar logic design group in charge of the development of 'analogics' for consumer products. He holds 9 patents.

E. D. van Veldhuizen graduated in electrical engineering at The Hague in 1958. Initially, he worked with electronic office equipment, but soon changed over to computers. In 1964, he joined Philips Data Systems, where he was involved in the design of main-frame and mini-computers and the testing of prototypes. In 1976, he moved to the Central Application Laboratory of Elcoma, where he is now responsible for the applications of bipolar LSI circuits.

Electronic components and materials

for professional, industrial and consumer uses

from the world-wide Philips Group of Companies

Argentina: FAPESA I.y.C., Av. Crovara 2550, Tablada, Prov. de BUENOS AIRES, Tel. 652-7438/7478.
Australia: PHILIPS INDUSTRIES HOLDINGS LTD., Elcoma Division, 67 Mars Road, LANE COVE, 2066, N.S.W., Tel. 427 08 88.
Austria: ÖSTERREICHISCHE PHILIPS BAUELEMENTE Industrie G.m.b.H., Triester Str. 64, A-1101 WIEN, Tel. 62 91 11.
Belgium: M.B.L.E., 80, rue des Deux Gares, B-1070 BRUXELLES, Tel. 523 00 00.
Brazil: IBRAPE, Caixa Postal 7383, Av. Brigadeiro Fari Alima, 1735 SAO PAULO, SP, Tel. (011) 211-2600.
Canada: PHILIPS ELECTRONICS LTD., Electron Devices Div., 601 Milner Ave., SCARBOROUGH, Ontario, M1B 1M8, Tel. 292-5161.
Chile: PHILIPS CHILENA S.A., Av. Santa Maria 0760, SANTIAGO, Tel. 39-40 01.
Colombia: SADAPE S.A., P.O. Box 9805, Calle 13, No. 51 + 39, BOGOTA D.E. 1., Tel. 600 600.
Denmark: MINIWATT A/S, Emdrupvej 115A, DK-2400 KØBENHAVN NV., Tel. (01) 69 16 22.
Finland: OY PHILIPS AB, Elcoma Division, Kaivokatu 8, SF-00100 HELSINKI 10, Tel. 1 72 71.
France: R.T.C. LA RADIOTECHNIQUE-COMPELEC, 130 Avenue Ledru Rollin, F-75540 PARIS 11, Tel. 355-44-99.
Germany: VALVO, UB Bauelemente der Philips G.m.b.H., Valvo Haus, Burchardstrasse 19, D-2 HAMBURG 1, Tel. (040) 3296-1.
Greece: PHILIPS S.A. HELLENIQUE, Elcoma Division, 52, Av. Syngrou, ATHENS, Tel. 915 311.
Hong Kong: PHILIPS HONG KONG LTD., Elcoma Div., 15/F Philips Ind. Bldg., 24-28 Kung Yip St., KWAI CHUNG, Tel. NT 24 51 21.
India: PHILIPS INDIA LTD., Elcoma Div., Band Box House, 254-D, Dr. Annie Besant Rd., Prabhadevi, BOMBAY-25-DD, Tel. 457 311-5.
Indonesia: P.T. PHILIPS-RALIN ELECTRONICS, Elcoma Division, 'Timah' Building, Jl. Jen. Gatot Subroto, P.O. Box 220, JAKARTA, Tel. 44 163.
Ireland: PHILIPS ELECTRICAL (IRELAND) LTD., Newstead, Clonskeagh, DUBLIN 14, Tel. 69 33 55.
Italy: PHILIPS S.p.A., Sezione Elcoma, Piazza IV Novembre 3, I-20124 MILANO, Tel. 2-6994.
Japan: NIHON PHILIPS CORP., Shuwa Shinagawa Bldg., 26-33 Takanawa 3-chome, Minato-ku, TOKYO (108), Tel. 448-5611.
(IC Products) SIGNETICS JAPAN, LTD., TOKYO, Tel. (03) 230-1521.
Korea: PHILIPS ELECTRONICS (KOREA) LTD., Elcoma Div., Philips House, 260-199 Itaewon-dong, Yongsan-ku, C.P.O. Box 3680, SEOUL, Tel. 794-4202.
Malaysia: PHILIPS MALAYSIA SDN. BERHAD, Lot 2, Jalan 222, Section 14, Petaling Jaya, P.O.B. 2163, KUALA LUMPUR, Selangor, Tel. 77 44 11.
Mexico: ELECTRONICA S.A. de C.V., Varsovia No. 36, MEXICO 6, D.F., Tel. 533-11-80.
Netherlands: PHILIPS NEDERLAND B.V., Afd. Elonco, Boschdijk 525, 5600 PD EINDHOVEN, Tel. (040) 79 33 33.
New Zealand: PHILIPS ELECTRICAL IND. LTD., Elcoma Division, 2 Wagener Place, St. Lukes, AUCKLAND, Tel. 867 119.
Norway: NORSK A/S PHILIPS, Electronica, Sørkedalsveien 6, OSLO 3, Tel. 46 38 90.
Peru: CADESA, Rocca de Vergallo 247, LIMA 17, Tel. 62 85 99.
Philippines: PHILIPS INDUSTRIAL DEV. INC., 2246 Pasong Tamo, P.O. Box 911, Makati Comm. Centre, MAKATI-RIZAL 3116, Tel. 86-89-51 to 59.
Portugal: PHILIPS PORTUGESA S.A.R.L., Av. Eng. Duharte Pacheco 6, LISBOA 1, Tel. 68 31 21.
Singapore: PHILIPS PROJECT DEV. (Singapore) PTE LTD., Elcoma Div., P.O.B. 340, Toa Payoh CPO, Lorong 1, Toa Payoh, SINGAPORE 12, Tel. 53 88 11.
South Africa: EDAC (Pty.) Ltd., South Park Lane, New Doornfontein, JOHANNESBURG 2001, Tel. 24/6701.
Spain: COPRESA S.A., Balmes 22, BARCELONA 7, Tel. 301 63 12.
Sweden: A.B. ELCOMA, Lidingövägen 50, S-115 84 STOCKHOLM 27, Tel. 08/67 97 80.
Switzerland: PHILIPS A.G., Elcoma Dept., Allmendstrasse 140-142, CH-8027 ZÜRICH, Tel. 01/43 22 11.
Taiwan: PHILIPS TAIWAN LTD., 3rd Fl., San Min Building, 57-1, Chung Shan N. Rd. Section 2, P.O. Box 22978, TAIPEI, Tel. 5513101-5.
Thailand: PHILIPS ELECTRICAL CO. OF THAILAND LTD., 283 Silom Road, P.O. Box 961, BANGKOK, Tel. 233-6330-9.
Turkey: TÜRK PHILIPS TICARET A.S., EMET Department, Inonu Cad. No. 78-80, ISTANBUL, Tel. 43 59 10.
United Kingdom: MULLARD LTD., Mullard House, Torrington Place, LONDON WC1E 7HD, Tel. 01-580 6633.
United States: (Active devices & Materials) AMPEREX SALES CORP., Providence Pike, SLATERSVILLE, R.I. 02876, Tel. (401) 762-9000.
(Passive devices) MEPCO/ELECTRA INC., Columbia Rd., MORRISTOWN, N.J. 07960, Tel. (201) 539-2000.
(IC Products) SIGNETICS CORPORATION, 811 East Arques Avenue, SUNNYVALE, California 94086, Tel. (408) 739-7700.
Uruguay: LUZILECTRON S.A., Rondeau 1567, piso 5, MONTEVIDEO, Tel. 9 43 21.
Venezuela: IND. VENEZOLANAS PHILIPS S.A., Elcoma Dept., A. Ppal de los Ruices, Edif. Centro Colgate, CARACAS, Tel. 36 05 11.

A12

Printed in The Netherlands

9398 7014 0011